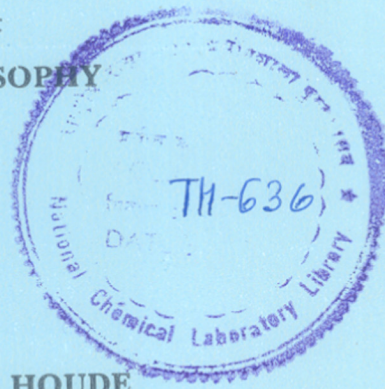# SORPTION AND PERMEATION
OF GASES IN POLYMERS

A THESIS

SUBMITTED TO THE

UNIVERSITY OF POONA

FOR THE DEGREE OF

DOCTOR OF PHILOSOPHY

(IN CHEMISTRY)

BY

AJAY YASHVANTRAO HOUDE

M. Sc.

POLYMER SCIENCE AND ENGINEERING GROUP

CHEMICAL ENGINEERING DIVISION

NATIONAL CHEMICAL LABORATORY

PUNE-411 008 (INDIA)

SEPTEMBER 1991

DEDICATED TO THE MEMORY

OF MY FATHER

DECLARATION

Certified that the work incorporated in the thesis **"SORPTION AND PERMEATION OF GASES IN POLYMERS"** submitted by Mr. Ajay Y. Houde was carried out by the candidate under my supervision. Such material as has been obtained from other sources has been duly acknowledged in the thesis.

[DR. M.G. KULKARNI]

Research Guide

ACKNOWLEDGMENTS

Last, but not least, I wish to thank my wife Anita for the encouragement, support, and assistance given during the course of preparation of this thesis.

(Ajay Y. Houde)

Candidate

CONTENTS

CHPTER I

CHAPTER II

i

CHAPTER III

CHAPTER IV

iii

LIST OF TABLES

LIST OF FIGURES

                              viii

ix

CHAPTER - I

LITERATURE   SURVEY

1.0.0 Literature survey

1.1.0 Introduction

Membrane separation processes have emerged as a low energy intensive unit operation. Membrane technology today competes and/or compliments conventional separation techniques. The major membrane separation processes are Microfiltration (MF), Ultrafiltration (UF), Reverse Osmosis (RO), Dialysis, Electrodialysis (ED), Pervaporation and Gas separation.

The world wide membrane market has been estimated to have grown from less than $ 5 million in 1950 to more than $ 500 million in 1981 (Lonsdale 1982). The current market is estimated at $ 4 billion in 1990 (Riedinger and Faul 1988). These figures relate only to the value of membrane/membrane modules ; the value of the complete technology may be about 3-10 times higher.

Gas separation and solvent recovery, either as vapor or by pervaporation, are relatively new and exciting areas. It is estimated that nearly $ 100 million are spent worldwide for research and development in gas separation alone (Riedinger and Faul 1988).

The utility of polymeric membranes for separating a gas mixture was known even in the 19th century. Mitchell (1831) reported that under equivalent conditions, rubber membranes were more permeable to carbon dioxide than hydrogen. This was the first known report of permselectivity of a membrane. Graham (1866), postulated that the permeation process in polymers involved a solution-diffusion mechanism.

1

1.1.1 Permeation of gases in polymers

In a membrane separation process, the components of a gaseous mixture are separated as a result of the difference in their rates of permeation through the membrane. The ability of a molecule to pass through the membrane depends upon the size and shape of the penetrant molecule, the membrane structure and morphology as well as the interaction between the membrane and penetrant.

The transport of small molecules in polymers has been the subject of extensive efforts since the classical work of Graham (1866). Prior to 1950, most research investigations dealt with rubbery polymers ($T>T_g$). As a result, theories of molecular diffusion in rubbery systems evolved. However, these often failed to explain sorption and diffusion in glassy materials.

Gas permeation in dense polymers occurs by a solution-diffusion mechanism. The permeation process and the mathematics of permeation has been discussed extensively in the literature. Von Wroblewski (1879), provided a mathematical analysis of the process of permeation through polymer films. He defined the permeability coefficient P, as,

$$P = J.l \, / \, \Delta p \tag{1}$$

where, J is the steady-state flux, $\Delta p = p_2 - p_1$, p_2 and p_1 are the pressures on high pressure and low pressure side of the membrane respectively, and 'l' is the membrane thickness. The permeability coefficient P is often expressed in units of $cc(STP).cm/cm^2.sec.cmHg \times 10^{-10}$ or barrers.

As shown in the Fig. 1.1 the upstream condition at x = 0 is

2

DOWNSTREAM

(Condition "1")

Low Pressure

P_1

C_2

$O \sim C_1$

Flux

l

x o

UPSTREAM

(Condition "2")

High Pressure

P_2
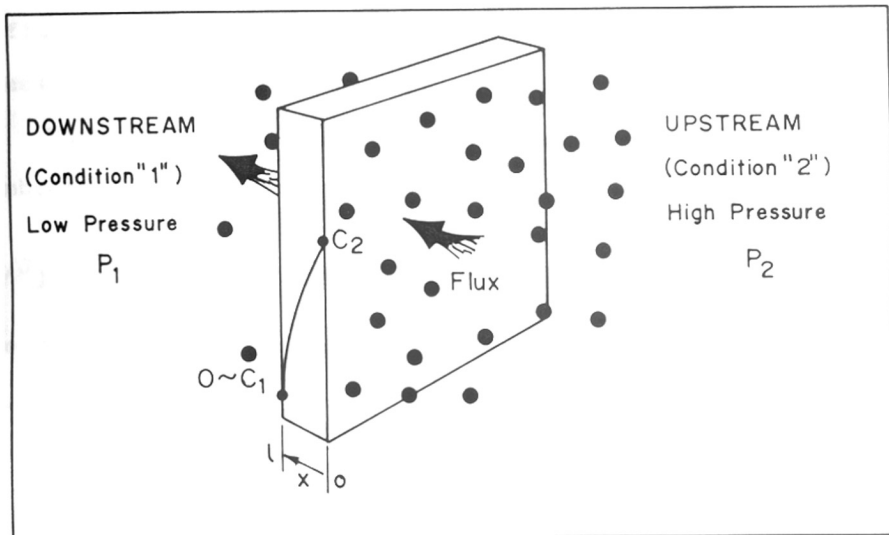
FIG. 1·1: PERMEATION THROUGH A MEMBRANE

distinguished by a subscript "2" and the downstream condition at x = 1 by subscript "1". This convention assumes that the flux occurs in the positive x direction.

Thus for the ith component of gaseous mixture,

$$J_i = K_i . D_i [p_{i(2)} - p_{i(1)} / 1] \qquad (2)$$

where, J_i denotes the flux, K_i and D_i denotes the solubility and diffusivity coefficient, and $p_{i(1)}$ and $p_{i(2)}$, the partial pressures of the ith component on either side of the membrane.

The relative flux for two gases permeating through a membrane is described by,

$$J_i/J_j = [K_i . D_i/K_j . D_j] . [(p_{i(2)} - p_{i(1)})/(p_{j(2)} - p_{j(1)})] \qquad (3)$$

The intrinsic permselectivity of the membrane can be expressed as,

$$\alpha_{ij} = [K_i / K_j] [D_i / D_j] \qquad (4)$$

Thus, the intrinsic permselectivity of a membrane towards various gases is governed by the relative solubilities and diffusivities of the gases being separated.

The solubility of a noncondensible gas in an amorphous polymer can be correlated with the Lennard-Jones potential (ϵ /k) (Michaels and Bixler 1961) or critical temperature (T_c) of the gas (Stern et al 1969). As an empirical rule, gases which have higher critical temperatures and/or smaller molecular diameters permeate faster.

1.1.2 Diffusional transport in polymers

Permeation of gases through non porous membranes involves five steps viz., a) diffusion through the boundary layer, b) sorption into the membrane, c) diffusion through the membrane, d) desorption from the membrane, and e) diffusion from the boundary layer. In the case of amorphous glassy polymers the diffusion through the membrane is the rate controlling step (Vrentas et al 1975).

The transport behavior in nonporous amorphous polymers depends on the characteristics of penetrant and the polymer as summarized in Table 1.1.

The characteristics of the diffusive transport can be predicted from the diffusion Deborah number $[DEB_D]$, which is the ratio of the relaxation time for the polymer-penetrant system to the diffusion time. The diffusion Deborah number is a function of temperature and penetrant concentration ; its magnitude may change during the processs of diffusion. The various regimes of diffusion defined by the penetrant concentration and the phase state of the polymer are shown in Fig. 1.2.

When the polymer is far below the T_g and penetrant activity is low, the time scales associated with the relaxation process are very large. Thus the polymer structure remains unaltered during the diffusion process. Although the medium is not a purely viscous fluid, the phenomena can be analyzed by the classical diffusion theory. Diffusion in this regime (III) is characterized by $[DEB < < 1]$ and is known as Fickian.

At the other extreme, the polymer structure has very high degree of mobility and the relaxation time is much shorter than

5

TABLE 1.1

Transcript in amorphous polymers[*]

	$T > T_c$	$T < T_c$
	Fickian diffusion, single mode sorption	
$T > T_g$	Ideal Fickian diffusion concentration independent diffusion coefficient	Concentration dependent diffusion expalined by free volume theories
	Henry's law obeyed, constant energy of activation	Apparent energy of activation dependent on penetrant concn. and temp.
	Dual mode sorption	
$T < T_g$	Energy of activation shows break near T_g	Non-Fickian and anomalous diffusion
		Case II and super case II transport

[*] Reference (Frisch 1980).
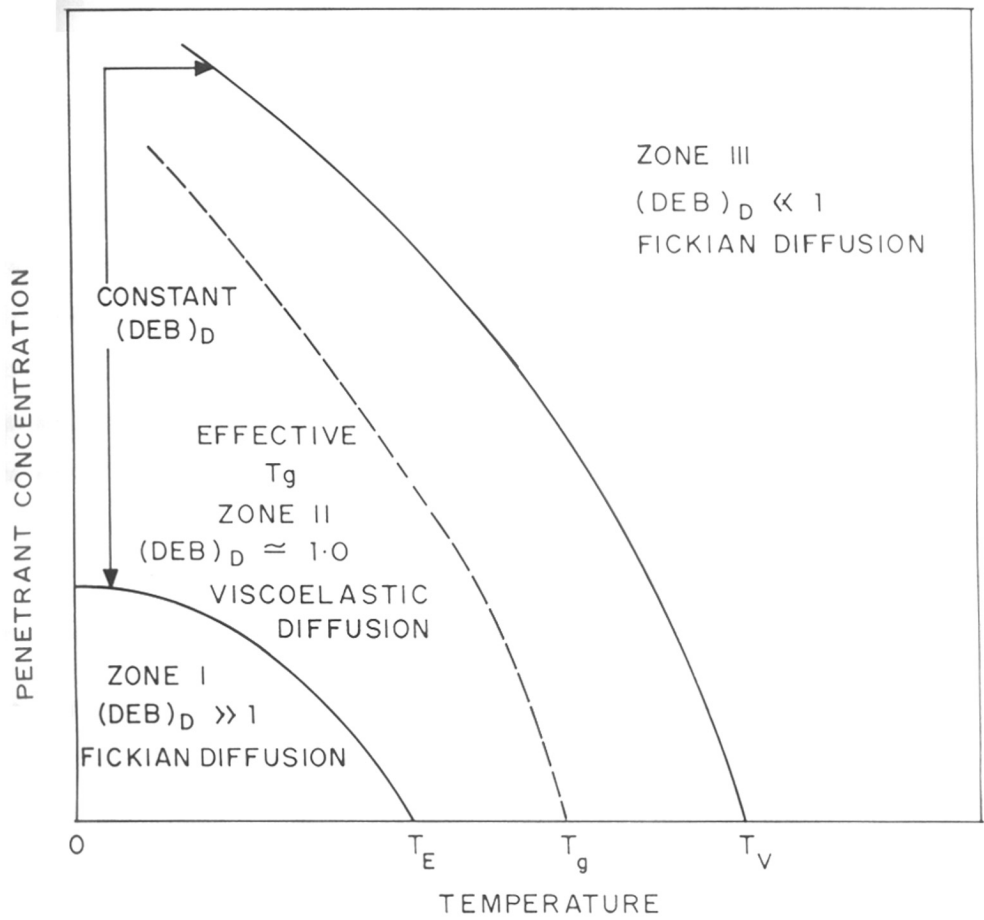
FIG.1·2:REGIMES OF DIFFUSIONAL TRANSPORT

the diffusion time [DEB << 1 Regime (I)]. The conformational changes in the polymer structure at any penetrant concentration take place almost instantaneously. The diffusion can be considered to take place in a purely viscous liquid and is described by Fickian diffusion equations with a concentration dependent diffusion coefficient.

The intermediate range ($0.1 < DEB_D < 1$) is classified as Regime II. In this regime, the penetrant activity is reasonably high and the polymer penetrant system is close to the glass-transition temperature. The time scales associated with the polymer relaxation are comparable to those associated with diffusion. The coupling of diffusion and relaxation results in "anomalous" sorption, the so called case II and supercase II transport (Jaques et al 1974).

Before introducing models of sorption and transport in the glassy state, it would be useful to review the phenomenological model of gas sorption and transport in rubbery polymers.

1.2.0 Sorption and transport in rubbery polymers [$T > T_g$]

A simple model has emerged for sorption and transport process for gases in amorphous polymers above their T_g. This stems from the experience that, generally the sorption obeys Henry's law and diffusion follows Ficks law (Stannett 1968),

$$C = k_D \cdot p \tag{5}$$

$$N = - D \cdot dc/dx \tag{6}$$

where, C, is the concentration of the gas in the polymer, in

cc(STP)/cc(polymer; k_D is Henry's law constant expressed in cc(STP)/cc(polymer).atm ; N is the diffusive flux in cc(STP)/cm^2.sec and D is the constant diffusion coefficient in cm^2/sec.

The time lag technique of Daynes (1920) and Barrer (1939) yields two observable parameters, the time lag Θ and steady-state permeability, P. For systems that obey equations 5 and 6, these parameters are simply related to the membrane thickness, l, the Henry's law constant for the gas, k_D and the diffusion coefficient D, by equation 7 and 8 where,

$$P = k_D.D \qquad (7)$$

$$\Theta = l^2 / 6D \qquad (8)$$

The meanings of these terms can be understood in terms of Fig. 1.3. As shown in Fig. 1.1, when a constant gas pressure is imposed on one side of the initially degassed membrane, a period of transient transport occurs as gas dissolves at the upstream membrane surface, diffuses through the membrane and is released giving rise to increasing pressure in the downstream gas receiver of known volume. Eventually a steady state is established and the slope of the line in Fig. 1.3 can be related to the permeability, P. The extrapolation of this steady state line to the time axis yields the time lag Θ. Experience indicates that the diffusion coefficient in equation 6, 7 and 8 is often independent of upstream driving pressure especially at low overall pressures and for gases with limited solubility.

9

$$P = \frac{N_{ss} \times l}{P_2}$$
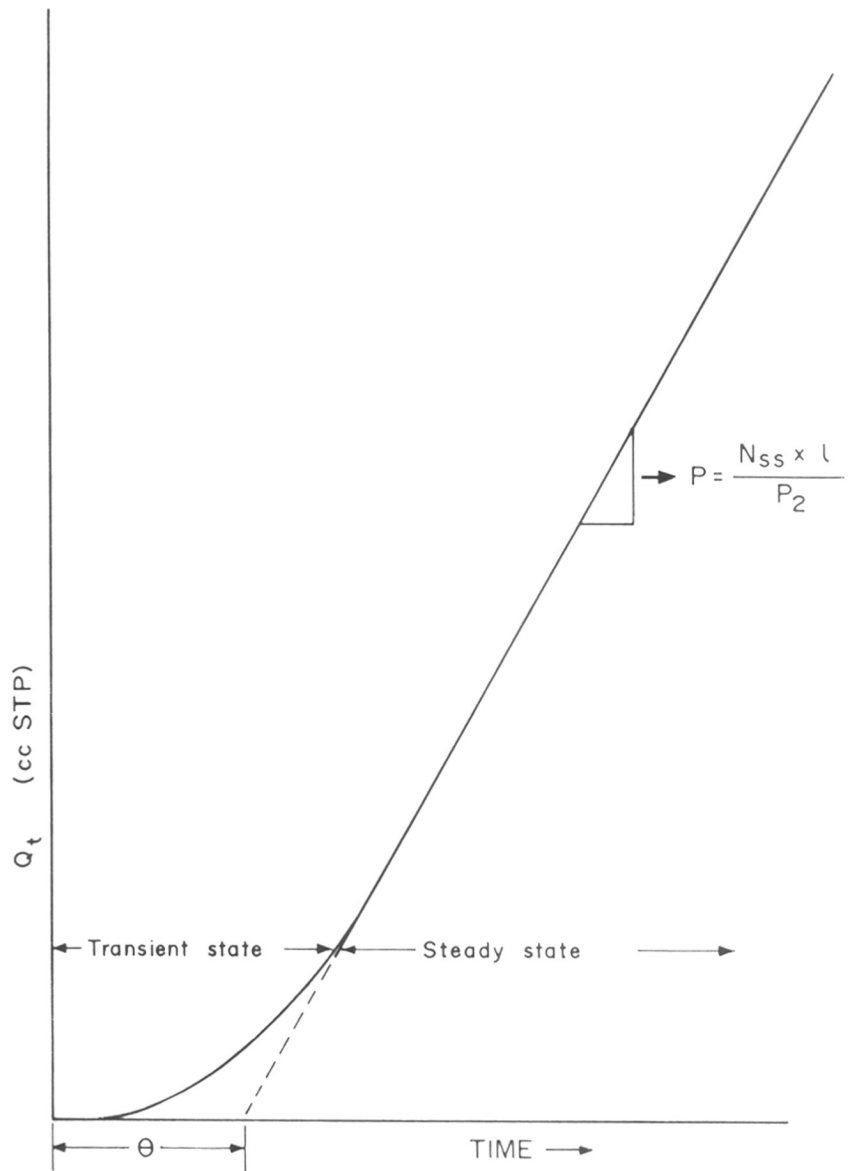
FIG.1·3: SCHEMATIC REPRESENTATION OF A TRANSIENT TRANSPORT EXPERIMENT

Diffusion Coefficient

The diffusion coefficient for gases in rubber can be described by,

$$D = D_o \cdot \exp [-E^* / RT] \qquad (9)$$

The activation energy E^*, is interpreted as the thermal energy that must be concentrated in the polymer adjacent to a diffusing molecule to open a passage of sufficient free volume, to allow the penetrant to execute a diffusional jump. The concept of "free-volume" or "empty" volume used to describe the transport of gases and liquids in polymers have been reviewed in the literature (Berry and Fox 1968, Kumins and Kwei 1968, Stern and Frisch 1981).

Henry's law coefficient

The Henry's law constant, k_D, appearing in equations 5 and 7 can be related to the Lennard-Jone's potential, that provides a measure of the ease of condensation of the gas (Michaels and Bixler 1961, Ulhmann et al 1976). Alternatively critical point or boiling point of the gas can also be chosen as a correlating parameter, with equally good results (Stern et al 1969).

1.3.0 Sorption in glassy polymers [T < T_g]

For rubber polymers, the solubility constants calculated from time lag data are in good agreement with solubilities obtained from equilibrium sorption data (Fujita, 1968). However, Meares (1958)[a] observed that in the case of poly(vinyl acetate), at $T < T_g$, the solubility coefficients for Helium, Neon etc. obtained from sorption data were higher than the values obtained

11

obtained from sorption data were higher than the values obtained from the time lag data. Meares (1958)[b], postulated two types of gas populations to explain this discrepancies.

In a glassy polymer at temperatures lower than T_g, additional free volume is effectively "frozen" in, as a result of the non equilibrium nature of the glass. This gives rise to two distinct populations of sorbed molecules. Those molecules which are dissolved in the polymer matrix and diffuse through it are relatively mobile and follow a Henry's law. Another population is adsorbed into the "holes" present in the polymer matrix, resulting in a Langmuir type sorption. The equilibrium sorption measurements account for the total amount of gas taken up by the polymer, whereas in the time lag analysis only the mobile species is measured. Hence the resultant solubility constant would be expected to be smaller.

1.3.1 Dual-sorption theory

There is considerable evidence suggesting that the Henry's law model (linear isotherm) which applies for gas sorption and transport in rubbery polymers is not adequate for sorption in amorphous polymers below their glass-transition temperature [T_g] (Berens 1974 and 1975). Instead non linear isotherms are observed which may be described by the mathematical form (Michaels et al 1963[a] and Barrer et al 1958).

$$C = C_D + C_H = k_D.p + C_H'.b.p \,/\, 1 + b.p \qquad (10)$$

where, C is the concentration of the gas (cc(STP) / cc(polymer)), C_D is the "dissolution" or Henry's law term and the C_H is the

12

"hole-filling" or Langmuir type sorption term. Parameter k_D is Henry's law term (cc(STP) / cc(polymer).atm), C_H' is the hole saturation constant (cc(STP) / cc(polymer)), b $(atm)^{-1}$ is the hole affinity constant and p is the pressure of the penetrant at equilibrium (atm). The dual-sorption model in this form provides reasonably good description of the sorption process in most glassy polymers (Stern and DeMeringo 1978, Koros and Paul 1978, Wonders and Paul 1979, Chern et al 1984).

In order to determine C_H' and b, the sorption isotherm must be measured over a wide pressure range. The physical significance of the parameters C_H' and b can be better understood from Fig. 1.4 , which illustrates that C_H' is a capacity factor and b is equal to the inverse of the pressure at which one half of the Langmuir sites are filled [i.e. $C_H' = 1/2.C_H$, when $p = b^{-1}$]. The parameter b can be identified as an equilibrium constant equal to the ratio of sorption and desorption rate constants for the Langmuir sites.

Pulsed NMR data (Assink 1975) for NH_3 in polystyrene supports the existence of two distinct sorbed gas populations (C_D and C_H) in local equilibrium with each other. Additional evidence for the two types of sorbed gas populations has been reported by a number of researchers (Michaels et al 1963[a], Vieth and Sladek 1965, Koros 1977).

1.3.2 Significance of dual-sorption parameters

According to the dual-sorption theory, the overall solubility constant of a gas in a glassy polymer [T < T_g] is given by equation 10. At low pressures, equation 10 reduces to
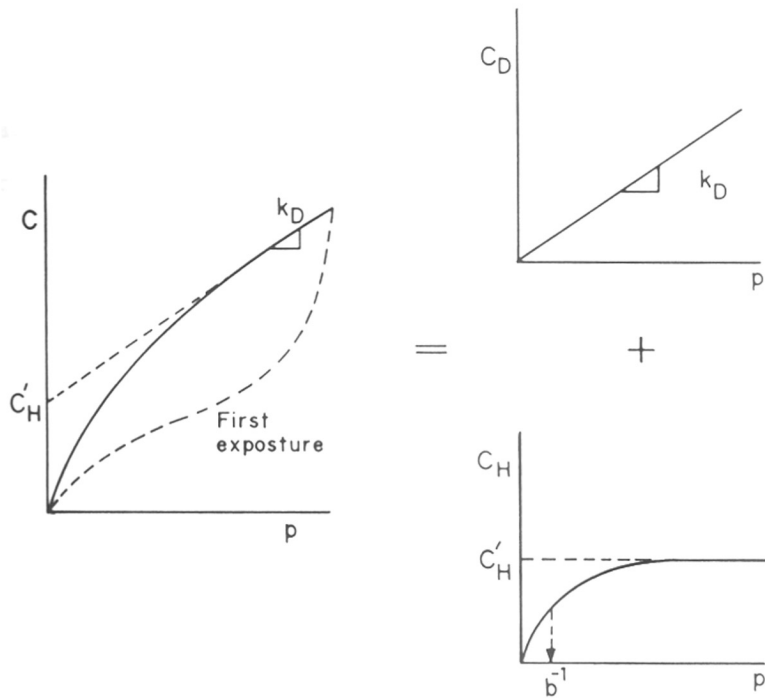
$$C = C_D + C_H$$

$$C = k_D\,p + \frac{C'_H\,bp}{1+bp}$$

FIG.1·4: SCHEMATIC ILLUSTRATION OF THE DUAL-SORPTION MODEL

equation 11.

$$C = k_D \cdot p + C_H' \cdot bp = K'p \tag{11}$$

where,

$$K' = (k_D + C_H' \cdot b) \tag{12}$$

Thus at low pressures, the overall solubility constant K has two components : k_D and $C_H' \cdot b$; $C_H' \cdot b$ is usually much larger than k_D. Hence, at low pressures, hole filling is more important than Henry's law dissolution. Similarly at high pressures, equation 10 reduces to,

$$C = k_D \cdot p + C_H' = K'p \tag{13}$$

where,

$$K' = k_D + C_H' / p = k_D \tag{14}$$

Hence, at high pressures, hole filling becomes less important and dissolution is the main sorption mechanism.

The term k_D in equation 10 is interpreted as the Henry's law constant. The solubility of gases in low molecular weight liquids (Jolley and Hildebrand 1958) and rubbery polymers (Michaels and Bixler 1961, Michaels et al 1963[a]) has been correlated with the Lennard - Jones force constant ϵ / K. Similar correlations have been reported for glassy polymers as well by Vieth et al (1966) and Koros et al (1977). Vieth et al (1966) expressed k_D by the following expression.

$$\ln k_D = 0.026 \ (\epsilon / k) - 1.68 \ \Delta Hm + I \tag{15}$$

where, ΔHm is the partial molar heat of mixing and I is a

constant characteristic of the polymer. Equation 15 is obtained from the integrated Clausius - Clapeyron equation where the heat of solution was taken as the sum of ΔHm and the heat of condensation ΔHc. ΔHc can be related to ϵ/k empirically. The use of the Clausius - Clapeyron equation implies that a plot of $\ln k_D$ vs $1/T$ is linear.

The hole affinity constant b, represents the ratio of the rate constants of sorption and desorption of gas (Vieth et al 1976, Brunauer 1977). The variation of b with T can be described by,

$$b = b_o.\exp(Q/RT) \tag{16}$$

where, Q is the energy, a mole of solute must gain in order to desorb from the Langmuir sites. Using the definition of the isoteric heat of sorption, Vieth et al (1966) have described the following relation at 25°C.

$$\ln b = 0.026 \, \epsilon/k + \ln(\Theta / 1 - \Theta) - I' \tag{17}$$

where, Θ is the fraction of sites filled and I' is a constant. According to Koros et al (1977) the term 'Q' in equation 16 can also be correlated empirically with ϵ/k thus being consistent with equation 17.

The parameter C_H' represents the saturation limit of the gas being sorbed into holes. Assuming that this sorption is a monolayer adsorption process, Vieth et al (1966), derived the following expression which correlates C_H' with surface area,

$$C_H' = [(RTs.Sf / N_A.Ps) . (1/A)] \tag{18}$$

where, R is the gas constant, N_A is Avogadro number, Ts and Ps are the standard temperature and pressure, Sf is the surface area bounding the free volume, and A the area occupied by one sorbate molecule.

The parameter c_H' can be interpreted directly in terms of Fig. 1.5. The unrelaxed volume, $(V_g - V_1)$, corresponds to the net frozen excess volume in the glass. As the experimental temperature increases, the increased mobility of the polymer segments progressively reduces the Langmuir capacity of the glassy polymer. The decrease in c_H' with (T_g-T) is reported in the literature for various polymers such as PET (Koros 1977), PVB (Kamiya et al 1986)[a], PI (Hachisuka et al 1991).

These qualitative observations were quantified by Koros (1977). c_H' was related to the effective molar density of the gas by the equation,

$$c_H' = \{[(V_g - V_1) / Vg] \cdot \rho^* \}$$ (19)

where, V_g and V_1 are the specific volumes of the polymer in the glassy and rubbery states, and ρ^*, the molar density of the gas sorbed in the microvoids, was given by,

$$\rho^* = [\rho \cdot (22,400 / M.W. \text{ of gas})]$$ (20)

where, ρ is the density of gas. Koros (1977) found that at a constant temperature a plot of c_H' versus T_C or ϵ/k is linear.

If the second mode of sorption is related to the non equilibrium nature of the glass, the distribution of these regions of lower density is likely to be a complex function of
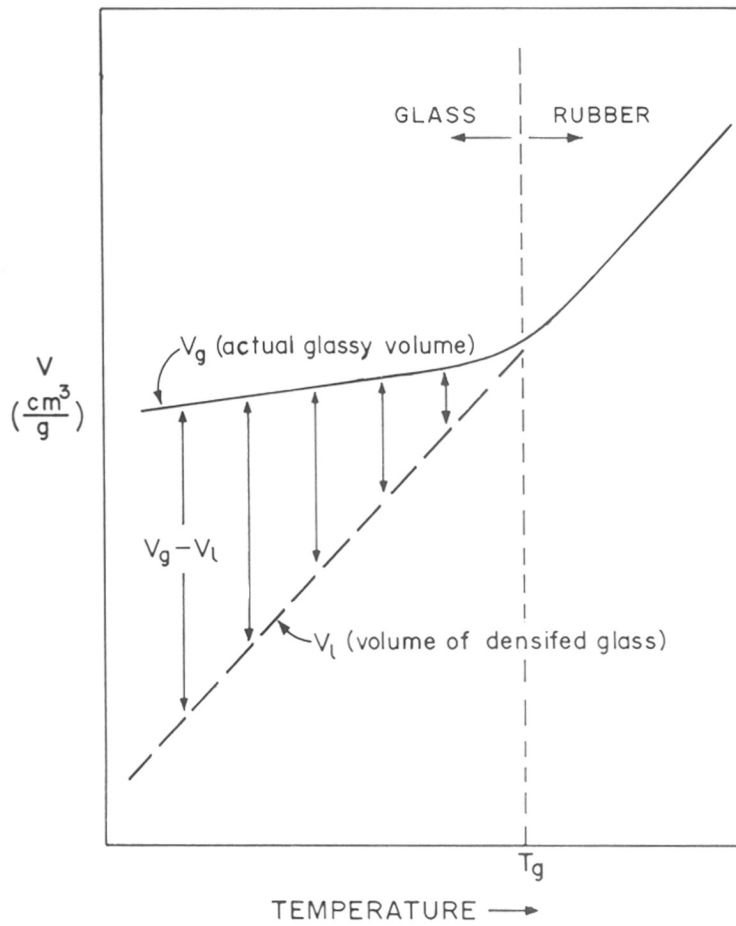
FIG.1·5: TEMPERATURE DEPENDENCE OF THE UNRELAXED
VOLUME (Vg−Vl) IN A GLASSY POLYMER

the sample history. The exposure of glassy polymers to high pressure of highly condensible gases such as CO_2 leads to an increase in c_H' (Chan and Paul 1979, Stern and Kulkarni 1982). Annealing below Tg may reduce the microvoids and a decrease in c_H' is observed (Chan and Paul 1980, Hachisuka et al 1991). Maeda and Paul (1987)[a,b], have reported a decrease in Langmuir capacity on the addition of a low molecular weight diluent to polysulfone and poly phenylene oxide as a result of antiplasticization.

1.3.3 Modified dual-sorption model

The sorption characteristics of a large number of glassy polymers could be satisfactorily correlated within the frame work of the dual-sorption model. However, the sorption behavior of gases in glassy polymers, such as poly vinyl benzoate [PVB] (Kamiya et al 1986)[a], polysulfone (Kamiya et al 1988) polythylene terephthlate (Mizoguchi et al 1987) poly phenylene sulfide (Bourbon et al 1990) could not be correlated satisfactorily.

Mauze and Stern (1983), modified the dual-sorption model in order to describe the sorption behavior of highly soluble penetrant-glassy polymer systems such as water - polyacrylonitrile (Mauze and Stern 1982) and vinyl chloride monomer - poly (vinyl chloride). It was assumed that c_D does not depend linearly on the pressure, but is represented by a function of concentration C and pressure p, that is,

$$c_D = k_D [\exp (\sigma . C)] . p \qquad (21)$$

where, σ is the parameter which represents the interaction between the gas and the polymer, and k_D is the solubility

coefficient in the limit of Henry's law. Thus the total concentration C of gas sorbed in polymer is given by,

$$C = \{k_D [\exp (\sigma . C)]p + [C_H' bp/(1 + bp)]\} \tag{22}$$

This model reduces to the original dual-sorption model in cases where the concentration of penetrant is very low or when $\sigma = 0$. However, the effect of penetrant concentration on Langmuir saturation constant i.e. C_H' was not taken into account.

Pace and Datyner (1981), pointed out the possibility that a decrease in C_H' could be caused by the plasticizing effect of sorbed gas. It was assumed that the presence of a significant concentration of Henry's law species might plasticize the polymer sufficiently to allow the relaxation of some of the initial excess free volume over the experimental time scale. The possibility of such a decrease in C_H' was also suggested by Petropolous (1985).

Kamiya et al (1986)[b], made an attempt to extend the dual-mode sorption model to gas-polymer systems in which the polymer is thus plasticized by the sorbed gas. Combining the results of Mauze and Stern (1983) with Kamiya et al (1986) the extended dual-mode sorption was given by,

$$C = \{[k_D p + [C_{H0}' bp(1 - C^*/C_g)] / 1 + bp\} \tag{23}$$

where, C_{H0} is hole saturation constant at concentration $C = 0$ and C_g is the glass transition concentration (Mauze and Stern 1983). The effective concentration of sorbed gas C^* can then be described as,

$$c^* = c_D + fc_H \qquad\qquad 0 \leqslant f \leqslant 1 \qquad\qquad (24)$$

where, f is the ratio of the plasticizing ability of the gas in the Langmuir species (H) to that in the Henry's law mode (D).

1.3.4 Mixed gas sorption in glassy polymers

The extension of dual-sorption theory to mixed gas permeation lies in the physical interpretation of the Langmuir capacity parameter. Competition between the penetrants for the available Langmuir sites is expected during mixed gas sorption. The resulting model putforth by Koros (1980) was given by,

$$c_A = \{k_{DA} \cdot p_A + [(c'_{HA} \cdot b_A \cdot p_A) / (1 + b_A \cdot p_A + b_B \cdot p_B)]\} \qquad (25)$$

$$c_B = \{k_{DB} \cdot p_B + [(c'_{HB} \cdot b_B \cdot p_B) / (1 + b_A \cdot p_A + b_B \cdot p_B)]\} \qquad (26)$$

where, k_{Di} is the Henry's law constant, b_i is the Langmuir affinity constant, and c'_{Hi} is the Langmuir capacity parameter for each component 'i'. The parameters in equations 25 and 26 are pure component sorption parameters. In principle, once the pure component parameters are known, equation 25 and 26 can be used to predict the sorption behavior of any mixture of the two components (Sanders et al 1984, Story and Koros 1991).

The total concentration of gas sorbed in the polymer matrix was given by,

$$c = \{k_{DA} \cdot p_A + k_{DB} \cdot p_B + [(c'_{HA} \cdot b_A \cdot p_A + c'_{HB} \cdot p_B) / (1 + b_A \cdot p_A + b_B \cdot p_B)]\} \qquad (27)$$

Equations 25 and 26 reveal that the presence of the component B in the gas stream results in a decrease or increase

in the apparent affinity constant of the component A as compared to their respective pure component values.

1.4.0 Transport of gases in glassy polymers [T < T$_g$]

1.4.1 Partial immobilization model

In the earlier formulation of the dual-sorption model, it was assumed that the gas sorbed by the Henry's law mode was free to diffuse while that sorbed by the Langmuir mode was completely immobilized. This led to the conclusion that the time lag would be pressure dependent while permeability would be constant as given by equation (7). Although most of the data on permeability of gases in glassy polymers reported in the literature can be explained on the basis of dual-sorption model ; the complete immobilization model was inadequate to explain the transient permeation experiments. In particular, the observed diffusion time lag is considerably less pressure dependent than that predicted by the total immobilization model (Koros et al 1981). Also, the permeability determined by the steady-state method decreases significantly with increasing upstream driving pressure in contrast to the predictions based on total immobilization model (Paul 1969). This anomaly was resolved by Koros (1977) by postulating that the gas sorbed by the Langmuir mode has a finite mobility, although much smaller than that of the gas sorbed by the Henry's law mode.

The dual mobility model was formulated in two ways,

1) Diffusion coefficient defined in terms of chemical potential gradients (Petropolous 1970).

2) Diffusion coefficient defined in terms of concentration

gradient (Paul and Koros 1976).

1.4.2 Modified mobility model

The dual-mode mobility model described in the preceeding sections has not been extensively tested in the literature. Sada et al (1988)[b] reported that even the dual-mode mobility model failed to explain the pressure dependence of mean permeability coefficient for various gas polymer systems.

Barrer (1984) suggested that the gas molecules sorbed in the glassy polymer matrix by Henry's law mode (D) and Langmuir mode (H) may execute four kinds of diffusion steps viz., $D \rightarrow D$, $D \rightarrow H$, $H \rightarrow D$ and $H \rightarrow H$.

Sada et al (1987) derived two modified mobility models, one based on the concentration gradient analogous to that derived by Paul and Koros (1976) and another based on the chemical potential gradient approach put forth by Petropolous (1970).

Pressure dependence of the mean permeability coefficient was given by,

$$P = k_D D_{DD} + [2k_D D_{DH})/b(p_2 - p_1)] \ln [(1 + bp_2) / (1 + bp_1)] + [C_H' b(D_{HH} + D_{HD}) - k_D D_{DH} / (1 + bp_2) (1 + bp_1) \qquad (28)$$

The pressure dependence of permeability results for CO_2 and CH_4 in Polyimide and Polysulfone could be simulated better over the entire pressure range by the modified mobility model than the dual-mode mobility model (Sada et al 1988)[a].

1.4.3 Concentration dependent transport model

The interpretations of the permeation behavior of gases in

23

glassy polymers based on dual-sorption model discussed so far, have assumed that the diffusion coefficient of the penetrant is independent of concentration. The results therefore are applicable only to those gases which exhibit a very low solubility in polymers, e.g., N_2, CH_4. However, the diffusion coefficient of plasticizing gases and diluents could be highly concentration dependent (Stern and Saxena 1980). According to this model the effective or apparent diffusion coefficient, D_{eff} is given by ,

$$D_{eff} = D(o) \exp. \left[\beta \cdot c_D [1 + FK / (1 + \alpha c_D)] \right] \cdot$$
$$\{ [1 + (FK / (1 + \alpha c_D)^2] / $$
$$[1 + (K / (1 + \alpha c_D)^2] \} \qquad (29)$$

where, $D(o)$ is the diffusion coefficient in the limit $c_m \rightarrow 0$, c_m is the concentration of the mobile part of the penetrant gas, β is an empirical constant which depends on the nature of the penetrant-polymer system, $K = c'_H \cdot b / k_D$, $\alpha = b / k_D$ and F is the fraction of the gas in the Langmuir mode which has a finite mobility.

For the transport of gas across planar nonporous membrane of thickness d, maintained at upstream pressure p_2 and downstream pressure $p_1 \rightarrow 0$, P_{eff} was then given by the equation,

$$P_{eff} = D(o) / \beta \cdot p_2 \left(\exp [\beta k_D p_2 (1 + FK / (1 + bp_2))] - 1 \right) \qquad (30)$$

The transport model incorporating a concentration dependent diffusion coefficient can be exploited to predict the optimum conditions under which selective permeation of gaseous mixture can be anticipated. The ideal operating pressure for the

separation of the multicomponent mixture will depend on the relative positions and magnitudes of minima in P_{eff} vs p_2 curves as well as on the composition of the mixture.

1.4.4 Mixed gas permeation model

In order to predict the performance of membranes during actual use, a methodology must be developed to predict the permeability of membranes to mixed gases, from pure component data.

When the down stream pressure is low in comparison to the upstream pressure, the permeability of the pure gases was given by,

$$P = k_D \cdot D_D \ [1 + FK \ /(1 + bp_2)] \qquad (31)$$

where, $K = C'_H \cdot b \ / \ k_D$ and $F = D_H \ / \ D_D$.

The dual-mobility model was generalized to describe the transport of mixed gases in glassy polymers (Koros et al 1981). The permeability of component A in a binary component feed was given by,

$$P_A = k_{DA} \cdot D_{DA} \ [1 + F_A \cdot K_A \ / \ (1 + b_A \cdot p_A + b_B \cdot p_B)] \qquad (32)$$

The additional term appearing in the denominator of the second term of equation (32) contributes to a decrease in permeability of component A owing to the competition of component B for sorption (see section 1.3.4) and transport in the membrane. Experimental evidence has been reported for variety of systems (Chern et al 1983[c], 1984, Pye et al 1976[b], Robenson 1969, O'Brien et al 1986, Sada et al 1990, Barbari et al 1989).

1.4.5 Gas-Polymer-Matrix Model

In an alternative approach, it has been suggested that there is only one population of sorbed gas molecules in polymers at any pressure and the sorbed gas alters the sorption and transport characteristics as a result of the change in the co-operative main chain motions in the polymer (Sefcik and Schaefer 1983). Raucher and Sefcik (1983)[a] later proposed that the gas-polymer interaction reduces the interchain potential of the polymer, and hence decrease the activation energy for polymer chain separation as well as the activation energy for the diffusion. Since the gas-polymer interaction alters the interchain energy, solubility coefficients also vary as the structure and dynamics of the polymer matrix change.

The gas-polymer-matrix model is based on the experimental evidence putforth by the authors that even permanent gases interact with polymeric chains, resulting in changes in the solubility and diffusivity coefficient as a function of pressure.

According to this model, the concentration of the sorbed gas is given by,

$$C = \sigma_o \cdot p \ / \ (1 + \gamma^* \cdot C) \qquad (33)$$

where, σ_o is the solubility coefficient in the zero-concentration limit. γ^* is a constant relating $\sigma^* k$ to the concentration C, σ^* is a constant relating the excess free energy of mixing to the depression of the glass-transition temperature of the polymer by the gas and k is defined by,

$$k = [T_{g(o)} - T_{g(c)}] \qquad (34)$$

where, $T_{g(o)}$ and $T_{g(c)}$ are the glass-transition temperatures of the pure polymer and polymer-gas mixture.

The sorption data for the system CO_2-polycarbonate could be correlated equally satisfactorily in the framework of the dual-sorption model as well as the gas-matrix interaction model (Sefcik et al 1983).

The diffusion coefficient D is given by equation (35) which was formulated using the diffusion model of Pace and Datyner (1979) and the theory of corresponding states (Prigogine 1957).

$$D = D_o (1 + \beta^*.K) \exp (\beta^*.K) \qquad (35)$$

where, D_o is the diffusion coefficient in the zero concentration limit, and β^* is a constant relating the excess activation energy of chain separation to the depression of the T_g of the polymer by the gas.

In equations (33) and (35) the terms σ_o and D_o reflect the fact that glassy polymers are heterogeneous and contain a distribution of structural and dynamic states (Ferry 1980), which are dependent on the nature of the penetrant and polymer (Pace and Datyner 1979), as well as the distribution properties in the polymer. Parameters γ^* and β^*, denote the effectiveness of gas-polymer interaction in inducing changes in solubility and diffusion coefficients, respectively.

The permeability constant P was given by,

$$P = D_o.\sigma_o [(1 + \beta^*.C) / (1 + \gamma^*.C)] \qquad (36)$$

At pressure less than 1 atm, the matrix model predicts a strong apparent pressure dependence of permeability. However, the dual-mode model predicts only a weak dependence.

1.5.0 History dependence of thermal, mechanical and transport properties

The gas transport properties of polymers are significantly affected by annealing (Chan and Paul 1980, Hachisuka et al 1991), orientation (Hibri and Paul 1985), blending (Chiou et al 1985[b], Maeda and Paul 1985) conditioning (Wonders and Paul 1979, Stern and Kulkarni 1982, Chiou et al 1987, Jordan et al 1989, Houde et al 1991) and by additives (Maeda and Paul 1987)[a,b,c]. Also, film preparation procedures, including casting conditions, solvent evaporation rate, thermal history influence the transport properties (Erb and Paul 1981, Wonders and Paul 1979, Chiou et al 1987).

An understanding of conditioning phenomena is critical in a number of areas involving gas separations and barrier research. The increased sorption levels due to conditioning provide a possible means of enhancing permeability of gases and consequently, increased productivity. Li and Long (1969) observed for the first time the plasticization effect of penetrants in polymers. The changes in membrane permeability and selectivity on plasticization have been well documented for various polymers such as CA (Donohue et al 1989, Sada et al 1990) and PC (Jordan and Koros 1990). An understanding of the cause-effect relationships is obviously important.

The increase of permeability and diffusivity with increasing penetrant pressure is commonly seen for rubbery polymers (Stern

et al 1983). In contrast, in glassy polymers, permeability usually decreases, even though the diffusivity increases with increasing the pressure. This type of behavior is well documented and adequately described by the dual-mode sorption and transport models for various gas-polymer systems including polysulfone (Erb and Paul 1981), polycarbonate (Barbari et al 1989), polyarylates (Sheu et al 1988), and polyimides (Chern et al 1984, Stern et al 1989).

It is well known that sorption of vapors and liquids in polymers can cause significant decrease in T_g (Bernier and Kambour 1968, Kambour et al 1972, 1974, Kambour and Gruner 1978). The resulting change is very small in the sorption of non condensible gases in polymers since the solubility level is quite low. However, condensible gases like CO_2 are soluble in glassy polymers such as polycarbonate (Koros et al 1976) and polysulfone (Erb and Paul 1981). Various investigators (Chiou et al 1985[a], Wonders and Paul 1979, Fried et al 1989) have reported a decrease in the glass transition temperature induced by the sorption of CO_2 for various polymers such as PVC, PSt, PET, PC, CA, PMMA, PSF, PI. In some cases plasticization may occur to an extent where the polymer would no longer be glassy e.g. PEMA (Chiou and Paul 1989), PPO (Hachisuka et al 1990), PPS (Bourbon et al 1990).

In most cases such as He, H_2, O_2, N_2 and CH_4, decrease in permeability with increasing pressure is observed and is in accordance with the predictions of the dual-sorption theory. On the other hand, the permeability coefficients of CO_2 increase with·increasing pressure in CA (Sada et al 1990, Donohue et al

1989), various polyacrylates (Chiou and Paul 1987 and 1989) and PVC (Hibri et al 1985). Chiou and Paul (1987) first called attention to these two contradictory patterns of behavior in glassy polymers and emphasized the need to understand the seemingly contradictory permeation characteristics. Sanders (1988) attributed the permeability profile of CO_2 in CA and PMMA to the increased mobility of their pendent groups on plasticization. Several investigators (Sada et al 1990, Donohue et al 1989) have successfully modelled the permeation characteristics of CO_2 in CA on the basis of concentration dependent diffusivity in combination with the classical dual-sorption theory.

Various techniques have been used to probe the observed diverse permeation characteristics interms of the polymer-penetrant interaction. The plasticization of polymers can lead to a) a modification of the interchain potential energy function and / or b) a structural change in the polymer such as an increase in the intersegmental chain spacing. Characterization techniques such as DSC (Chiou et al 1985)[a], DMA (Fried et al 1989) and NMR (Sefcik and Schaefer 1983), reflect changes in chain mobilities arising from structural as well as energetic considerations and have been extensively used to investigate the effect of polymer-penetrant interaction on the molecular motions in polymers. It has been recently shown that Wide Angle X-Ray Diffraction Spectroscopy (WAXD) technique can be satisfactorily used to monitor the changes in the average intersegmental spacing (Kulkarni et al 1990). Also, volume dilation in various gas-polymer pairs has been quantified (Kamiya et al 1986[b], Bourbon et

al 1990, Fleming and Koros 1990). However, WAXD provides a more direct and quantitative measure of the average intersegmental spacing in the polymer. The correspondence between WAXD and volume based measurements have been discussed recently (Charati et al 1991).

In summary, the plasticization of glassy polymers has been modeled on the basis of the effect of pressure on solubility and / or diffusivity within the framework of the dual-sorption theory. Thus, various investigators have proposed an exponential dependence of (i) diffusivity on solute concentration (Stern and Saxena 1980) (ii) Henry's law constant on concentration (Mauze and Stern 1983) or (iii) a decrease in the microvoid sorption saturation constant with increasing the concentration (Kamiya et al 1988). Also, an alternative, matrix model (Raucher and Sefcik 1983[b]) is itself based on the assumption of solute-glassy polymer interaction incorporated in the parameters β^* (diffusivity depression) and γ^* (solubility depression).

1.6.0 Material selection considerations

The commercial viability of gas separation processes using permselective polymer membranes has been established during the last decade (Strathmann 1981, Lonsdale 1982, Schell 1985, Kurz and Narayan 1986). The development of higher performance membrane materials would probably enhance the market share of membrane processes in the growing gas separation business. The major performance criteria are : (a) productivity (b) selectivity , and (c) durability. The first generation membrane materials, however, were selected rather empirically than on the basis of

31

systematic studies. Research efforts are now directed towards tailoring polymer structure for developing entirely new materials to enhance the intrinsic performance characteristics of polymeric membranes.

Polymers which exhibit high permeability usually exhibit low selectivity, and vice versa. However, synthesis of novel polyimides (Hoehn 1974, Stern et al 1989, Coleman and Koros 1990, Kim 1988, O'Brien et al 1988), polysulfones (Pilato et al 1975, Yamamato et al 1990, Aitken et al 1990, McHattie et al 1991) and polycarbonate (Muruganandam et al 1987) opened new avenues for simultaneous enhancement in permselectivity and permeability.

At downstream pressure very low, permeability (P) and permselectivity (α) is given by,

$$P = S. \; D \tag{37}$$

$$\alpha = [D_A \; / \; D_B] \; [S_A \; / \; S_B] \tag{38}$$

The solubility coefficient, S, is a thermodynamic quantity and is influenced by the inherent condensibility of the penetrant, by polymer-penetrant interaction, and by the free volume of the glassy polymer (Koros 1977, Koros and Paul 1976, Koros 1985). The average diffusion coefficient, D, is a measure of the mobility of the penetrant. This parameter is governed by packing density and mobility of the polymer segments as well as by the size of the penetrant molecule.

The mobility selectivity (D_A/D_B) is based on the inherent ability of the polymer matrix to function as a size and shape

selective medium as a result of segmental mobility and intersegmental packing. The solubility selectivity (S_A/S_B) is determined by the differences in condensibility of the two penetrants and interactions with the membrane material. Thus from equations (37) and (38) it is clear that increasing either diffusivity or solubility of the desired gas by structural variations in polymers would enable enhancement in the permeability as well as selectivity.

Certain principles for the design of glassy polymers which would offer intrinsically higher permeabilities and separation factors were enunciated by Hoehn and Richter (1980) and elaborated by Chern et al (1985). Recently it has been demonstrated that significant increase in diffusivity and diffusivity selectivity can result from simultaneous inhibition of intersegmental chain packing and interaction mobility in a series of polyimides (Stern et al 1989, Kim 1988, O'Brien et al 1988).

A recent report (Schwaar 1990) describes a large number of patents for newer polymers for gas separations. These belong to the family of modified polysulfones, polysiloxanes, substituted poly acetylenes, polyimides and fluorine containing polymers.

In the selection of materials for membranes, it is instructive to consider four levels of membrane structures. These were first proposed by Hoehn and Richter (1980) in connection with aromatic polyamide membranes. These levels consist of (1) segmental structure of the polymer (2) steric relationships in

the segmental structure, (3) morphology of the membranes and (4) morphology of the thin film composite membranes. The first two levels relate to the chemical constitution of the polymer whereas the latter two relate to membrane properties which can be manipulated by the membrane fabrication conditions. In this section, we will primarily discuss the material selection considerations based on the first two levels.

The intrinsic separation factor is given by the eqn. (38) and can be factored into two components. The values of the two parameters for a few polymers are summarized in Table 1.2. Clearly the key to develop polymers with high ideal separation factors lies in combining high solubility selectivity with high diffusivity selectivity. In addition, the polymer has to be highly resistant to the plasticization by the penetrant gas so that the selectivity is retained at high operating pressures.

An examination of Table 1.2 reveals that polyphenylene oxide is not seriously deficient in diffusivity selectivity ; however, it lacks solubility selectivity. Koros (1985) showed that the solubility of a gas like CO_2 can be qualitatively correlated with the $C = O$ and $S = O$ "group densities" in the polymer. Thus it has been shown that carboxylation of polyphenylene oxide which increases the carboxyl group density leads to an enhanced solubility selectivity for CO_2/CH_4 separation (Koros 1985).

In contrast to solubility selectivity, the mobility selectivity can be manipulated over a wide range by appropriate choice of the polymer structure. Yet any increase in the diffusivity selectivity is usually accompanied by a decrease in the absolute permeability. The most challenging aspect of polymer

34

TABLE 1.2

Choice of polymers for CO_2/CH_4 separation[*]

Polymer	S_A/S_B	D_A/D_B	P_A/P_B
PPO	2.08	7.21	15.0
PC	3.6	6.81	24.4
CA	7.3	4.21	30.8
PSF	3.2	8.85	28.3
PI	4.1	15.38	63.6

*Reference (Chern et al 1985)

selection lies in tailoring polymers which would offer high selectivity along with high permeability. Polymers which contain a) bulky structures in the backbone and thereby prevent compact chain packing along with (b) restricted chain mobility as to provide size and shape selectivity are expected to offer high permeability as well as high separation factors in gas separations (Hoehn and Richter 1980). Polyimides which offer these characteristics have been discussed by Kim et al (1987), Stern et al (1989).

A further extension of the above concept is illustrated in the development of poly [1-(trimethylsilyl)-1-propyne] (PMSP) membranes. The high permeability of CO_2 in PMSP stems from high T_g and high frozen free volume in the polymer as a result of bulky substituents in the polymer structure. This is reflected in the very high value of C_H' (Ichiraku et al 1987). Since the polymer lacks any functional groups with which CO_2 could interact, the b value is very low. In this case a tremendous increase in the permeability is accompanied by a decrease in the selectivity (Ichiraku et al 1987). Nonetheless, this development indicates that it is possible to design glassy polymers having permeabilities as high as rubbery polymers.

Major applications of membranes for gas separation

There are three major applications of membranes in gas separation processes. i) Separation of H_2 from various purge gas streams ii) CO_2 separation from CH_4 from landfill gases and in recycling of CO_2 from enhanced oil recovery projects iii) The separation of O_2 from N_2.

An extraordinarily small molecular size of H_2 enables it to diffuse rapidly through the polymer membranes (Stannett 1968). However, it is difficult to separate H_2 from CO_2 and H_2S which are bulkier molecules. This can be explained on the basis of eqn. (37). Although H_2 has a high diffusivity, it has very low solubility in membranes (Bixler and Sweeting 1971). Therefore, a gas such as CO_2 which has low diffusivity yet higher solubility may have a steady-state permeability comparable to that of H_2, since the permeability of a component through the membranes is governed by the product of solubility and diffusivity. High solubilities of CO_2 and H_2S in membranes at low partial pressures, coupled with the relatively low solubility and diffusivity of the bulky methane molecule, enable the separation of CO_2 and CH_4.

In the case of the systems H_2-NH_3 and CO_2-CH_4, the difference in permeability between permeate and retentate gases is more than 20-fold. Highly enriched streams can be obtained in a single pass. Unfortunately, currently available polymer membranes have only moderate selectivities to separate O_2 and N_2. With a selectivity of 2, the product gas can be enriched to 35-40 % ; with a selectivity of 4, a product gas of 60 % can be produced.

Polydimethyl siloxane was known for a long time, to have the highest permeability to O_2 (6×10^{-8} cc(STP).cm/cm^2.s.cmHg) among the existing polymers. This polymer however, is a rubbery material, and difficult to cast into thin films. Poly [1-(trimethylsilyl)-1-propyne] films show an O_2 permeability even

higher (83×10^{-8} cc(STP).cm/cm^2.s.cmHg) (Masuda et al 1983) than that of PDMS films. However, both of these PDMS and PTMSP exhibit low selectivities. A selectivity of 4 is only obtained with polymers of having low permeabilities (Masuda et al 1983). This follows from eqn. (37). The size and shape (and hence diffusivity) of O_2 and N_2 are quite similar, besides there are no significant differences in their solubility characteristics. The ideal separation factor (eqn. 38) is therefore low. The development of high-permeability, high-selectivity membranes for the system O_2/N_2 is a challenging area of considerable research.

Another mechanism for separation viz. facilitated transport, is being developed and in principle could lead to much higher membrane permeabilities and selectivities compared with those possible using polymer membranes operating by the solution-diffusion mechanism. This would lead to dramatic reductions in process costs. A facilitated transport membrane is illustrated in Fig. 1.6 (Baker and Blume 1986). The membrane contains a carrier that selectively and reversibly binds O_2 such as, liquid compounds (Baker and Blume 1986), transition metal ions (Dong et al 1989), silicon-bound cobaltporphyrin (Nishide et al 1989) etc. These systems offer higher selectivities and permeabilities than the existing polymer membranes and, would represent a breakthrough in performance if developed commercially. However, membranes made to date are relatively unstable and rather thick (100 - 200 um) compared to the membranes which effect separation through passive diffusion wherein thickness are typically 0.2 - 5.0 μm.

Membranes which can preferentially permeate N_2 could find

Feed stream
atmospheric air

Product stream
at lower pressure

Membrane

21 % O_2
78 % N_2
1 % Other

Carrier

88 % O_2
12 % N_2

O_2

Carrier·O_2

O_2
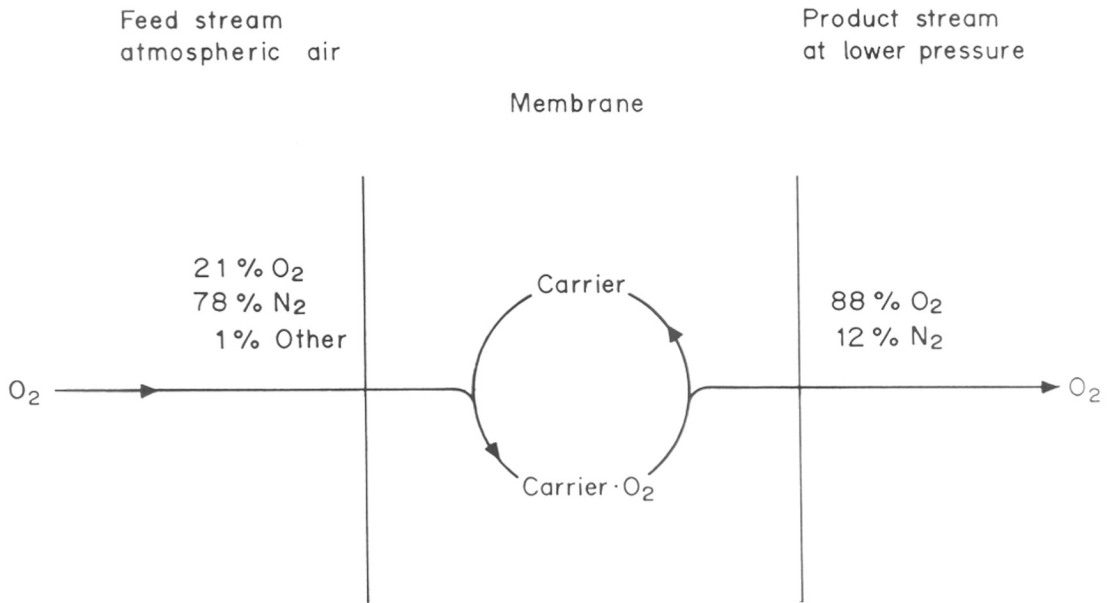
FIG. 1·6 : FACILITATED   TRANSPORT : SCHEMATIC

applications in the separation of trace amounts of N_2 (5 - 15 %) in the natural gas. Unfortunately, polymers exhibit lower permeability for N_2 than for CH_4. The solubility of N_2 is lower than that of CH_4 due to the lower critical temperature of N_2 (126 °K vs 191°K for CH_4). On the other hand the diffusivity of N_2 is higher than that of CH_4 due to the smaller kinetic diameter of N_2 (3.64 Å vs 3.8 Å for CH_4) (Svehla 1962). Amongst conventional rubbery and glassy polymers, the diffusivity selectivity of N_2 over CH_4 is small and the overall selectivity is dominated by the solubility selectivity for CH_4 over N_2 (Kim 1988). Consequently, the permeability of N_2 is smaller than that of CH_4 in almost all polymers (Kim et al, 1987). However, aromatic polyimides exhibit relatively higher permselectivity for the system N_2/CH_4 (1.67 - 2.18) since the diffusivity selectivity factor dominates (Kim et al 1987).

Summary

In summary, this chapter discusses theories and models developed in the past to describe sorption and permeation characteristics of gases in polymers. The scope for the research in the gas separation area is discussed in brief. Criteria for material selection and the effect of exposure to high pressure gases on properties of polymers have also been reviewed.

CHAPTER - II

RATIONALE   AND   OBJECTIVES

2.0.0 Rationale and objectives

2.1.0 Material selection considerations

Hoehn (1974) demonstrated for the first time that simultaneous enhancement in permeability and permselectivity can be brought about by the manipulation of the intrasegmental chain mobility and intersegmental chain packing. Subsequent studies by Stern et al (1989), Kim (1988) and Hellums et al (1989) have borne out the principles laid down by Hoehn (1974).

These studies lead to the conclusions that (Coleman and Koros 1990),

1) Substitutions which simultaneously inhibit chain packing and rotational mobility about flexible linkages on the polymer backbone tends to lead to an increase in both membrane permeability and permselectivity.

2) Substitutions which decrease the concentration of mobile linkages in the polymer backbone tend to lead to increased permselectivity without a large reduction in permeability provided the added moiety does not significantly increase the intersegmental packing density.

This study attempts to develop structurally modified polysulfones on the basis of above principles. The study seems especially warranted because of the importance of bisphenol-A polysulfone (PSF) as a membrane material for gas separation. PSF has been chosen for membrane applications because of its processibility, cost, toughness and high T_g, in addition to its desirable gas transport properties.

The aim of this work is ;

a) to elucidate the effect of polar / flexible groups such as -COO- and/or -O-, in the polysulfone backbone on its gas transport behavior,

b) to study the effect of bond location in the modified polysulfone, replacing meta disubstituted acid chloride by para disubstituted acid chloride on the sorption and permeation characteristics,

c) to study effect of substitution of the bulkier phthalide group for the isopropylidene moiety of the diol unit in the conventional polysulfone (Udel), on the sorption and transport characteristics.

2.2.0 History dependence of properties of glassy polymers

The sorption and transport behavior of CO_2 in glassy polymers has been extensively investigated. High levels of CO_2 sorption have been shown to plasticize the polymer and cause significant changes in the thermal (Chiou and Paul 1987, Sanders 1988), mechanical (Fried et al 1990) as well as transport (Wonders and Paul 1979, Fleming et al 1990, Houde et al 1991) properties of the polymers. However, the effect of plasticization on the permeation characteristics of different glassy polymers is not identical.

In rubbery polymers, both diffusivity and permeability of gases increase with increasing pressure (Stern et al 1983). The permeability of most glassy polymers to gases decreases with increasing pressure in accordance with the predictions of the dual sorption theory (Michaels et al 1963)[b]. However, the

permeability of cellulose acetate (CA) (Sada et al 1990, Donohue et al 1989), various polyacrylates (Chiou and Paul 1987 & 1989) and poly (vinyl chloride) (PVC) (Hibri et al 1985), to CO_2 increases with increasing pressure. This seemingly contradictory dependence of permeability on pressure merits detailed investigation.

Gas-polymer interaction can result in a) modification of the interchain potential energy function and/or b) a structural change in the polymer such as an increase in intersegmental chain packing. Characterization techniques such as DSC (Chiou et al 1987), DMA (Fried et al 1989) and NMR (Sefcik and Schaefer 1983), reflect changes in chain mobilities arising from structural as well as energetic considerations and have been extensively used to investigate the influence of gas-polymer interaction on the molecular motions in polymers.

The effect of sorbed gases on the transition temperature of bisphenol-A based glassy polymers has been attributed to possible enhancement in the intersegmental spacing (Fried et al 1989). However, no experimental validation has been reported. It is reasonable to expect that the observed enhancement in the gas diffusivity / permeability may result from an increase in the polymer intersegmental spacing as measured by WAXD.

In the second phase of work, the utility of wide angle X-ray direction measurements (WAXD) as a probe to measure the intersegmental chain spacing in various glassy polymers and in the interpretation of the diverse permeation characteristics of glassy polymers following exposure to CO_2 at elevated pressures has been investigated. Effect of CO_2 exposure on sorption,

transport, thermal and volumetric behavior of phenolphthalein based polysulfone has also been studied.

Summary

The proposed investigation has been undertaken with the following objectives.

* To synthesize polysulfones which would offer better separation characteristics for the system CO_2/CH_4.

* To investigate the effect of chemical composition on the sorption and transport characteristics of a series of polysulfones.

* To investigate the effect of conditioning by CO_2 on the physical and transport properties of phenolpththalein based polysulfone and aromatic polyesters synthesized during this work.

* To investigate plasticization behavior of a wide range of glassy polymers and attempt to interpret their permeation characteristics.

* To illustrate the role of structural attributes in a series of bridge and ring substituted aromatic polyesters on the permeation characteristics of the polymers and their hysteresis behavior

CHAPTER - III

EXPERIMENTAL

3.0.0 Experimental

3.1.0 Materials

3.1.1 Monomers and polymers

The various polymers used in this investigation are summarized in Table 3.1. The sources and purities of monomers, solvents and catalyst used for the synthesis of PSF-PPHA and PAES are described in Appendix III-1. All the raw materials were purified before use according to the standard procedures (Perrin and Armarego 1988).

Polymer A was based on condensation of phenolphthalein and 4,4'-difluorodiphenylsulfone (PSF-PPHA). Polymer B containing ester linkage in the backbone (PAES) was synthesized by the condensation of bisphenol-A with 4,4'-sulfonyl dibenzoyl chloride. Polysulfones C (PA-1), D (PA-2) and E (PA-3) containing ether and ester linkages in the backbone were based on condensation of bisphenol-A and 4,4'- (SPCl) / 3,3'- (SMCl) or equimolar mixture of SPCl and SMCl isomers of sulfonyl bis(p-phenenyleneoxy) dibenzoyl chloride respectively. Polymers C, D and E were supplied by Dr. B.B. Idage.

Aromatic polyesters (F-K) were synthesized by the condensation of equimolar mixture of isopthaloyl and terephthlaloyl chlorides and substituted diols. Polymers L and M were synthesized by condensation of phenolphthalein and (25:75) or (50:50) molar mixture of isophthaloyl and terephthaloyl chlorides respectively. These polymers were supplied by Mr. S.G. Charati.

45

TABLE 3.1

Polymers identified

Sr. No.	Polymer	Composition	
		Diol	Dihalide
A)	Phenolphtha-lein based polysulfone **[PSF-PPHA]**	PPHA	DFDPS
B)	Polyaryl-estersulfone **[PAES]**	BIS-A	4,4'- SDBCl
C)	Polyaryl-ether ester sulfone **[PA1]**	BIS-A	SPCl
D)	Polyaryl-ether ester sulfone **[PA2]**	BIS-A	SMCl
E)	Polyaryl-ether ester sulfone **[PA3]**	BIS-A	SPCL : SMCl
F)	Bis(phenol-A)-I/T **[(BIS-A-I/T)]**	BIS-A	IPC : TPC
G)	Bis(methyl-ethyl ketone)-I/T **[BIS(MEK)-I/T]**	BIS(MEK)	IPC : TPC
H)	Bis(methyl iso butyl ketone)-I/T **[BIS(MIBK)-I/T]**	BIS(MIBK)	IPC : TPC
I)	Bis(aeto-phenone)-I/T **[BIS(ACETO)-I/T]**	BIS(ACETO)	IPC : TPC
J)	Dimethylbis-phenol-A-I/T **[DMBIS-I/T]**	DMBIS	IPC : TPC

K)	Tetramethyl-bisphenol-A-I/T **[TMBIS-I/T]**	TMBIS	IPC : TPC
L)	Phenolphtha-lein-I/T **[PPHA-25I/75T]**	PPHA	IPC(25) : TPC(75)
M)	Phenolphtha-lein-I/T **[PPHA-I/T]**	PPHA	IPC(50) : TPC(50)

Chloroform was used as a solvent for the polymers A-M.

The polymers poly(methyl methacrylate) (PMMA), cellulose acetate (CA), polycarbonate (PC), polysulfone (PSF), polyethersulfone (PES) and polystyrene (PSt) used for plasticization study were all commercial samples. Sources, specifications and solvents used for the purification of these are tabulated in Appendix III-2.

3.1.2 Gases

Helium (He), Argon (Ar), Oxygen (O_2), Nitrogen (N_2), Methane (CH_4) and Carbon dioxide (CO_2) were used for sorption and permeation studies without further purification. The standard gas mixture of CO_2 : CH_4 (55:45) (mole fractions) was used for mixed gas permeation studies. The purities and suppliers are listed in Appendix III-3.

3.2.0 Synthesis of polyarylestersulfone (PAES) based on bisphenol-A and 4,4'-sulfonyl dibenzoyl chloride

The reaction scheme for the preparation of 4,4'-sulfonyl dibenzoyl chloride (5) is summarized in Fig. 3.1.

Synthesis of 4,4'-ditolyl sulfone (3)

The compound 4,4'-ditolyl sulfone (3) was prepared by Fridel-Crafts nucleophilic substitution method from tosylchloride (1) and toluene (2) using the procedure described in the literature (Holt and Pagdin 1960).

To a two necked 250 ml round bottom flask, equipped with reflux condenser, and a thermowel was added 19.05 g (0.1 mole) tosylchloride (1), 16.70 g (0.125) mole anhydrous $AlCl_3$, and 50
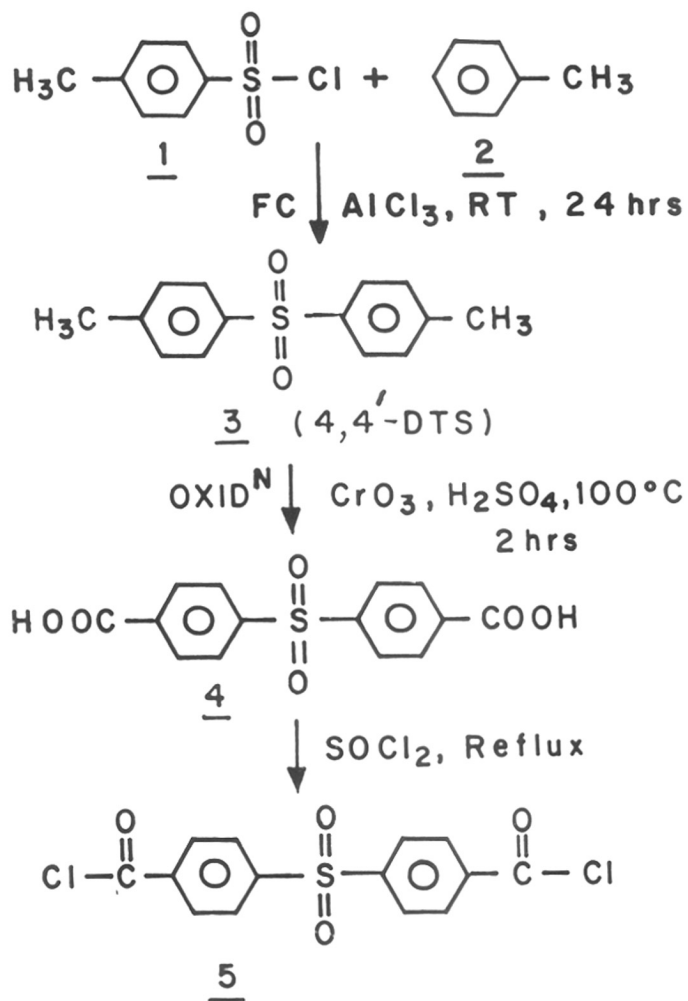
FIG. 3·1: SYNTHESIS OF 4,4'-SULFONYL DIBENZOYL
CHLORIDE (5)

ml dry 1,2-dichloro ethane (EDC). The mixture was stirred for 45 minutes at room temperature using a magnetic stirrer. The clear solution was decanted from undissolved aluminum chloride into a two necked 250 ml round bottom flask equipped with reflux condenser and thermowel, containing a mixture of 10.12 g toluene (distilled and dry), and 50 ml EDC (dry). The reaction mixture was stirred overnight at room temperature, the solution was then poured into ice and 5 ml conc. hydrochloric acid (HCl). EDC layer was separated and dried after being washed successively with water, dil. sodium hydroxide solution, and water again. After concentration, the solution was kept at room temperature for crystallization. The solid material separated was filtered and dried in a vacuum oven at 50°C for two days.

[Yield : 75 %, M.P. : 152 $^{\circ}$C (found), 157-158°C (Holt and Pagdin 1960)]

Molecular formula : $C_{14}H_{14}O_2S$, Molecular weight : 246

IR (Nujol) : 1110 cm^{-1} and 1150 cm^{-1} (S=O)

(^{1}H) NMR (CDCl$_3$) : δ 2.35 (S, 3H phenyl CH$_3$), δ 7.35 (M, 4H aromatic H$_a$), δ 7.86 (M, 4H aromatic H$_b$).

The NMR spectrum is shown in Fig. 3.2a.

Synthesis of 4,4'-sulfonyl dibenzoic acid (4)

4,4'-sulfonyl dibenzoic acid (4) was synthesized as reported in the literature (Milan and Jiri 1960). A solution of 25 g of 4,4'-ditolyl sulfone (3) in 200 ml glacial acetic acid (GAA) was warmed to 40-50°C, in a four necked 1 liter round bottom flask equipped with reflux condenser, thermowel, glass stirrer, and a hot dropping funnel. To this was added a solution of 75 g
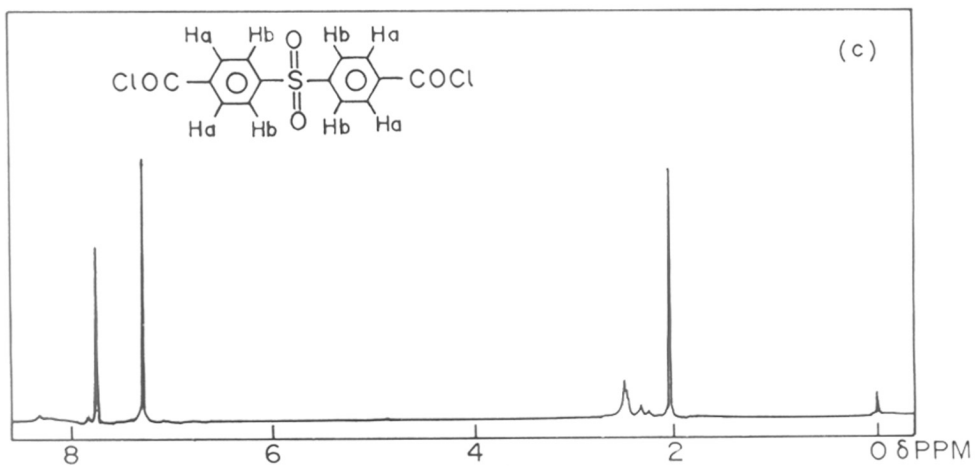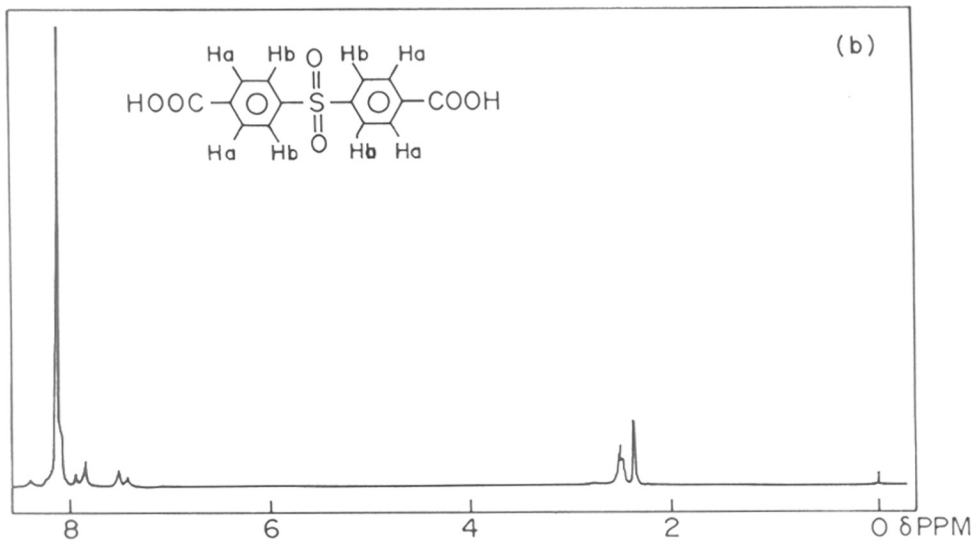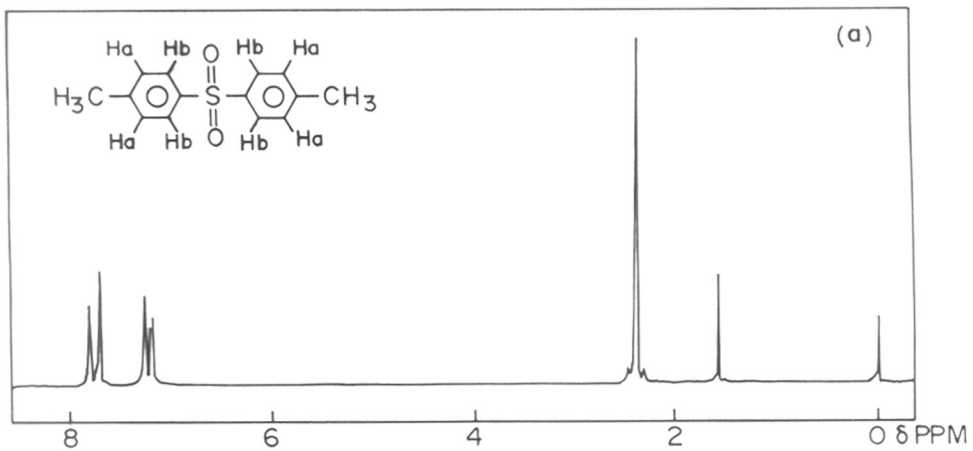
FIG. 3·2: NMR SPECTRA OF (a) 4,4'-DITOLYLSULFONE
(b) 4,4'- DICARBOXY DIPHENYLSULFONE (c) 4,4'-SULFONYL
DIBEZOYL CHLORIDE

51

chromium trioxide (CrO_3), in 125 ml H_2O, 200 ml GAA and 125 ml conc. H_2SO_4, previously heated to $70^\circ C$. Addition time was 30 minutes; the temperature was maintained at $100-110^\circ C$ during the addition and then at $100^\circ C$ for another 15 minutes. The mixture was cooled and diluted with 800 ml H_2O and treated with SO_2 for 10 minutes to reduce excess CrO_3. Filtration and washing with hot water (2-3 times) yielded 28 g of crude product, which was purified by dissolving in aq. sodium carbonate (Na_2CO_3) solution and reprecipitating with dil. HCl.

[Yield : 88 %, M.P. : $355-360^\circ C$ (found), $370^\circ C$ (Buechler and Masters 1939)]

Molecular formula : $C_{14}H_{10}O_6S$

Molecular weight : 306

IR (Nujol) : 1110 cm^{-1} and 1170 cm^{-1} (S=O), 1690 cm^{-1} (acid C=O), 1590 cm^{-1} and 1610 cm^{-1} (COO^- stretch), 2540 cm^{-1} and 2690 cm^{-1} (acid bonded -OH)

(^1H) NMR (DMSO-d_6) : δ 7.37 (M, 4H aromatic H_a), δ 7.84 (M, 4H aromatic H_b), δ 8.10 (S, 1H carboxylic).

The NMR spectrum is shown in Fig. 3.2b.

Synthesis of 4,4'-sulfonyl dibenzoyl chloride (5)

To a 100 ml round bottom flask equipped with reflux condenser, guard tube and stirring arrangement, was added 15.3 g (0.05 mole) diacid [i.e 4,4'-sulfonyl dibenzoic acid (4)] and 7.14 g (0.06 mol) thionyl chloride. The mixture was heated to the reflux temperature for 2 hrs., after which 3-4 drops of dimethylformamide (DMF) were added. The heating was continued for another 2-3 hrs. and then the contents were left overnight at

room temperature. Excess thionyl chloride was removed under reduced pressure at 40-50°C. The dry crude product was recrystallized from dry benzene. [Yield : 15.95 g (93 %), M.P : 160°C (found), 165°C (Adamek et al 1960)]

IR (Nujol) : 1100 cm^{-1} and 1150 cm^{-1} (S=O), 1790 cm^{-1} (acyl chloride C=O)

(^{1}H) NMR (DMSO-d_6) : δ 7.31 (S, 4H aromatic H_a), δ 7.82 (S, 4H aromatic H_b)

The NMR spectrum is shown in Fig. 3.2c.

Synthesis of polyarylestersulfone (PAES)

The reaction scheme for synthesis of polyarylestersulfone (PAES) is shown in Fig. 3.3.

In a two necked 100 ml round bottom flask equipped with nitrogen sparge tube, condenser fitted with moisture trap, and magnetic stirrer, were placed 2.28 g (0.01 mole) of purified bisphenol-A and 20.4 ml of 1 M aqueous sodium hydroxide. The mixture was stirred and 60 g of benzyl triethylammonium chloride (BTEAC) was added. To this solution was added, all at once a solution of 3.42 g (0.01 mole) of 4,4'-sulfonyl dibenzoyl chloride (5) in 20 ml of methylene chloride (DCM), and vigorous stirring was continued for 1 hr. at room temperature. The mixture was poured into 700 ml of boiling water containing 2 ml concentrated HCl. The precipitated polymer was collected, washed with water, and dried at 100°C in vacuum.

[Yield : 4.96 g (99.4 %)]

Molecular formula of repeat unit structure : $C_{29}H_{22}O_6S$

Molecular wt. of repeat unit : 498.5 g/mole
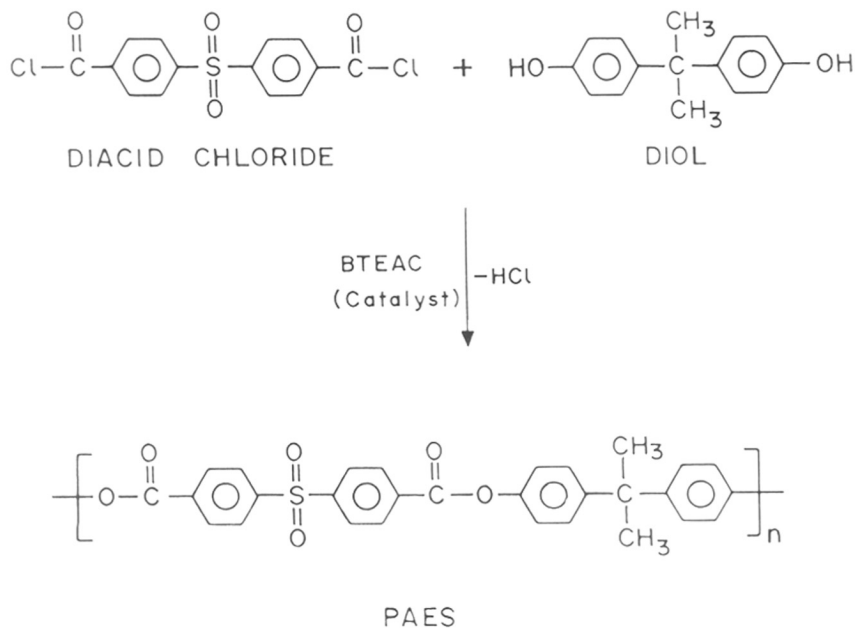
FIG. 3·3 : PREPARATION OF POLYARYLESTERSULFONE (PAES)

Elemental analysis :

Calculated for $C_{29}H_{22}O_6S$: C, 69.86 % ; H, 4.44 % ; O, 19.23 % ;

S, 6.43 %.

Found : C, 69.5 % ; H, 4.25 % ; S, 6.5 %.

Glass transition temperature : 267 ^{O}C (by DSC) (Manami et al 1990)

235 ^{O}C (by DSC) (Found)

The DSC scan for quenched sample is shown in Fig. 3.4.

3.3.0 Synthesis of phenolphthalein based polysulfone (PSF-PPHA)

Polycondensation reactions require reaction stoichiometry to be critically maintained in order to achieve high molecular weights. Hence the monomer purity is a critical factor. The reaction scheme for synthesis of phenolphthalein based polysulfone is given in Fig. 3.5.

Phenolphthalein (ACS reagent, Loba) was purified twice according to a standard procedure (Perrin and Armarego 1988). Purified product was dried at 75°C for 12 hrs., cooled, powdered in mortar and pestel and dried again for 12 hrs. at 80-90°C. This was essential to remove the last traces of solvent. Difluorodiphenylsulfone was recrystallized thrice from hot benzene. Similar drying procedure was used to remove the traces of solvent.

Phenolphthalein based polysulfone (PSF-PPHA) was prepared by the condensation of 4,4'-difluorodiphenylsulfone (DFDPS) with phenolphthalein in N,N',-dimethylacetamide (DMAC) according to the procedure reported by Viswanath et al (1984). The route was preferred to the DMSO/NaOH (Johnson et al 1967) route which leads
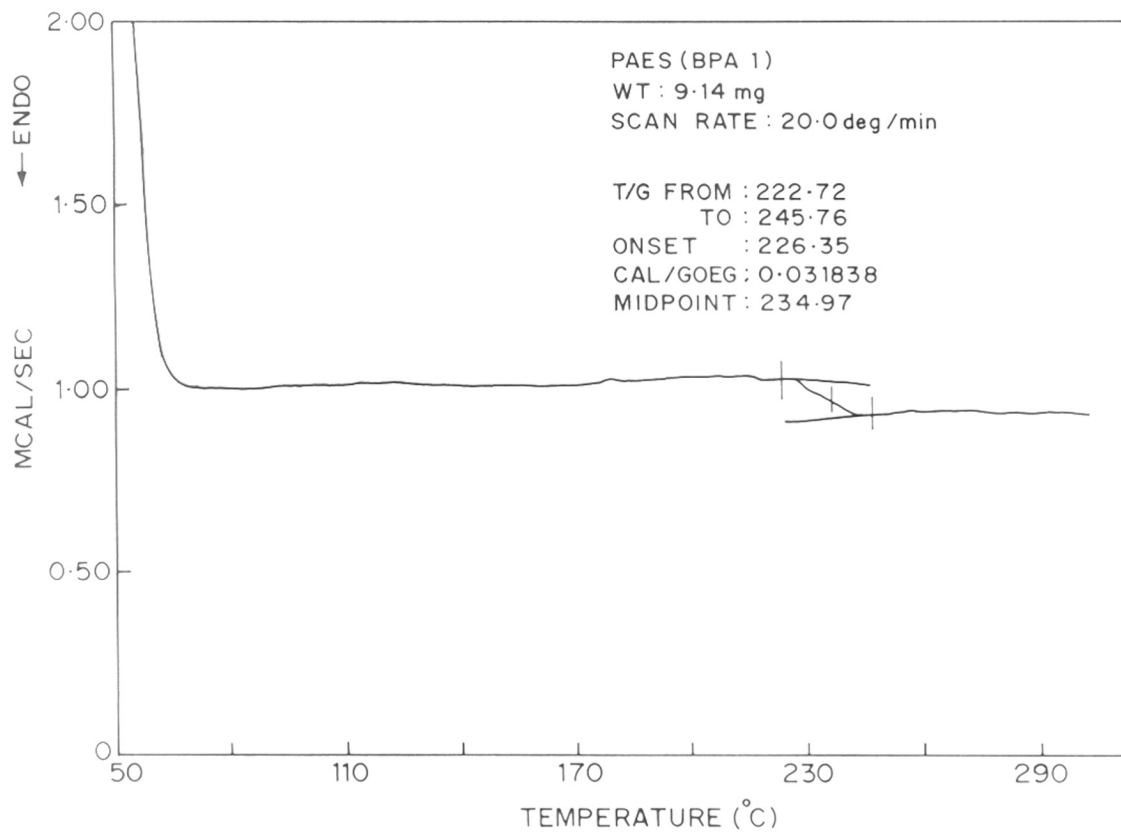
FIG.3·4:DSC SPECTRUM OF SOLUTION-CAST PAES
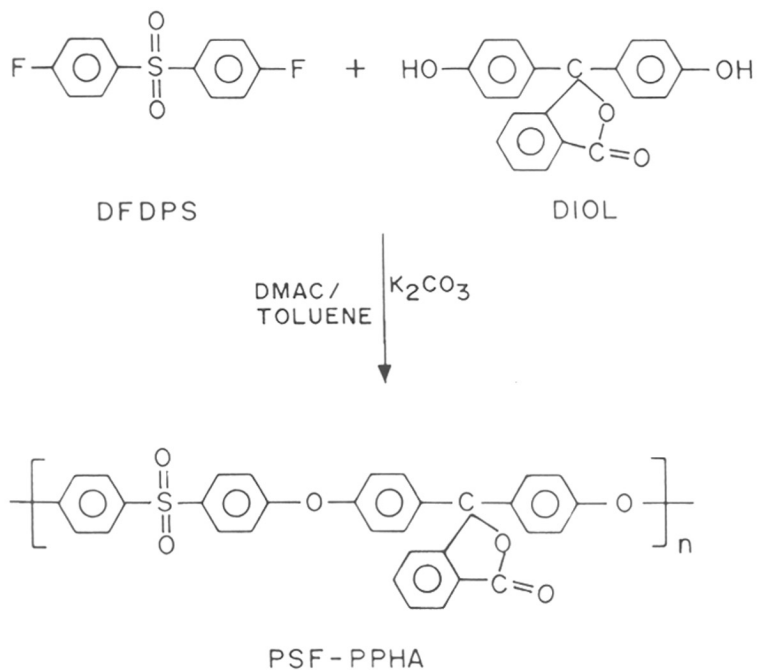
FIG. 3·5: PREPARATION OF PHENOLPHTHALEIN BASED
POLYSULFONE (PSF-PPHA)

to high molecular weight in a very short time. However, the synthesis is accompanied by the hydrolysis of the polymer and insolubility of the bisphenate.

A five necked 250 ml round bottom flask was equipped with a stirrer, nitrogen inlet sparge tube, thermometer, Dean-Stark trap and water condenser with moisture trap. A silicone oil bath with a magnetic stirring bar was used for heating and stirring the contents. Initially the reaction assembly was purged with dry nitrogen. 75 ml of N,N'-dimethylacetamide (freshly purified) was then added along with accurately weighed phenolphthalein (15.9 g, 0.05 mole), DFDPS (12.7125 g, 0.05 mole) and 6.9105 g (0.05 mole) of uniformly powdered, anhydrous potassium carbonate (K_2CO_3). These were added under a constant nitrogen purge and with good stirring. The aluminum weighing pans and powder funnel were rinsed with 37.5 ml dry toluene. The reaction mixture was stirred vigorously and heated to reflux ($140^{o}C$). The temperature was maintained at $130^{o}C-140^{o}C$ for 2 hrs or long enough until water was completely distilled over into the Dean-Stark trap. Toluene was removed continuously from the trap to increase the bath temperature to $150^{o}C$ after almost all the water had already been removed. The reaction mixture which appeared lightly colored was maintained at this temperature for nearly 10-12 hrs. At this stage the reaction was assumed to be complete. The reaction mixture was cooled to about $100^{o}C$ and 38 ml of chlorobenzene was added to dilute the solution and precipitate the inorganic salts. The mixture was filtered through a medium pore size sintered glass funnel. The filtrate was neutralized with acetic acid. The clear neutralized solution was precipitated in water/methanol

58

(1:1 by volume) mixture. The precipitate was filtered and washed with methanolic water and finally with water. It was then boiled in water for 1 hr. to remove any trapped salts, filtered and dried in a vacuum oven at 100°C.

[Yield : 26.42 g (99.28 %)]

Molecular formula of repeat unit : $C_{32}H_{20}O_6S$

Molecular weight of repeat unit : 532.5 g/mole

Elemental analysis :

Calcd for $C_{32}H_{20}O_6S$: C, 72.17 % ; H, 3.78 % ; S, 5.98 %.

Found : C, 72.22 % ; H, 3.69 % ; S, 5.98 %.

Glass transition temperature : 290°C (by DMA) (Nurmukhametov et

al 1976)

291°C (by DMA) (Found)

260.5° (by DSC) (Found).

DMA and DSC spectra are given in Fig. 3.6 and 3.7 respectively. The solution-cast PSF-PPHA sample does not show clear transition (Fig. 3.6a), while on reheating it shows a transition (Fig. 3.6b) which matches with the T_g value reported in the literature (Nurmukhametov et al 1976). Details are discussed in the section 4.2.1.

3.4.0 Casting of films

2.5 % (w/v) solutions of polymers in their respective solvents were prepared. These were filtered through sintered disks and were cast on flat surface petrie dishes floating on mercury at room temperature. After initial evaporation of solvent, the films were peeled off and dried for two days in a vacuum oven at 50°C. The final thickness of the film was about 50
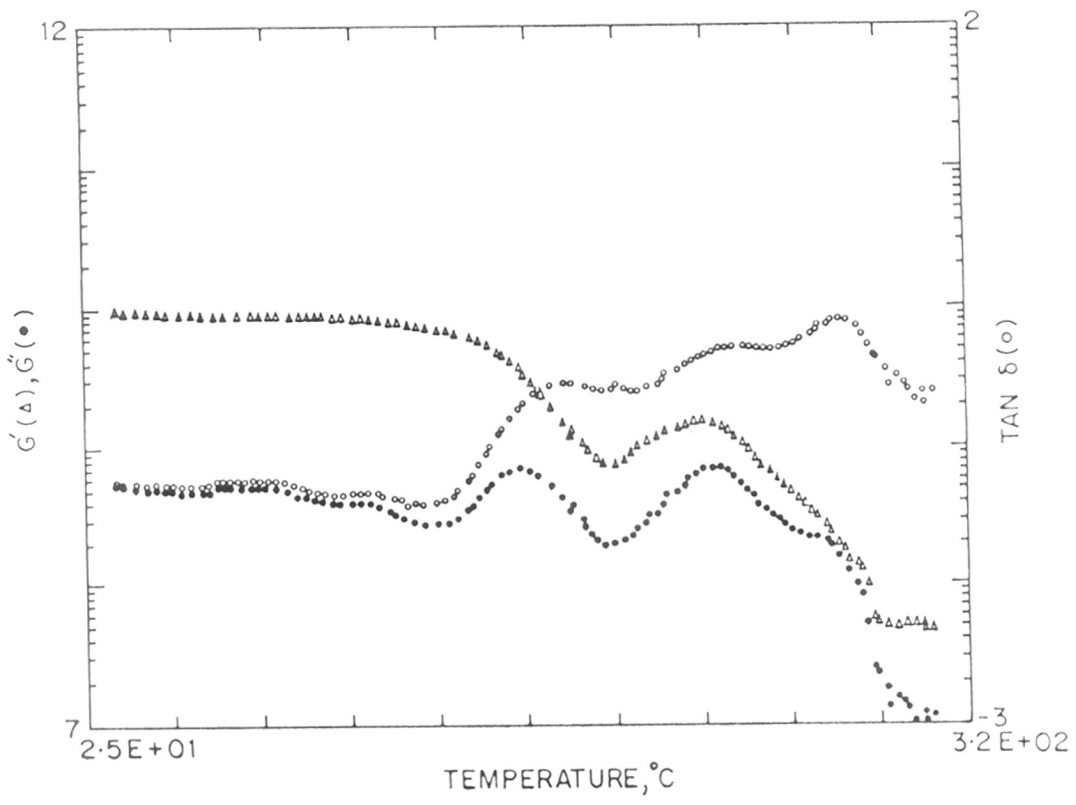
FIG. 3·6a : DMA SPECTRA FOR PSF — PPHA (SOLUTION-CAST)
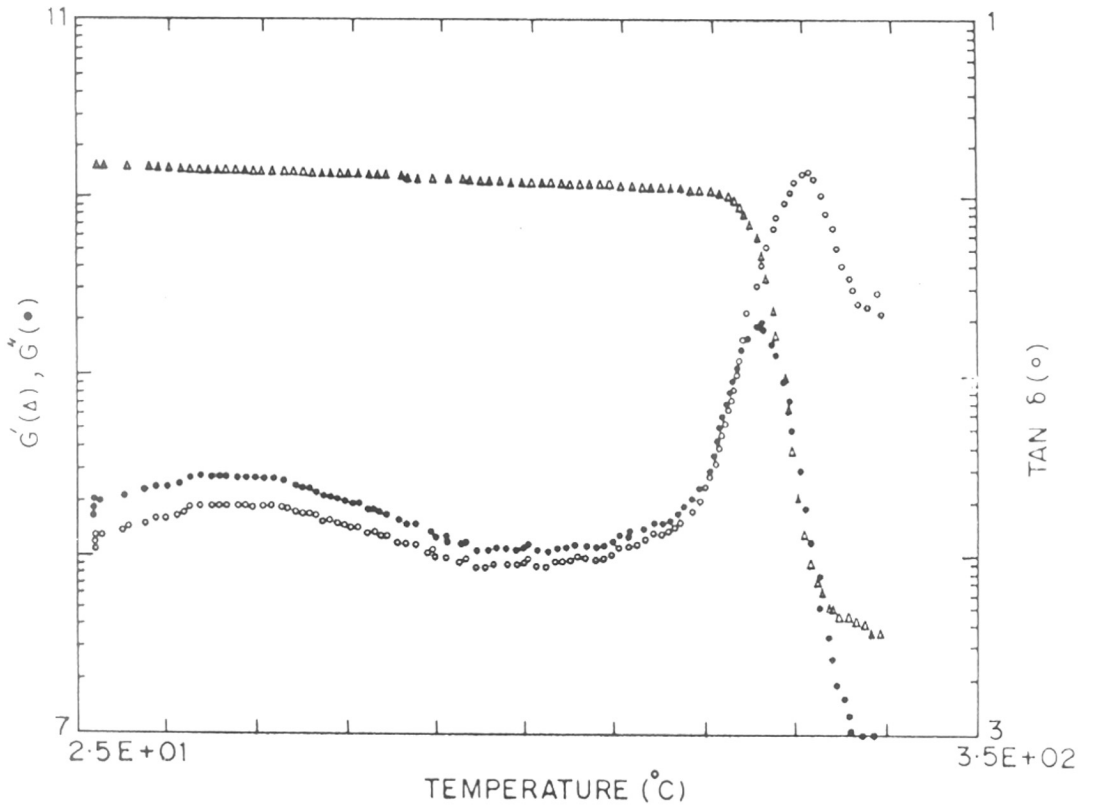
FIG. 3·6b: DMA SPECTRA FOR PSF-PPHA (ANNEALED)

FIG.3·7:DSC SPECTRUM OF SOLUTION - CAST PSF-PPHA

The chart contains the following annotations:

- Y-axis (left): ← ENDO, MCAL / SEC with markings at 2·00, 1·50, 1·00, 0·50, 0
- X-axis: TEMPERATURE (°C) with markings at 50, 110, 170, 230, 290

PSF (PPHA) FH
WT : 10·64 mg
SCAN RATE : 20·0 deg/min

T/G FROM : 256·02
        TO : 268·14
ONSET   : 256·68
CAL/GOEG : 3·98647E-02
MIDPOINT : 260·46
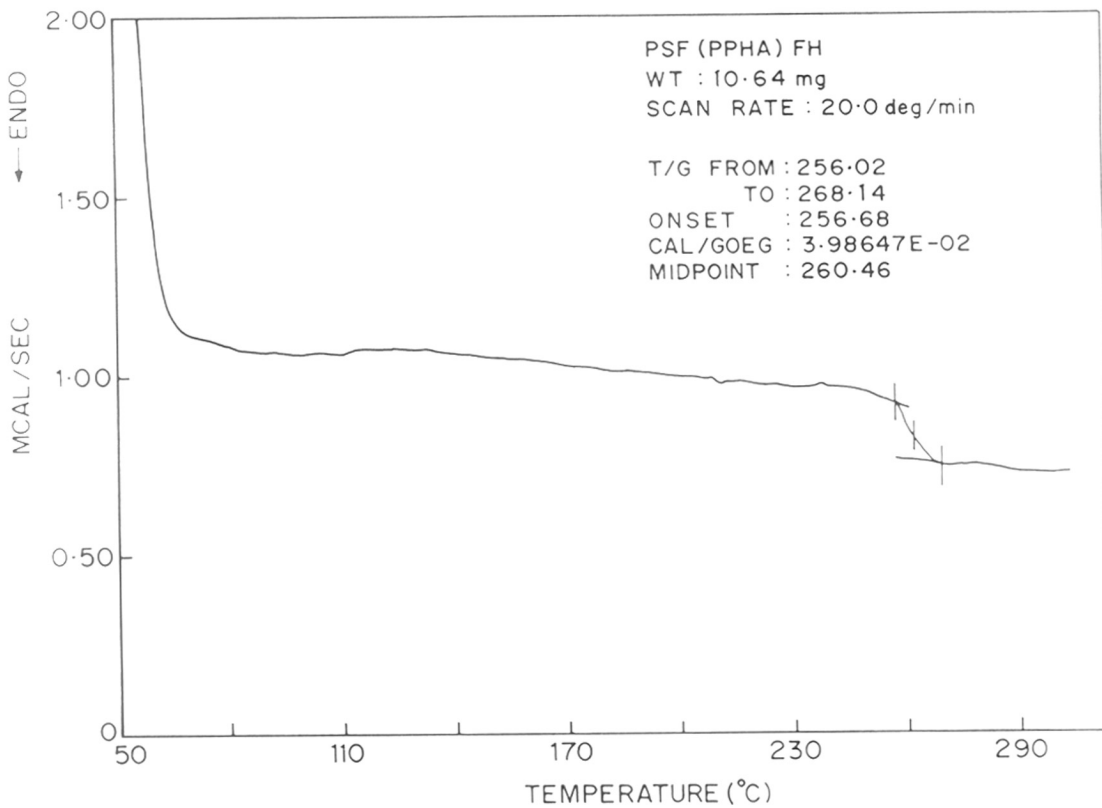
um (2 mil). Films of higher thickness (1.5 - 2 mm) were also cast by the same procedure using 10 % (w/v) solution, and were dried for 15 days in vacuum oven for 8 days at 50°C before use.

3.5.0 Polymer characterization

All the polymers were purified twice by reprecipitating the polymer solutions into suitable nonsolvents. The solvents used for purification are summarized in Appendix III-2.   The physical properties of the polymers synthesized in our laboratory are listed in Table 3.2.

3.5.1 Viscosity measurements

The solution viscosities of the polymer in chloroform were determined using an Ubbelohde viscometer in a constant temperature bath maintained at 30° C +/- 0.1^{O}C. The calculated inherent viscosity values are listed in Table 3.2.

3.5.2 Thermal behavior

The effect of structural modification i.e substitution of phthalide ring on bridge carbon atom of diol unit in the polysulfone back-bone (PSF-PPHA) or replacement of the ether linkage in the main chain by ester linkage (PAES) on thermal stability of polysulfone was studied by thermooxidative degradation. To evaluate this effect, themogravimetric analysis (TGA), differential thermal analysis (DTA), and derivative thermogravimetry (DTG) were performed simultaneously by heating the polymer at a constant rate of 10°C/min in air. Polymer samples were dried at 100°C for 48 hrs under vacuum before subjecting them to analysis. The initial decomposition

TABLE 3.2

Properties of polysulfones synthesized

Polymer Property	PSF-PPHA	PAES
η_{inh} (dl/g)[a]	0.63	0.43
T_g (°C)[b]	268	239
d_{sp} (Å)[c]	5.03	5.33
ρ (g/cc)[d]	1.3395	1.2687
IDT (°C)[e]	422	357

a. Measured in chloroform, at 30°C

b. Determined by DSC

c. Determined by wide angle X-ray diffraction spectra, using Bragg's equation $n\lambda = 2d\sin\theta$

d. Determined by flotation method, at 25°C.

e. Determined by TGA

temperature (IDT), is the point where the trace begins to display evidence of weight change and was calculated from the original TGA curve. The IDT values for the polymers synthesized in our laboratory are given in Table 3.2.

3.5.3 DSC Measurements

Solution-cast films approximately 50 μm thick were dried in a vacuum oven at 50°C for 8 days. The analysis was carried out on a Perkin Elmer DSC II coupled to a data station. The scanning was carried in the temperature range room temperature to 10°C above the glass transition temperature at heating rate 20°C/min.

3.5.4 DMA measurements

Normally, solution-cast specimens, approx. 1.5 mm thick, were dried in a vacuum oven at 50°C for 15 days before analysis. Samples employed in the conditioning experiments were equilibrated at 20 atm. CO_2 pressure in a high pressure stainless steel vessel at room temperature for two days. The DMA measurements were made on Rheometrics Dynamic Mechanical Spectrometer (RDS-II, Model 7700) at a frequency of 100 Hz in the temperature range -150°C to 325°C at a heating rate of 10°C/min.

3.5.5 WAXD measurements

The WAXD (Wide Angle X-ray Diffraction Spectrometer) measurements were carried out on an X-ray diffraction unit (Phillips PW 1730) with a CuK α beam at a scanning speed of 2000 counts per second. The peak maximum was identified by curve fitting as well as by the digital read-out of the intensity values. Both methods gave identical values. The average values

reported in Table 4.12 are based on 3 replicate measurements. The standard deviation of an individual d_{sp} measured was estimated to be 0.05 A, based on 9 replicate measurements carried with virgin and polycarbonate sample exposed to CO_2. Based on this standard deviation, the 95% confidence interval bounds on the mean of 3 replicate measurements are calculated to be +/- 0.06 Å. 50 μm thick samples were used for most WAXD analysis. Higher thickness films (2 mm) were also examined in the case of PMMA ; however, the WAXD results were unchanged.

3.5.6 Density measurements

A Dilatometer, described by Tyagi and Deshpande (1989), was used for density measurements. Polymer samples of 1.5 mm thickness were used. Densities were determined within the accuracy of +/- 0.1 %.

The floatation method was used for determining the density values within the accuracy of +/- 0.01 %. $FeCl_3$ solutions of varying concentrations were used. All the measurements were made at 25° C +/- 0.1°C. The sample thickness used was 50 um (approx.).

3.6.0 Sorption measurements

3.6.1 Sorption techniques

Sorption measurements in polymers can be carried out by two methods.

a) Pressure decay method : In this method a known amount of gas enclosed in a fixed volume, is exposed to sample. The amount of gas sorbed in the polymer sample is calculated by

66

monitoring the decrease in pressure in the gas phase (Michaels et al 1963)[a].

b) Gravimetric method : In this method a quartz spring balance is used for the study of sorption and desorption of gases at low pressures (McBain and Baker 1926). The technique has been modified recently by Kamiya et al (1986)[a], to study the solubility of various gases in poly (vinyl benzoate) in the pressure range of 0 - 50 atm.

For the present study, a pressure decay method was employed. The design of the sorption cell used in this work is similar to that reported previously in the literature (Vieth and Sladek 1965, Stern and DeMeringo 1978, Koros et al 1976).

3.6.2 Sorption equipment

A schematic of the sorption apparatus used in this work is shown in Fig. 3.8. The cells and reservoirs were fabricated from 316 stainless steel. The detailed dimensions of the reservoirs A and B are shown in Fig. 3.9a and 3.9b respectively. The sample cells A and B containing polymer samples were connected to the gas reservoir R through valves 3 and 2 respectively. The gas reservoir R was connected, in turn, through valve 1, to either a vacuum line capable of maintaining vacuum of the order of 10^{-6} Torr or to the gas cylinder via valve 4 and 5 respectively. Stainless steel 316 tubing of dia 3 mm (1/8th inch) (OD) was used for all the connections. Both the sample cells as well as gas reservoir were mounted on a brass stand and were immersed in a water bath controlled to +/- 0.1°C, by means of a fully automatic solid state electronic control with a PT-100 sensor.

67
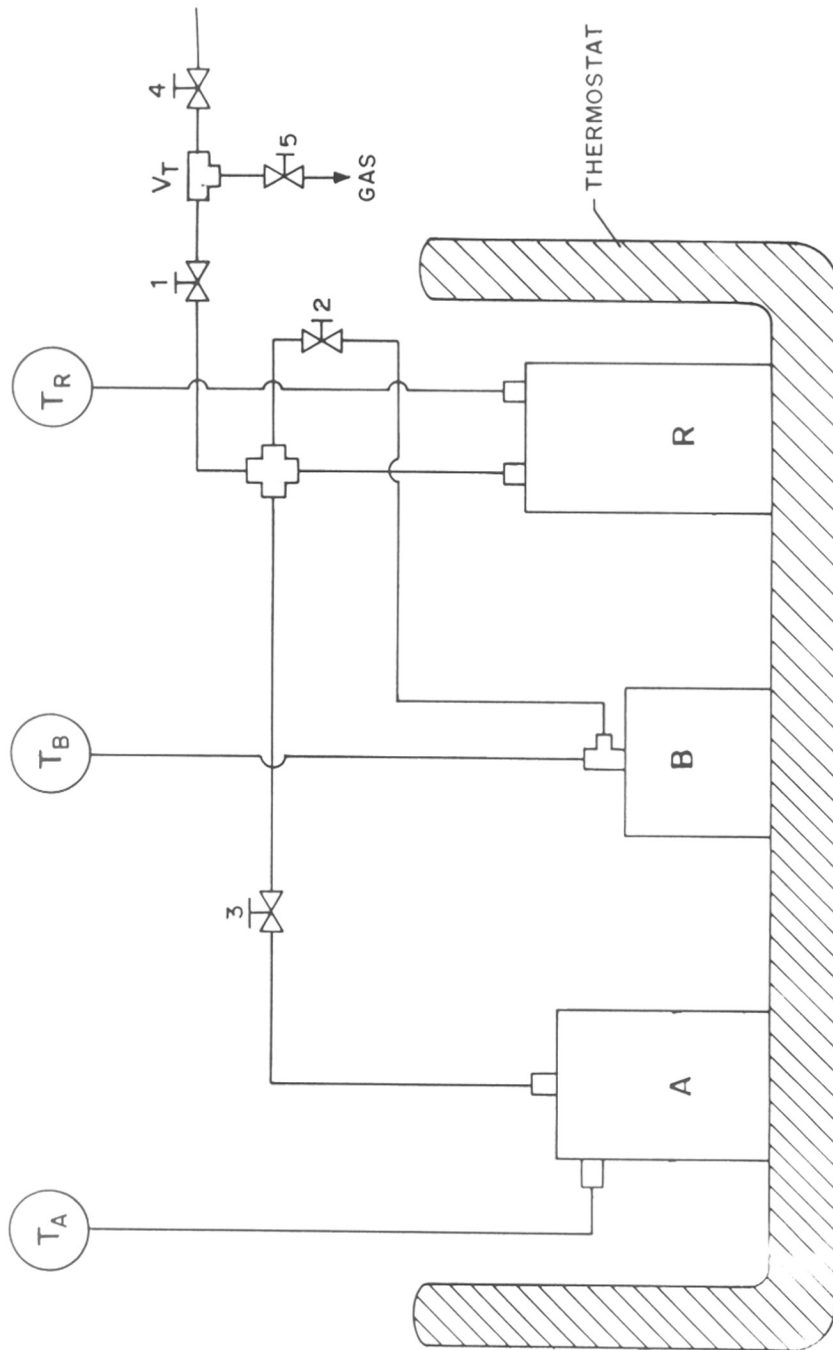
FIG. 3·8 : SORPTION EQUIPMENT : SCHEMATIC
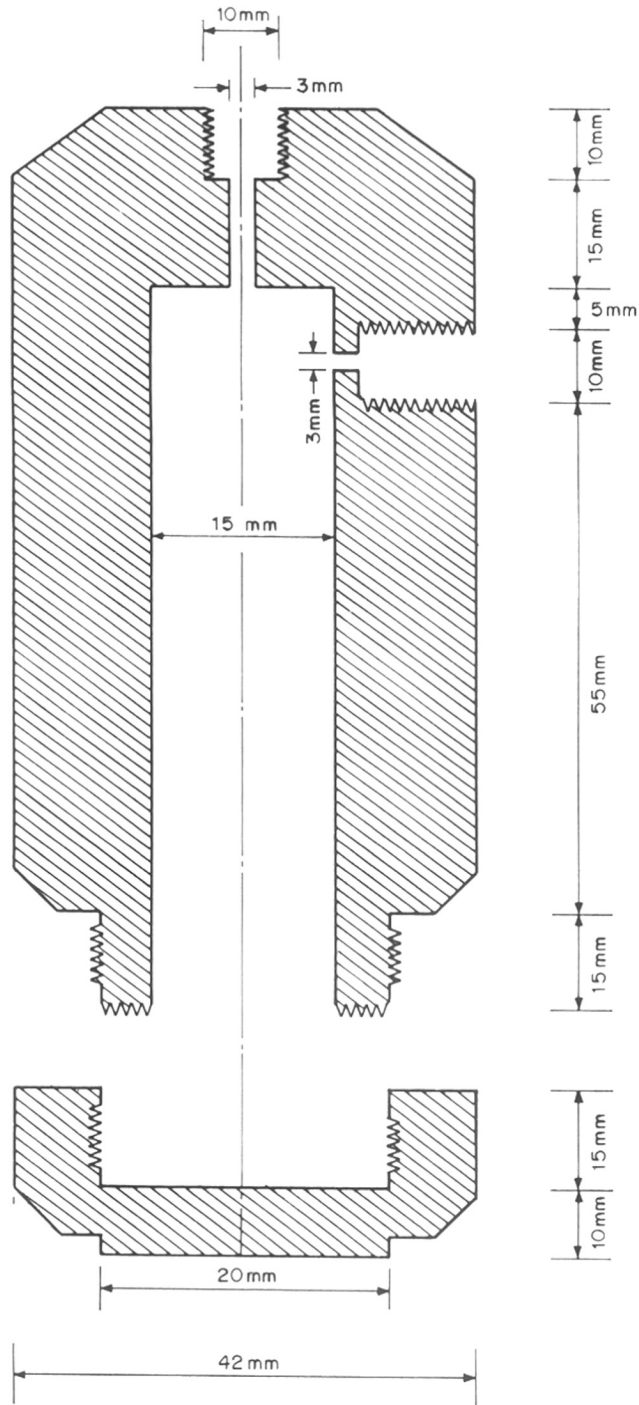
FIG. 3·9a : CROSS-SECTION OF SORPTION RESERVOIR -A

69
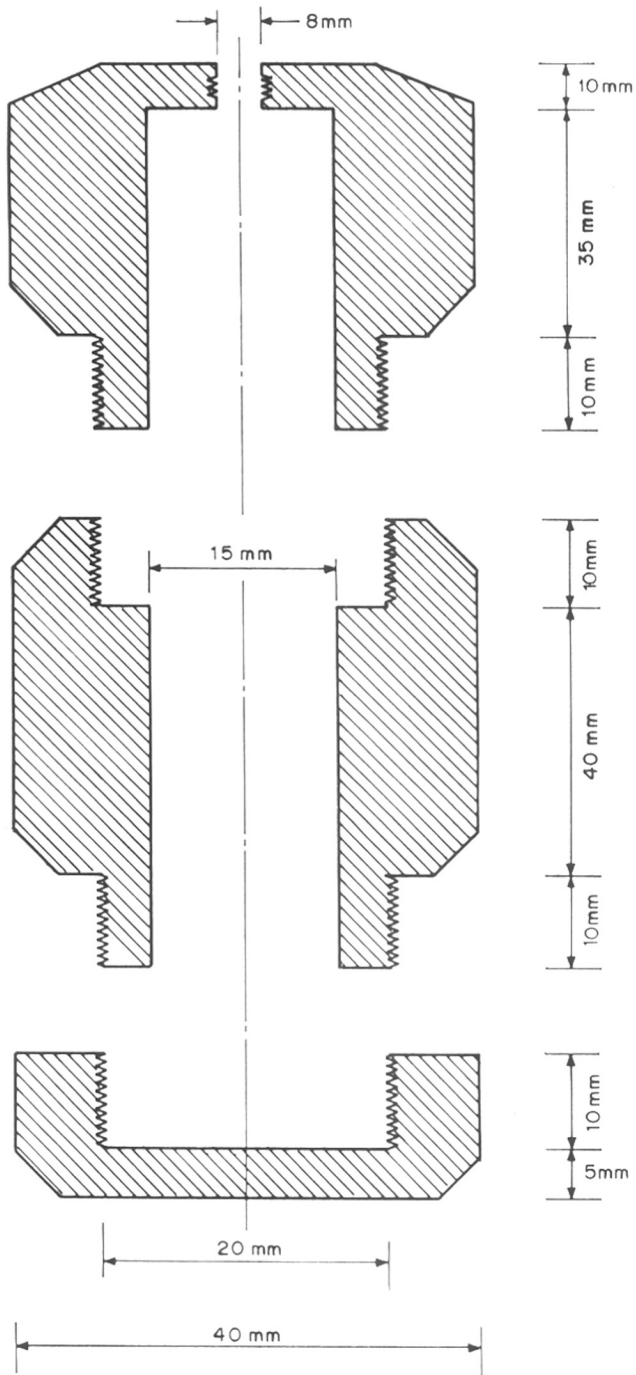
FIG. 3·9b: CROSS-SECTION OF SORPTION RESERVOIR-B

The sorption apparatus set up is shown in Fig. 3.10. This can be used to determine solubility of gas in two polymer samples simultaneously.

The pressure inside the sample chambers A, B and R was monitored by indicators connected to an absolute pressure transducer. The electronics were powered by an automatic voltage regulator. The indicators as well as the transducers were housed in a cabinet fabricated from acrylic sheet and provided with a fan for air circulation as to eliminate temperature shifts in the electronic component (see Fig. 3.11).

The specifications, materials of construction and the sources of the various components used are summarized in Appendix III-4.

3.6.3 Calibration of sorption cells and reservoir

Before undertaking the actual calibration, the transducers T_A, T_B and T_R were calibrated over the entire range using Heise pressure gauge as a reference by setting a series of arbitrary pressures in the reservoirs A, B and R. This calibration procedure ensured that all the transducers would read the same value at a given pressure.

The volumes of the empty sample cells A and B, as well as gas reservoir R were calibrated by the expansion of the gas at various pressures in the pressure range 100-300 psia using ultrapure Helium (99.995% pure) and a standard reservoir (S). The volume of the reservoir S was determined by filling with water at 35°C. The following procedure was followed.

1. The entire system was evacuated through valve 4 keeping all
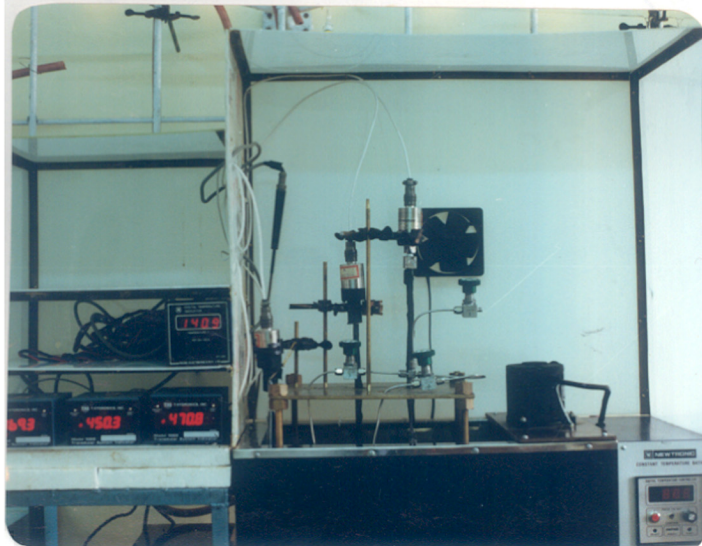
FIG. 3·10 : PHOTOGRAPH OF SORPTION EQUIPMENT
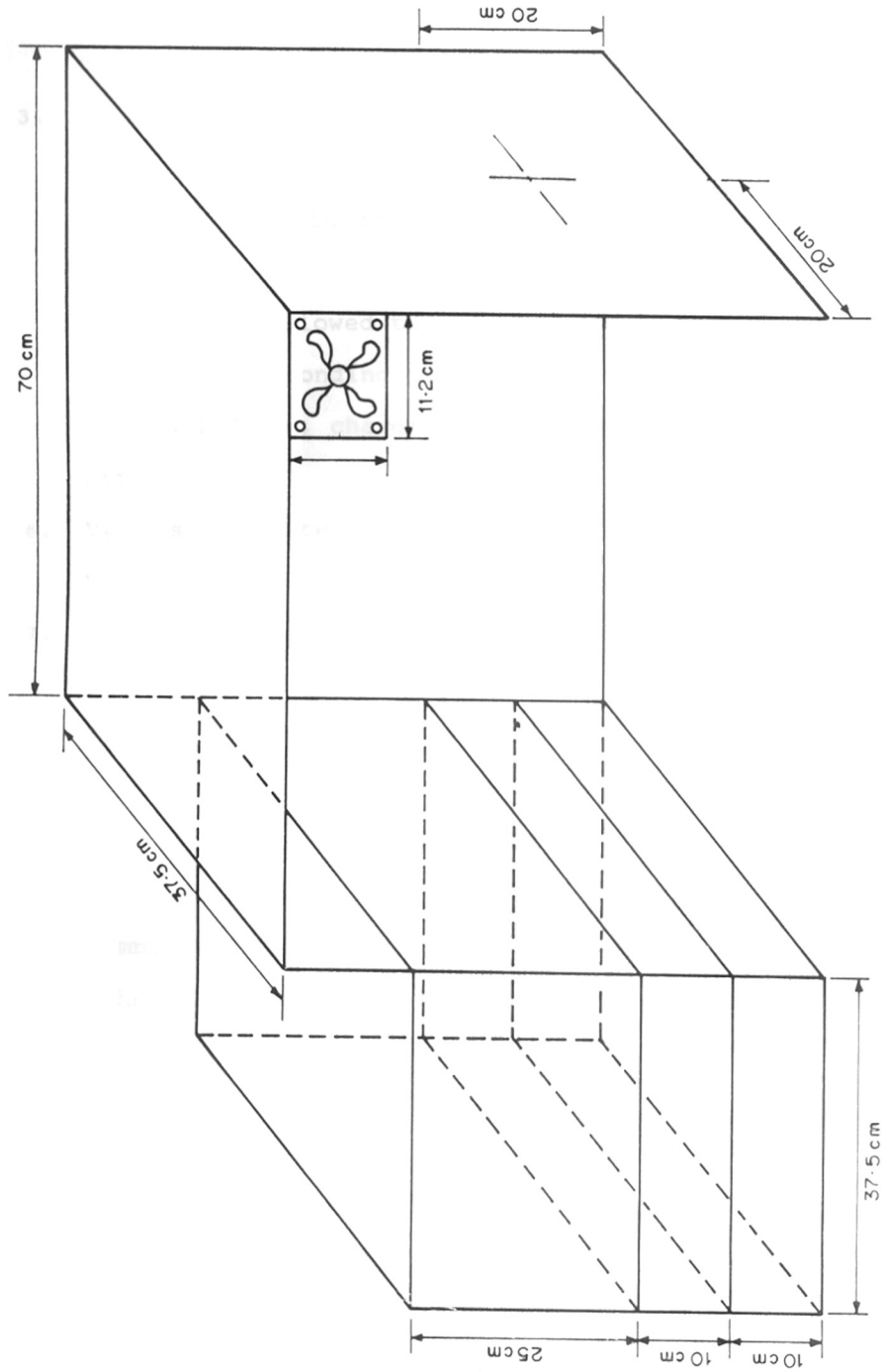
FIG. 3·11 : AIR - THERMOSTAT : SCHEMATIC

20 cm

20 cm

70 cm

11·2 cm

37·5 cm

37·5 cm

25 cm

10 cm

10 cm

valves except valve 5 open.

2. Valves were closed in the order 3,2,1 and 4. The system was connected through valve 5 to the He cylinder.

3. Reservoir V_R was charged to some initial pressure (200-500 psia) by opening valves 1 and 5. Valve 1 was then closed. The pressure (p_1) in the reservoir R was noted from transducer T_R.

4 The gas was allowed to expand from V_R to V_A through the valve 3. The corresponding pressure p_2 was read.

5. The cell B was charged by opening valve 2. Pressure p_3 was noted.

6. V_T was evacuated through valve 4 keeping valve 1 closed. Valve 4 was closed after about five minutes.

7. Valve 1 was opened to expand gas into V_T. The pressure p_4 was read.

8. Finally, the standard reservoir V_S was opened to the system through valve 5. The pressure was read as p_5.

The steps 1-8 were repeated 7 times and the respective volumes were calculated from averaging all the data. The results are summarized in Appendix III.5

The calculation of volumes of the various reservoirs was done using the following expressions,

$$X = V_S \cdot p_5 / (p_4 - p_5)$$
$$Y = X \cdot p_4 / p_3$$
$$Z = Y \cdot p_3 / p_2$$
$$V_R = Z \cdot p_2 / p_1$$
$$V_A = Z - V_R$$

74

$$V_B = Y - Z$$

$$V_T = X - Z$$

Polymer samples in flat sheet form having a volume of about 1.5 - 2.0 cc were used for the sorption studies. The sample preparation is discussed in section 3.4.0. The density of the polymer was measured by dilatometry accurate to +/- 0.01 g/cc and refined by the flotation method to 0.001 g/cc. These density values were used for determining the sample volume. The actual volume of the gas in the sample cell was obtained by subtracting this volume from V_A and V_B.

An accurately weighed (+/- 0.1 mg) polymer sample was filled into the sample cells A and B. The cell top was screwed down until the scribe marks on the top and cell body coincided. The machine threaded cap was retightened to the same scribe mark on each reassembly. This ensured that the volume of the sample chamber returns to the calibrated value. This was checked by recalibrating the volume after each reassembly.

3.6.4 Sorption procedure

Before the actual sorption run, the polymer sample was evacuated through valve 4 by keeping valves 1, 2, and 3 open (see Fig. 3.8) for at least 48 hours at 10^{-2} Torr. The bath temperature was maintained at $50^{\circ}C$ during desorption.

A sorption run was carried in the following manner. At this point all the valves were in closed position,

1. All gas supply lines were purged 2-3 times with the gas to be sorbed by feeding gas through valve 5 and evacuating through

valve 4.

2. Valve 1 was opened and reservoir R was charged with the penetrant gas of interest to some initial pressure. After about 2 hours (to ensure temperature equilibrium) the pressure p_1 in the reservoir R was read from the transducer T_R.

3. To start the sorption run for the sample in cell A, valve 3 was opened; the pressure p_2 was noted from transducer T_A after 30 seconds. Pressure p_2 was not used for calculations.

4. Valve 3 was kept open for 2 hrs, then closed and the pressure in transducer T_A was noted as p_3.

5. Steps 3 and 4 were repeated for performing sorption study in cell B ; the pressures for the respective steps 3 and 4 were p_4 and p_5.

6. The outputs from transducers A and B were recorded as a function of time and the time t was noted when no change in pressure was observed over 12 hrs. At this point the run was considered to be complete. The final pressure readings from transducers T_A and T_B were recorded as p_6 and p_7 respectively.

7. Steps 2-6 were repeated to obtain more sorption data at different pressures by varying the initial pressure p_1.

Care was taken to ensure that no more than two successive measurements were performed with sequential increase or decrease in pressure to avoid possible compaction or relaxation of the polymer. Otherwise, all measurements were made at randomly chosen pressures. All the measurements were carried out at $35^{\circ}C$.

The total concentration, C, of gas dissolved in the polymer,

at a given equilibrium pressure and temperature was calculated using the equation,

$$C = 22414 \ \Delta n_T \ / \ V_p$$

where, C is in cc (STP)/cc (polym), V_p is the volume of the polymer sample in cc and Δn_T denote change in the moles of gas at the beginning and at the end of the experiment. Following equations were used for calculations,

$$n_i = V_R \cdot (p_1) \cdot RT/1000$$

$$n_x = (V_R + V_A) \cdot (p_3) \cdot RT/1000$$

$$n_y = n_x \cdot V_A/(V_R + V_A)$$

$$n_f = V_A \cdot (p_6)/1000$$

$$\Delta n_T = (n_i - n_x) + (n_y - n_f)$$

Values p_3, p_5 and p_7 were used in the above equations instead p_1, p_3 and p_6 respectively for the calculation of sorption of gas for the sample loaded in the cell B

The solubility coefficient 'S' was calculated from,

$$S = C \ / \ p_E$$

where p_E, is the pressure of the gas at equilibrium (p_6 or p_7).

3.6.5 Estimation of dual-sorption parameters

The dual-sorption model parameters were estimated first by linearising the dual-sorption model and then refined by a non linear least square estimation procedure. For this purpose the

77

optimization procedure known as Box's complex method was used (see Appendix III-6).

3.7.0 Permeability measurements

3.7.1 Experimental techniques

Amongst the various methods employed for measuring gas permeabilities, three have received particular attention; these are 1) the variable volume method (Brubaker and Kammermeyer 1953, Stern et al 1963), 2) variable pressure method (Heilman et al 1956, Brown and Sauber 1959, Koros et al 1976, O'Brien et al 1986) and 3) variable concentration method (Landrock and Proctor 1952).

In the present investigations, the permeability measurements were based on the variable-volume method. High pressure gas at constant pressure (p_h) was allowed to contact one side of the polymer film and the gas permeated was allowed to expand on the low pressure side p_l ($p_l < p_h$) against atmospheric pressure. The change in the volume of the permeate was then measured as a function of time by following the displacement of the mercury column in the precision-bore borosilicate glass capillary using a cathetometer.

3.7.2 Diffusion cell

The diffusion cell, shown in Fig. 3.12 consists essentially of three parts viz a) top cell b) bottom cell and c) locking ring. Machined depressions in top and bottom cell halves form a cylindrical cavity when the cells are superposed. The cells were made of SS 316 and the locking ring was made of brass. The
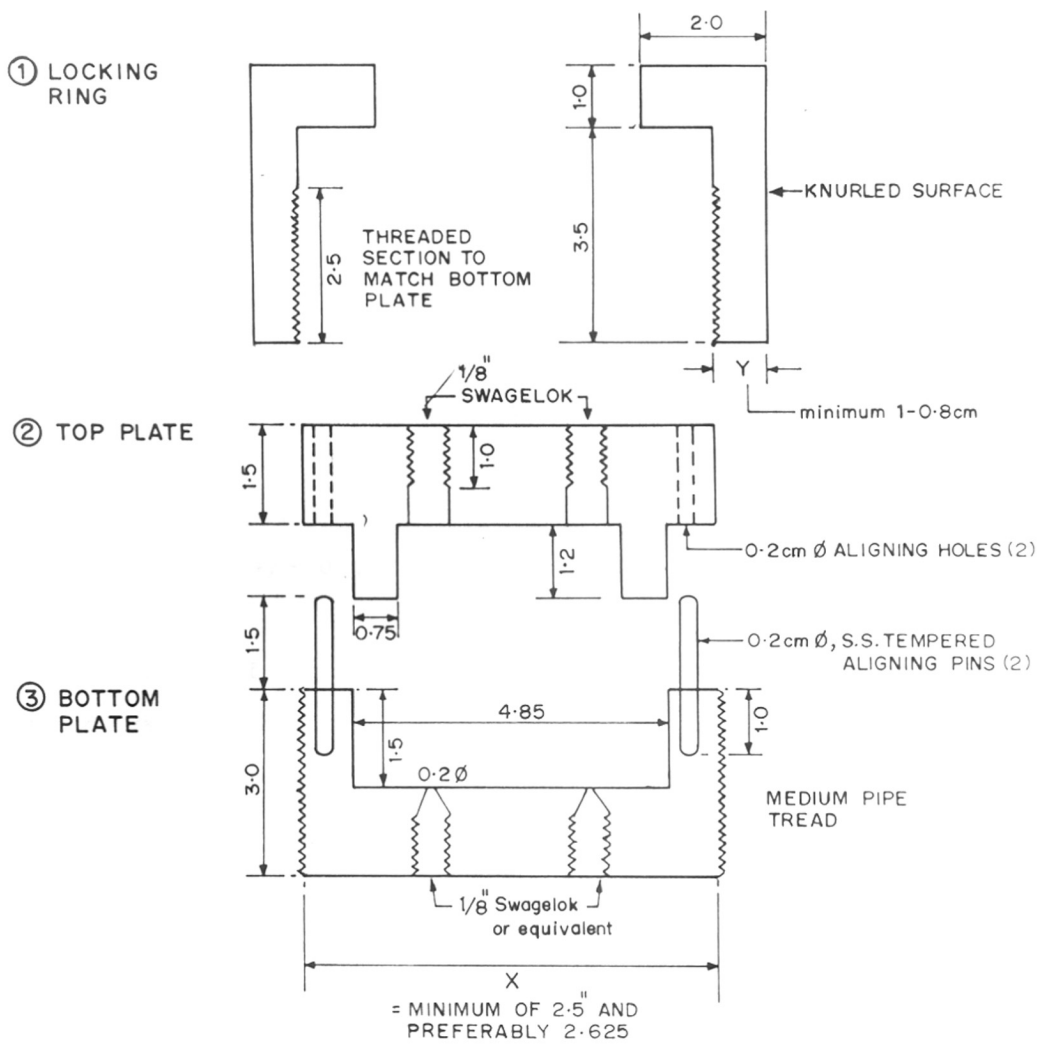
FIG. 3·12: DIFFUSION CELL : SCHEMATIC

detailed dimensions of each part are given in Fig. 3.12. The bottom cell plate was fitted with a stainless steel porous plate (5 micron) to provide a good membrane support without obstructing gas flow to the permeate side. The polymer film to be tested was clamped between two cells by tightening the locking ring. Use of a neoprene O-ring between the top cell and membrane ensured a pressure tight fit. Whatman filter paper was inserted between the porous plate and membrane as an extra support so as to avoid the deformation of the later around the porous plate.

3.7.3 Permeability apparatus

The permeability cell set-up is shown in the photograph in Fig. 3.13. The diffusion cell was housed in a modified GC oven with a working temperature up to 250°C. The cell temperature was controlled within +/- 0.1^{o}C by means of a temperature control module.

A schematic of the permeability cell set up for pure as well as mixed gas permeation studies is shown in Fig. 3.14. All connections were made using SS 316 tubing with 3 mm (1/8th inch) OD. The specifications, materials of construction and the sources of the various component used are summarized in Appendix III-4.

The upstream gas driving pressure was measured with a Heise gauge. A mercury thermometer was used to monitor the temperature of the diffusion cell bath. A calibrated borosilicate glass capillary containing a mercury slug was used to measure the flow rate of gas permeating through the membrane.

As shown in Fig. 3.14, the upstream end of the cell was connected through valve 1 to the outlet of the cylinder
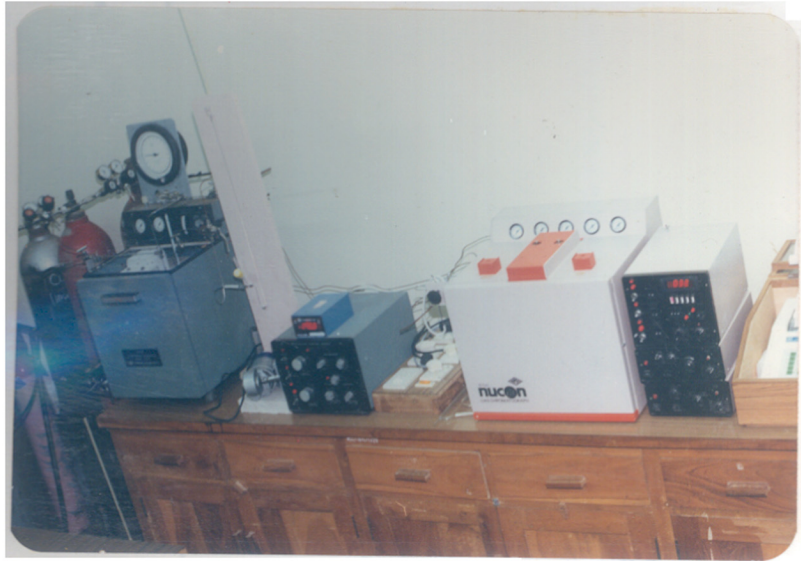
FIG. 3·13 : PHOTOGRAPH OF TRANSPORT EQUIPMENT
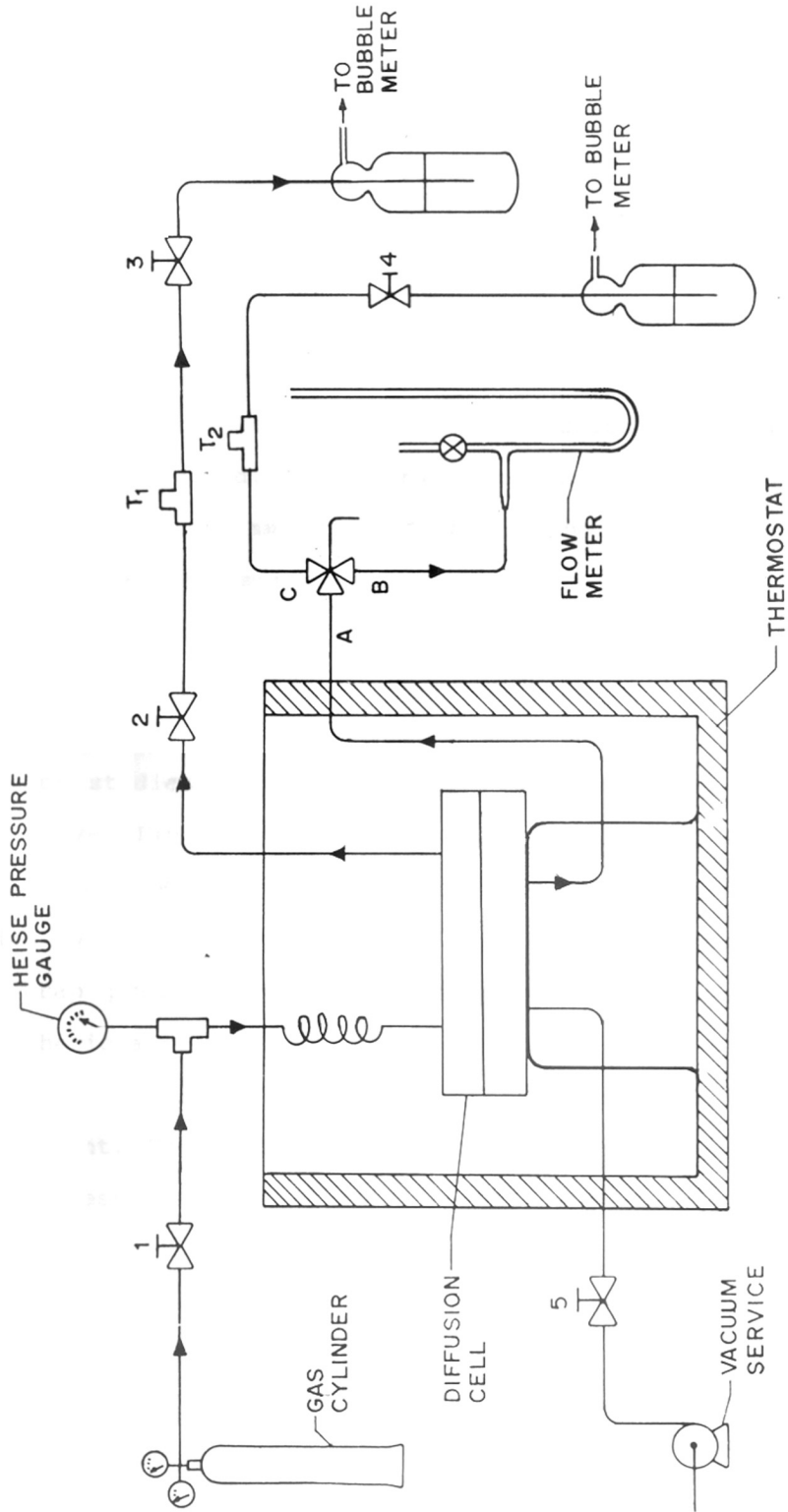
FIG.3·14: PERMEATION APPARATUS FOR PURE AS WELL AS MIXED GAS STUDY : SCHEMATIC

regulator. In the case of mixed gas system valves 2 and 3 were used to maintain constant gas composition on feed side by bleeding out the non permeated gas. The outlet of the bleed was connected to a bubble meter. Depending on the flow rate of fast gas permeating through the membrane, the feed/bleed rate was adjusted using valves 1,2 and 3. A silicone septum was installed for sampling the gas which was analyzed on a GC.

On the permeate side of the diffusion cell, a 3-way ball valve was connected. A calibrated borosilicate glass capillary (I.D. 1 mm, 1.58 mm or 2.16 mm depending on the gas flux) containing a small mercury slug (2-5 mm in length) was connected to end B (see Fig. 3.14). The displacement of the mercury slug was monitored by a vertical Cathetometer with a least count of 5 x 10^{-3} mm.

For studies on mixed gas systems, end C of the three way ball valve (Fig. 3.14) was connected to one end of the T-union (T_2). The other two openings of the union Tee, B and C were sealed by a silicone septum and an oil trap respectively. The oil trap prevents the contamination of permeated gas with atmospheric air.

The polymer film was exposed to vacuum before each measurement. Vacuum line was connected through valve 5. During this process, valves 1-3 and a three way ball valve connected to the other end of the permeate side (see Fig. 3.14) were kept closed. The degassing pressure was 10^{-2} Torr and the oven temperature was raised to 50°C during desorption. Generally degassing time was approximately five times the estimated maximum

time lag.

A Nucon 5700 gas chromatograph (GC) was used for gas analysis. A TCD was used in the present study. The detector signal lines were integrated and recorded using an integrator (Schimadzu, C-R3A model). Helium was used as the carrier gas to sweep samples from the sample loop to the GC. A gas tight micro syringe (Hamilton make, capacity 1 μl) was used for sampling the gas mixtures. The sample volume injected was 0.2 Ul.

The gas chromatograph was calibrated using standard gas mixtures of CO_2 : CH_4.

3.7.4 Permeability measurements : Pure gas system

Before the actual measurement it was confirmed that there was no leakage on either side of the diffusion cell using no membrane in the cell. The cell and membrane were then evacuated for a sufficient time through valve 5 keeping all other valves closed. The following sequence was adopted for each run.

1. Valve 5 was kept closed all the time during the permeation run. The teflon stop cock fitted on the flow meter X (see Fig. 3.14) was open to the atmosphere. This prevents expulsion of mercury slug from the flow meter in the case of membrane rupture or leakage to the permeate side.

2. Valves 1,2 and 3 were open. The upstream side of the membrane and supply lines were purged 2-3 times with the test gas, to eliminate trace impurities.

3. Valves 2 and 3 were closed and the desired pressure p_h was applied on the high pressure side of the membrane with the help of cylinder regulator and valve 1. This pressure was

noted from the Heise gauge as p_h.

4. The position of the 3-way ball valve was kept open to end B. The teflon stop-cock (X) was then closed slowly.

5. The position of mercury slug in the capillary was noted at time t equal to zero, using the vertical Cathetometer. The mercury column was displaced as a result of an increase in volume caused by the permeating gas flowing out of diffusion cell.

6. The slug position on Cathetometer was read after a finite time t.

7. 3-4 readings were taken in order to check that steady state had been attained. Steps 6 and 7 were repeated, if necessary, till a constant flow rate was attained.

A knowledge of the rate of displacement of mercury slug at pressure p_1 (1 atmosphere in this study), and the capillary cross section yield the flow rate of gas N [cc(STP)/sec].

The permeability coefficient P was calculated using the equation,

$$P = [(J \cdot \delta) / (p_h - p_1)]$$

where, J = N / A, A is the effective membrane area, in cm^2, δ denotes thickness of the membrane, in cm, p_h and p_1 are the pressures in cmHg on the feed and permeate side of the membrane respectively.

The permeability measurements were made at randomly selected pressures and at a constant temperature (35°C). Sequential increases or decreases in pressure were avoided except when the conditioning effect was studied in which case the pressure p_h

was increased in regular intervals (see section 3.7.6). The reproducibility of each experiment was confirmed thrice.

3.7.5 Permeability measurements : Mixed gas system

For this purpose, the first steps 1-8 were the same as described in section 3.7.4. However, the following additional operations were also involved :

1) The gas mixture on feed side was continuously flushed out through valves 2 and 3. The feed rate was adjusted using valves 1,2 and 3 simultaneously. The feed rate was kept at sufficiently high value to ensure that the maximum stage cut (ratio of permeate : feed flow rate) was less than 0.001.

2) The samples from feed side were analyzed at 10-15 min intervals to ensure that the feed composition remained constant throughout the experiment. For this purpose valve 3 was closed momentarily and a sample was withdrawn for GC analysis.

3) In order to check the composition of the permeated gas, the 3-way ball valve position was turned towards end C. For some time, the permeated gas was flushed through valve 4. This time period varied from 30 minutes to 3 hours, depending on the flow rate of the permeating gas. Valve 4 was then closed. A gas sample for the GC analysis was withdrawn using a gas tight micro syringe through the septum fixed at T_2 (see Fig. 3.14)

Step 3 was repeated at least 3 times to ensure that the permeate mixture composition was constant.

The following expression was used for calculating the

86

permeabilities of each gas in the binary mixture,

$$P_1 = \{(J_T \cdot y_1 \cdot \delta) / [A \cdot p_h (x_1 - (p_1/p_h) \cdot y_1)]\}$$

where, P_1 is permeability coefficient of gas '1', in $cc(STP).cm/cm^2 sec.cmHg$; J_T, denotes the permeate flux in $cc(STP)/sec$; A, denotes the effective area of the membrane, in cm^2; δ is the thickness of the membrane, in cm; p_h and p_1, denote the pressures, in cmHg, on the feed and permeate side of the membrane respectively $[p_h > p_1]$; x_1 and y_1, denote the mole fractions of gas '1' on the feed side and permeate side.

The validity of the mixed gas permeation measurements was verified using solution-cast Lexan polycarbonate films at $35^{\circ}C$ for $CO_2:CH_4$ separation. The results are summarized in Appendix III-7.

3.7.6 Conditioning and hysteresis study

The conditioning protocol consisted of maintaining the upstream face on the membrane at the conditioning pressure for the desired time period to allow the sample to creep slowly to a new stable steady-state value. At the end of this time, no significant drift in the permeability was observed, and subsequent depressurization from the conditioning pressure led to hysteresis effects.

CHAPTER - IV

RESULTS AND DISCUSSION

4.0.0 Results and discussion

4.1.0 Material selection considerations

The polymers used hitherto as membrane materials have exhibited a trade-off between permeability and permselectivity. Development of new membrane materials which would exhibit higher permeability and higher selectivity would significantly improve the economics of membrane separation processes. This would open up newer markets. Recent studies indicate structural modifications in polymers which would bring about simultaneous enhancements in permeability and selectivity (McHattie et al 1991, Stern et al 1989, Muruganandam et al 1987).

Bisphenol-A based polysulfone (Udel) (PSF) is a high performance, high-temperature resistant thermoplastic and is widely used as a membrane material. In this work, a series of structurally modified polysulfones, tailored as to lead to enhanced permeability and permselectivity for the gas pair CO_2/CH_4, have been investigated. The structures of the repeat unit of the polysulfones are presented in Fig. 4.1 which are reflected in the physical as well as the transport characteristics.

The first part of this chapter (section 4.1.1) deals with a series of polysulfones PAES in which the ether linkage in the PSF backbone is replaced by an ester linkage. Three other polymers (PA1-PA3) investigated, contain both ester and ether linkages. All these polymers were synthesized by condensation of bisphenol-A with various diacid chlorides containing sulfone linkages. The effect of change in diacid chloride linkage from

88
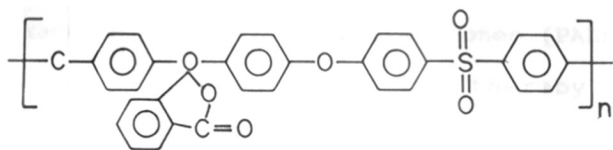
PSF-PPHA
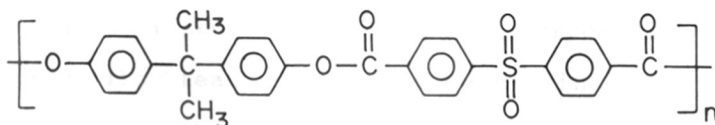
PAES
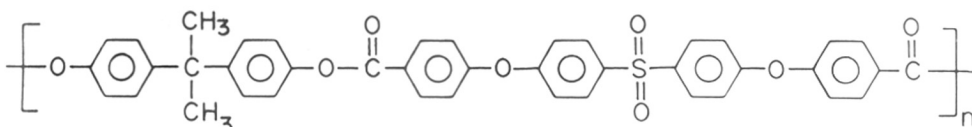
PA 1 (SPCL + BPA)
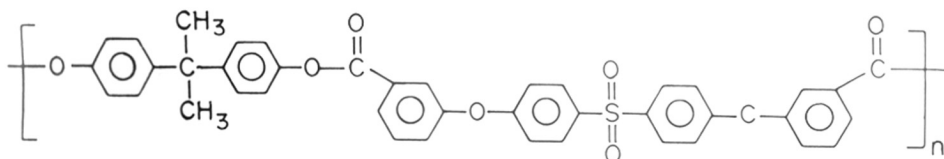
PA 2 (SMCL + BPA)
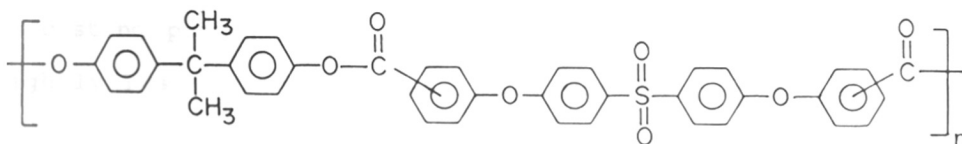
PA 3 (SPCL / SMCL + BPA)

FIG.4·1:POLYSULFONES IDENTIFIED (REPEAT UNIT STR)

para (PA1) to meta (PA2), has also been investigated (section 4.1.2). It was expected that the presence of the more polar ester linkage in the modified polysulfones (PAES and PA1) would enhance the solubility of CO_2, and thereby its permeability and permselectivity (Koros 1985).

The substitution of the isopropylidene unit in the bisphenol moiety in PSF by the phtlalide ring (PSF-PPHA) is discussed in section 4.1.3. The incorporation of the phthalide ring would lead to an increase in the polarity of the polysulfone. Similar results in the case of aromatic polyesters have been reported (Sheu et al 1988). Thus, the bulky phthalide ring connected to the bridge carbon via two bonds renders the backbone more rigid and hinders the effective packing of the polymer segments. Thus, the polymer PSF-PPHA is expected to be more permeable than PSF.

It is well known that the sorption and transport characteristics of the polymers are affected by the processing history. For example, permeability coefficient of the solution-cast PSF film for CO_2 or CH_4 is about 20-24 % higher than that of the melt-extruded material (Chiou et al 1987). The permselectivity for the system CO_2/CH_4 decreases from 23.8 for the melt-extruded specimen to 21.5 for the solution-cast film. The casting procedure yields films that are more permeable and slightly less selective than the corresponding melt-extruded films. This has been attributed to the annealing of the melt-extruded specimen (Chiou et al 1987).

In the present investigation, the films used for the

permeability studies were cast from chloroform. The samples were kept in a vacuum oven at $50^{\circ}C$ for eight days before initiating sorption and transport measurements. Measurements were made at $35^{\circ}C$ on virgin films as well as on films exposed to high pressure CO_2. The results are compared with those for the PSF films having the same history.

4.1.1 Effect of ester and ether linkages on physical and transport properties of polysulfones

The effect of substitution of ether linkage from PSF backbone by an ester and/or ether linkage on the various properties of PSF has been summarized in Table 4.1.

Physical properties of polymers

The physico-chemical properties of polymers govern the solubility and diffusivity of various gases. The solubility, S, is influenced by factors such as the inherent condensibility of the penetrant, polymer-penetrant interaction, and the frozen void volume in the glassy polymer (Koros 1977). The diffusivity, D, depends on the mobility of the penetrant in the membrane. This parameter is controlled by factors such as packing density and mobility of the polymer segments and also the relative size and geometry of the penetrant molecule.

The physical characteristics of polymers investigated are listed in Table 4.2. The values of T_g, V_f, density, d_{sp}, reflect the rigidity and openness of polymer. The solubility parameter 'δ', indicates the possible affinity between the penetrant and the polymer.

The average intersegmental spacing serves as a good measure

91

TABLE 4.1

Summary of results[*]

Polymer Properties	PSF	PAES	PA1	PA2	PA3
Group	Ether	Ester	Ether/ Ester	Ether/ Ester	Ether/ Ester
Linkage	Para	Para	Para	Meta	Para/Meta
T_g (^{O}C)	189	Higher	Same	Lowest	Lower
d_{sp} (Å)	4.95	Higher	Same	Lowest	Lower
(cal/cc)$^{0.5}$	10.55	Higher	Higher	Higher	Higher
Solubility[a] (S)					
CO_2	--	Higher	Higher	Higher	higher
N_2	--	Lower	Lower	Lowest	Lower
Ar	--	Lower	Lower	--	--
CH_4	--	Same	Same	Lowest	Lower
Diffusivity[a]	--	Same	Same/ Lower	Lowest	Lower

[*] Numerical values in subsequent tables

a. At 10 atm and 35°C

TABLE 4.2

Physical properties of polysulfones

Properties Polymer	T_g $(^oC)^a$	ρ $(g/cc)^b$	d_{sp} $(\overset{o}{A})^c$	V_f $(cc/cc)^d$	Solubility parameter $(cal/cc)^{0.5}$
PSF (Udel)	189	1.2482	4.95	0.3466	10.55
PAES	237	1.2703	5.33	0.3511	10.74
PA1	187	1.2799	4.98	0.3466	10.91
PA2	168.4	1.3009	4.76	0.3355	11.18
PA3	181	1.2892	4.92	0.3415	11.10

a. Determined by DSC

b. Determined by floatation method, at 25^oC.

c. Determined by wide angle X-ray diffraction spectra, using Bragg's equation $n\lambda = 2d\sin\theta$

d. Calculated using Van der Waals volume by a group-contribution method (Bondi 1964)

e. Calculated according to group-contribution method (Van Krevelen and Hoftyzer 1976).

of the openness of the polymer (Kim 1988, Stern et al 1989, Hellums et al 1989). The correlations based on average intersegmental spacing lead to more consistent results than the correlations based on the density or free volume. The parameter d_{sp} can be satisfactorily correlated with the diffusion coefficient (Charati et al 1991).

Substitution of the ether linkage in PSF with an ester linkage as in PAES leads to enhancement in both the rigidity and openness of the polymer matrix as can be seen from the value of T_g and d_{sp} respectively (Table 4.2). However, PA1 which contains both ether and ester linkages has almost the same values of T_g and d_{sp} as that for PSF. Thus it appears that the incorporation of the ether linkage (PA1) nullifies the enhancement in T_g and intersegmental chain spacing brought about by the incorporation of the ester linkage (PAES). Replacement of the para linkage (PA1) in the diacid chloride of the repeat unit by meta substituted diacid chloride (PA2) leads to a decrease in the T_g as well as d_{sp}. The values for the polymer containing both para/meta linkages lie within the two limits. Similar results have been reported for aromatic polyesters (Sheu and Chern 1989), polysulfone (Aitken et al 1990) and polyimides (Coleman and Koros 1990, Stern et al 1989).

The values of solubility parameter (δ) calculated for the six new polysulfones discussed herein are higher than that for PSF. This is attributed primarily to the addition of the polar ester group in the backbone.

Sorption and permeation

Pure gas permeabilities for the six gases measured, are summarized in Table 4.3. Polymers PAES and PA1 are more permeable to CO_2. This is the result of increased solubility coefficient inspite of decrease in diffusivity (see Table 4.3). A small change is observed in the case of CH_4. The permeabilities of less condensible gases viz. Ar, O_2 and N_2 are very low. Aitken et al (1990) have reported similar results for a series of polysulfones synthesized from ring substituted diol and 4,4'-dichloro diphenylsulfone.

The plots of ratio of permeability values for PAES and PA1 over PSF versus critical temperature of gas are shown in Figs. 4.2 and 4.3 respectively, indicate a reasonably good correlation. The results can be explained on the basis of the sorption data as follows.

Solubility values for CO_2, CH_4, Ar and N_2 at 35°C and 10 atm pressure for the polymers studied in this study are given in Table 4.3. For reasons of safety, the sorption study for oxygen was not carried out. The solubilities of these gases in PAES and PA1 decrease in the order CO_2 > CH_4 > Ar > N_2. Similar trends have been reported for PSF (Erb and Paul 1981), PES (Sanders 1988), polycarbonate (Wonders and Paul 1979) and polyesters (Sheu and Chern 1989).

Substitution of the ether linkage in PSF by an ester linkage (PAES) and ester/ether (PA1) leads to enhancement of the solubility of CO_2 in both polymers, while the solubility of methane remained unaltered. However, the solubility value, for Ar

TABLE 4.3

Contributions of solubility and diffusivity to permeability of for various gases in solution cast polysulfones at 10 atm and 35°C

Polymer	PSF			PAES			PA1			PA2			PA3		
Property	P	S	D	P	S	D	P	S	D	P	S	D	P	S	D
He	12.54	--	--	13.22	--	--	12.39	--	--	6.13	--	--	10.51	--	--
Ar	0.59	0.32	1.84	0.35	0.173	2.02	0.335	0.148	2.26	0.126	--	--	0.20	--	--
O_2	1.29	--	--	0.59	--	--	0.487	--	--	0.30	--	--	0.40	--	--
N_2	0.239	0.20	1.195	0.242	0.105	2.30	0.0845	0.08	1.05	0.0476	0.047	1.012	0.067	0.067	1.00
CH_4	0.243	0.55	0.44	0.236	0.56	0.42	0.217	0.52	0.41	0.050	0.37	0.135	0.073	0.414	0.176
CO_2	5.98	2.1	2.84	7.50	2.93	2.56	6.33	2.65	2.39	1.68	1.99	0.84	2.20	2.17	1.01
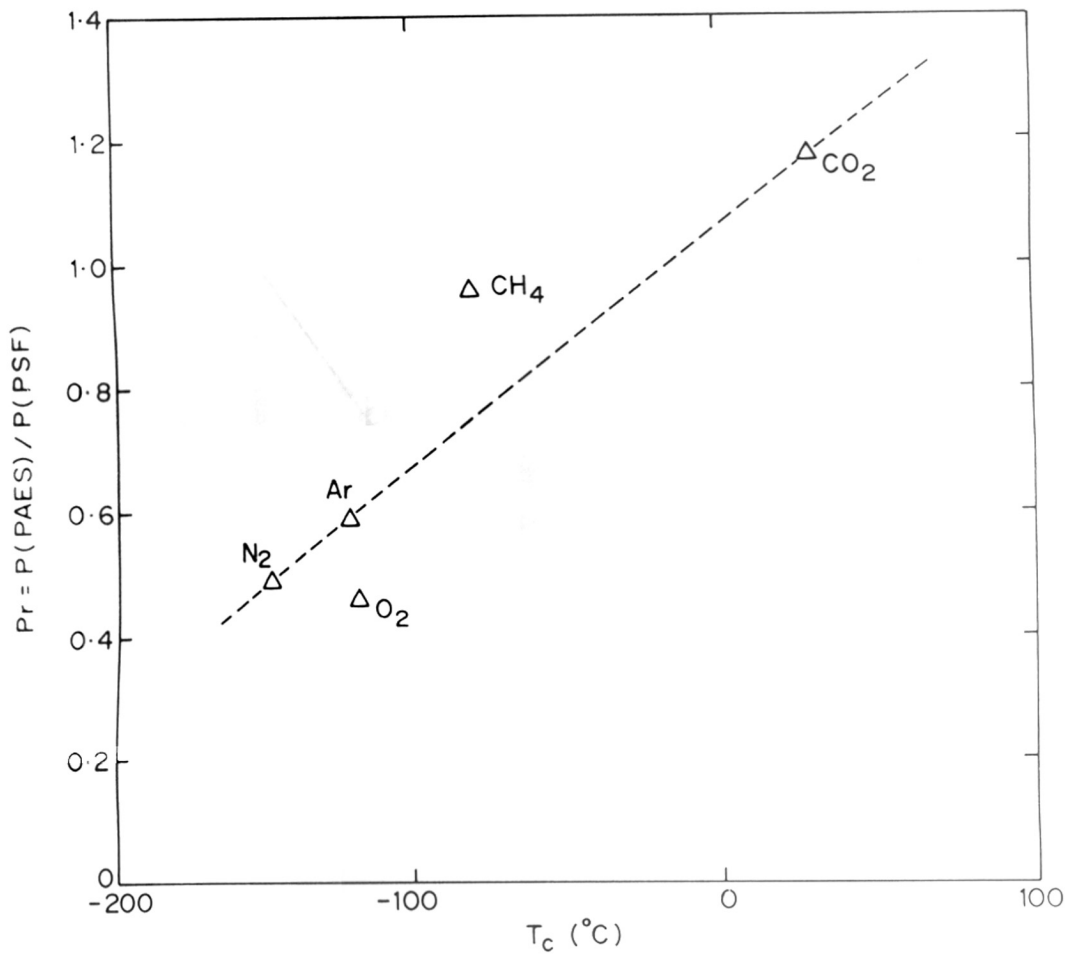
FIG.4·2 :PERMEABILITY IN SOLUTION-CAST PAES AT 35°C
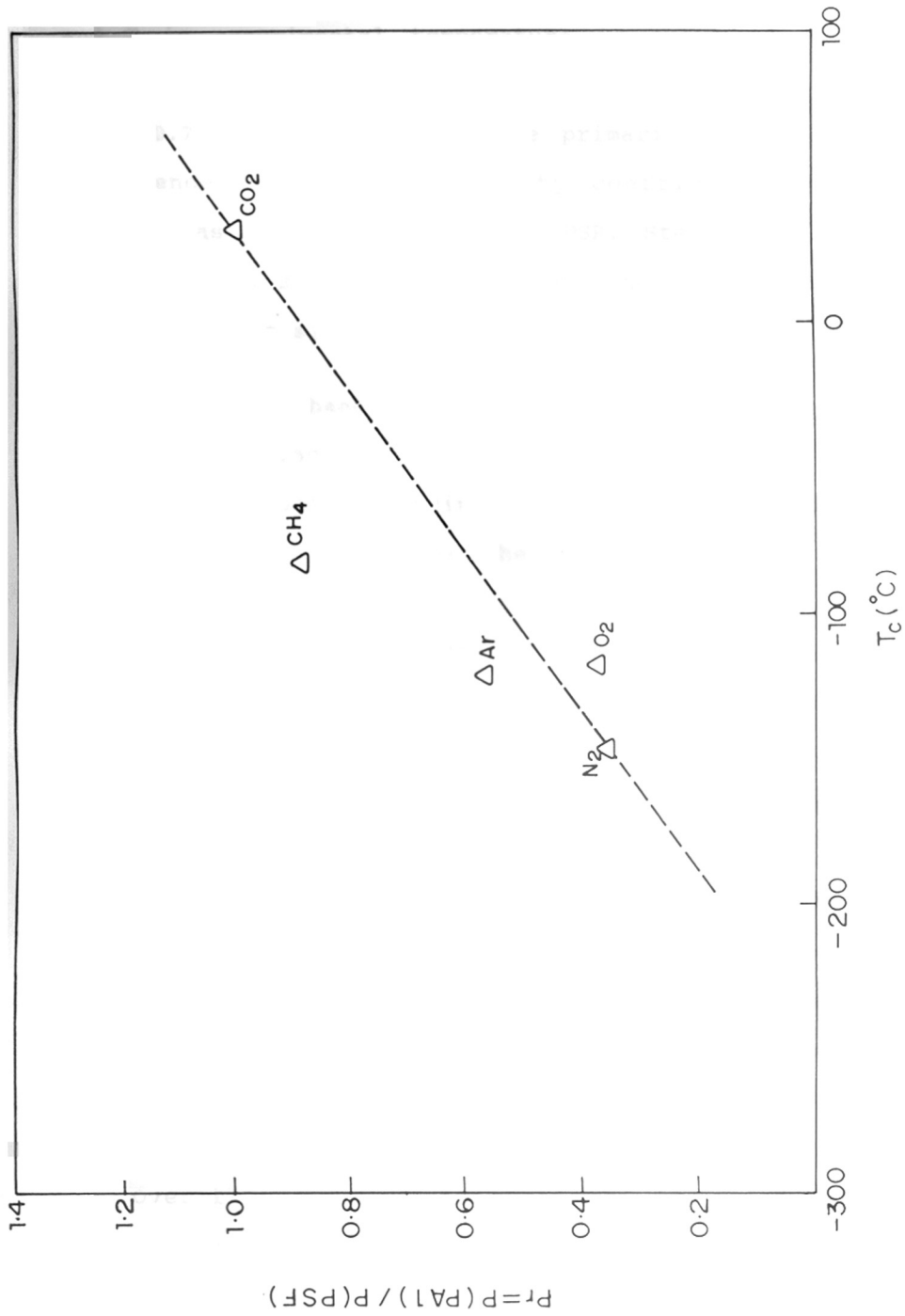
FIG.4·3: PERMEABILITY IN SOLUTION-CAST PA1 AT 35°C

and N_2 decreases. A plot of log S versus reduced temperature (T/T_c), where, T_c denotes the critical temperature of the gas, and T is experimental temperature is shown in Fig. 4.4. The differences in values of slopes for PAES (-1.03), PA1 (-1.08), PES (-0.72) and PSF (-0.62) are primarily responsible for the differences in the permeability coefficients of these two polymers as compared to that of PSR. Stern et al (1969) have explained the solubility of various gases in the polyethylene films using the similar plots.

Permselectivity changes

Modification of the polymer structure so as to simultaneously inhibit chain packing and the rotational mobility about flexible linkages in the polymer backbone, leads to an increased membrane permeability and permselectivity (Hoehn 1974, Chern et al 1985). The findings of the present investigation for PAES and PA1 for the gas pair CO_2/CH_4 and CO_2/N_2 show such effects.

In addition to the permeability, the permselectivity of a membrane material is another property of interest. The measured permeability coefficients and ideal separation factors for PAES, PA1 and PSF for various gas pairs are listed in Table 4.4. PAES which has the highest d_{sp} value exhibits lowest permselectivity for the system O_2/N_2. The permselectivity of these polymers for the system He/CH_4, which has greatest size difference is relatively less affected.

Overall selectivity is analyzed in terms of solubility selectivity and diffusivity selectivity for the CO_2/CH_4 and
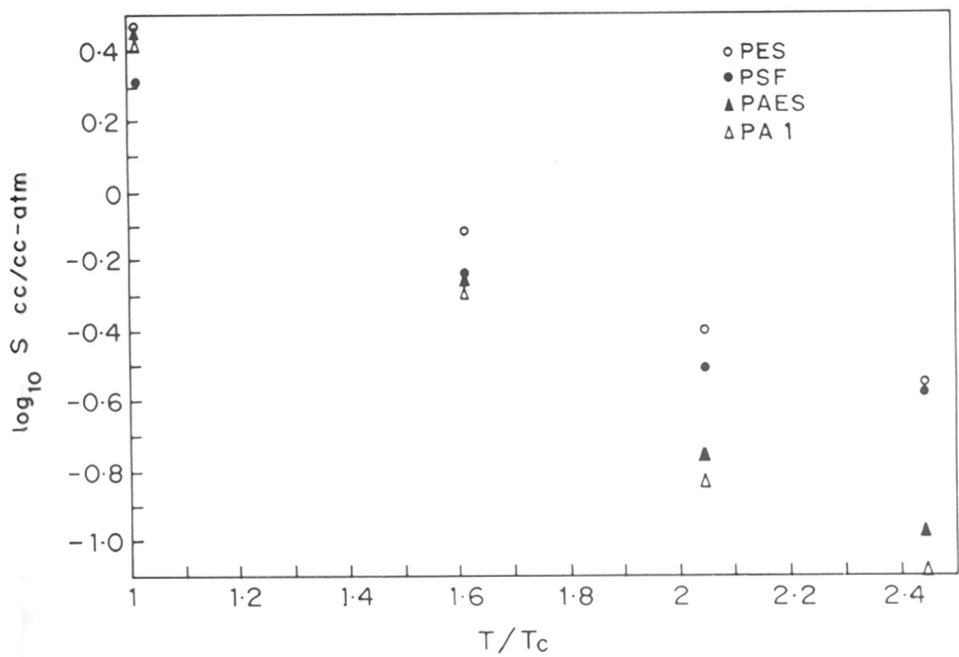
FIG.4·4 : GAS SORPTION IN SOLUTION-CAST PAES , PA1, PES AND PSF AT 35°C

TABLE 4.4

Comparison of CO_2 permeability and selectivity over CH_4 and N_2 in solution-cast PSF, PAES, PA1, PA2 and PA3 at 10 atm and $35^{\circ}C$

Polymer Property	PSF[*]	PAES	PA1	PA2	PA3
P^a_{CO2}	5.6	7.50	6.33	1.68	2.20
CO_2/CH_4	22	30.00	29.37	33.5	29.94
CO_2/N_2	--	60.10	74.95	35.33	33.19
S^b_{CO2}	2.1	2.936	2.665	1.996	2.176
S_{CO2}/S_{CH4}	3.7	5.22	5.075	5.41	5.25
S_{CO2}/S_{N2}	--	31.00	32.93	41.93	32.14
D^c_{CO2}	2.0	2.418	2.384	0.841	1.01
D_{CO2}/D_{CH4}	5.9	5.74	5.786	6.19	5.70
D_{CO2}/D_{N2}	--	1.94	2.27	0.842	1.03
O_2/N_2	5.4[#]	2.43	5.76	6.3	5.97
He/CH_4	51.6[#]	56.0	57.1	122.6	144

* Reference McHattie et al 1991.

This work

a $P - 10^{10}[cc(STP) \ cm/cm^2 \ Sec \ cmHg]$

b $S \ [cc(STP)/cc \ atm]$

c $D - 10^8 \ [cm^2/Sec]$

CO_2/N_2 systems. For both PAES and PA1, the permselectivity value for gas pairs CO_2/N_2 and CO_2/CH_4 is enhanced significantly (Table 4.4). As expected, the variation in selectivity among these polymers is primarily solubility-controlled. The presence of polar -COO- in addition to $-SO_2-$ in PSF improved the polymer-penetrant interaction for CO_2 which leads to enhancement in permeability and permselectivity.

4.1.2 Effect of isomerism

Stern et al (1989) reported the importance of polymer chain conformation in governing the solubility and diffusivity of gases. Thus polyimides comprising para disubstituted monomers are were found to be more permeable to CO_2 than those containing meta disubstituted monomers. The Polymers containing para disubstituted repeat units were also less permselective (Stern et al 1989, Coleman and Koros 1990).

In this section, the effect of type of linkage in diacid chloride on the transport properties of the polysulfone series PA1-PA3 is discussed. A comparison of the permeability coefficients and ideal separation factors for the polysulfones used for the gas pairs CO_2/CH_4, CO_2/N_2, and He/CH_4 are shown in Table 4.3 and 4.4.

The permeability of CO_2 in PA1 is more than 3.5 times of that in PA2, but the permselectivity has decreased merely by 13 %. The glass transition temperature and d_{sp} values for PA2 are lower than those for PA1. Similar results have been reported in the literature for para and meta substituted isomers in the case of polyimides (Stern et al 1989, Coleman and Koros 1990),

polysulfones (Aitkin et al 1990) and polyesters (Sheu and Chern 1989).

Since PA2 has a lower d_{sp} value than that PA1, one would expect lower permeability and higher permselectivity values for PA2. The changes in permselectivities of these materials are seen most dramatically for the system He/CH_4, in which the differences in size between the penetrants are the most significant. The measured permeability values for He and its selectivity over CH_4 for the polymers investigated are plotted as a function of d_{sp} (Fig. 4.5). As the d_{sp} is decreased from 5.33 $\overset{\circ}{A}$ (PAES) to 4.76 $\overset{\circ}{A}$ (PA2), there are marked changes in the diffusivity selectivity. Diffusivity is more dramatically affected for larger molecules such as CH_4 or N_2 than for smaller molecules such as He. This has significant effects on both permeability and permselectivity. Initially, both permeability and permselectivity increase slightly with an increase in the value of d_{sp} from 4.76 $\overset{\circ}{A}$ (PA2) to 4.92 $\overset{\circ}{A}$ (PA3). A sudden change is observed at d_{sp} = 4.95 $\overset{\circ}{A}$ (PSF, PA1) when He/CH_4 selectivity drops dramatically as the permeability of CH_4 is enhanced significantly. Subsequent increases in d_{sp} lead to relatively constant permeability and permselectivity values.

Another unusual effect is the variation in permselectivity for CO_2/N_2 in the isomer series PA1-PA3. As expected, PA2 (d_{sp} = 4.76 $\overset{\circ}{A}$) and PA3 (d_{sp} = 4.92 $\overset{\circ}{A}$) exhibit lower permeabilities for both CO_2 and N_2 (see Table 4.4). In PA1 (d_{sp} = 4.98 $\overset{\circ}{A}$), the permeability of CO_2 has increased markedly while the corresponding increase in the case of N_2 was far less significant. As a result the selectivity value for CO_2/N_2 in PA1
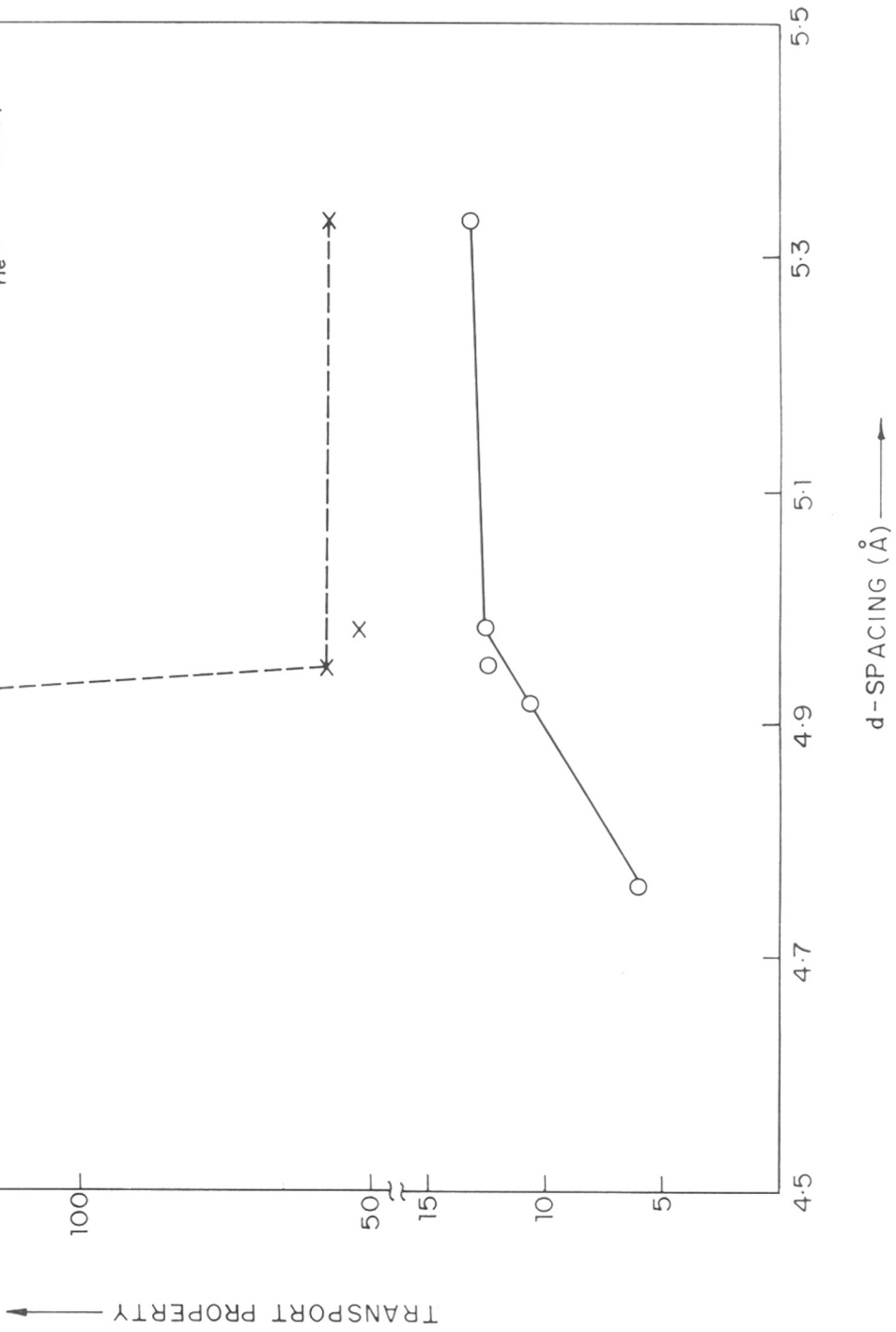
FIG. 4·5 : INTRINSIC SEPARATION FACTOR FOR He/CH₄ AND PERMEABILITY FOR He
AGAINST d_{sp}

x – α He/CH₄
O – P_{He} (BARRERS)

d–SPACING (Å) ⟶

TRANSPORT PROPERTY

104

is higher than that in PA2. These results demonstrate the effect of change in isomerism on d_{sp} (inturn diffusivity) and thereby transport characteristics for various gases with different physico-chemical properties.

4.1.3 Sorption and transport of various gases in phenolphthalein based polysulfone (PSF-PPHA)

In this section, the effect of replacing the isopropylidene unit of bisphenol-A based polysulfone (PSF) by a bulky phthalide ring containing a polar ester group is discussed. The results are compared with those for the solution-cast PSF (Udel) and PES (Victrex) samples. The polymer PSF-PPHA is more polar, has a higher T_g and a more open structure (as reflected in d_{sp}), compared to PSF and PES (see Table 4.5). It is therefore expected to exhibit higher permeability than the other two.

Sorption of gases

Sorption measurements were carried out for specimens subjected to pretreatment. Sorption data for CH_4 were collected for i) the virgin film and ii) for the specimen exposed to CO_2 at 20 atm for eight days. For CO_2, measurements were carried on the samples exposed to 20 atm CO_2 at $35^{\circ}C$ for eight days.

Results for the sorption of pure CO_2 and CH_4 in solution cast PSF-PPHA film are shown in Fig. 4.6a and 4.6b respectively. The sorption isotherms at $35^{\circ}C$ exhibit the characteristic non-linear shape characteristic of glassy polymers.

The dual-sorption parameters for PSF-PPHA are listed in Table 4.6 alongwith corresponding values for PSF and PES taken

TABLE 4.5

Physical parameters of PES, PSF and PSF-PPHA

Polymer Property	PES (VICTREX)	PSF (UDEL)	PSF-PPHA
$n\lambda(dl/g)$ [a]	0.44	0.48	0.63
T_g (^{o}C)	225	189	291[b]
d_{sp} ($\overset{o}{A}$) [c]	4.92	4.95	5.03
ρ (g/cc)	1.370	1.263	1.342
V_f (cc/cc) [d]	0.3462	0.3443	0.3440
$(cal/cc)^{0.5}$	9.64	10.55	11.74
Gr. density			
$=SO_2=$	27.6	14.5	5.2
$-CO_2-$	--	--	12.0

a. Measured in chloroform, at $30^{o}C$

b. Determined by DMA

c. Determined by wide angle X-ray diffraction spectra, using Bragg's equation $n\lambda = 2dsin\theta$

d. Calculated using Van der Waals volume by a group-contribution method (Bondi 1964)

e. Calculated according to group-contribution method (Van Krevelen and Hoptyzer (1976).
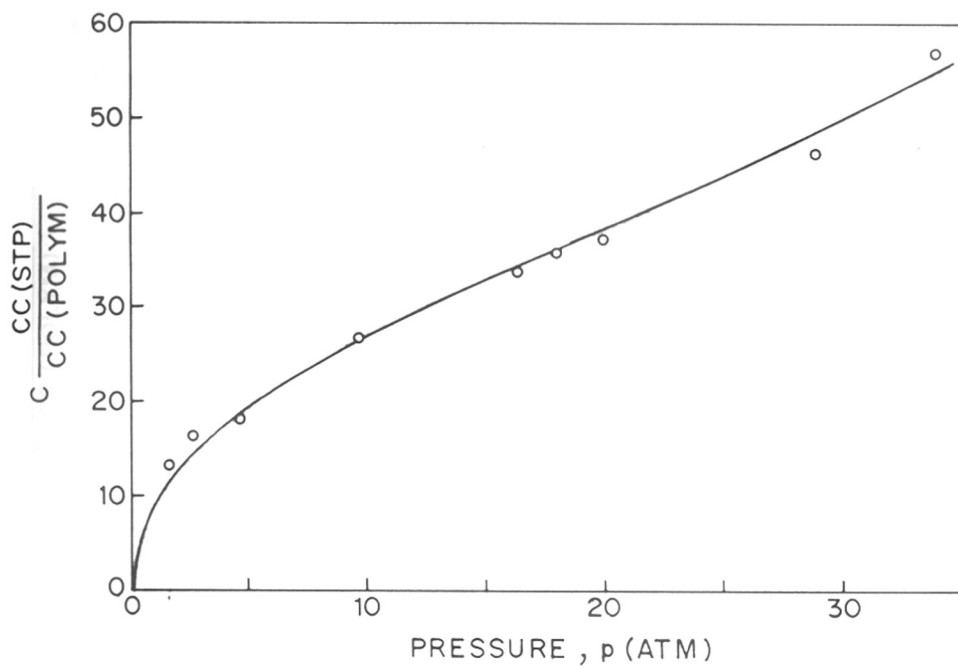
FIG.4·6a : HISTORY DEPENDENT SORPTION OF CO_2 IN SOLUTION-CAST PSF-PPHA, AT $35°C$
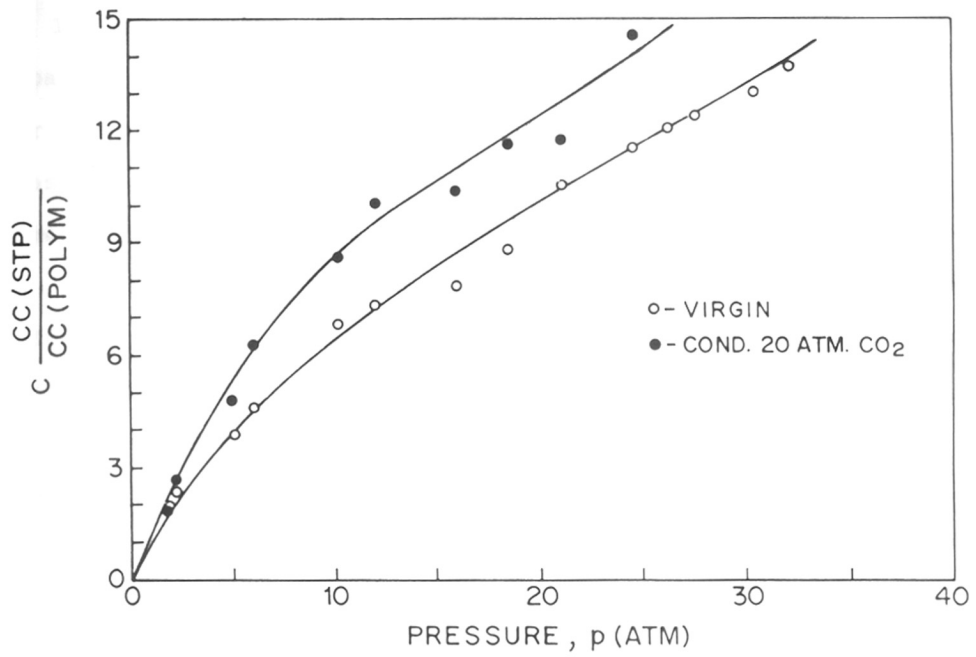
FIG. 4·6b: HISTORY DEPENDENT SORPTION OF CH4 IN SOLUTION-CAST PSF-PPHA, AT 35°C

from the literature (McHattie et al 1991, Sanders 1988). The solid lines in Figs. 4.6a and 4.6b represent the isotherms based on the dual-sorption model parameters listed in Table 4.6 and are in good agreement with the experimental data. The solubilities of both CO_2 and CH_4 in PSF-PPHA are almost the same as that for PES (Sanders 1988), and higher by 20-25 % than PSF (McHattie et al 1991). Inspite of the higher T_g, the Langmuir sorption capacity parameter, C'_H, for CO_2 in PSF-PPHA is lower than that for the other two polymers. However, the product ($C'_H b$) which is a measure of the sorption capacity in the glassy matrix is 1.7 times and 3 times higher than that of PES and PSF respectively. k_D and b values for PSF-PPHA are higher than the corresponding values for PSF, indicating higher affinity for the CO_2 molecule. The sulfonyl group density is highest in the case of PES followed by PSF and PSF-PPHA. Thus, though the T_g of PES is lower than that of PSF-PPHA by 68°, the marginally higher solubility of CO_2 in PES could be attributed to a higher sulfonyl group density in PES. The ratio of k_D for CO_2 over that for methane is highest in PSF-PPHA followed by PES and PSF. This can be attributed to the presence of additional ester group in the phthalide moiety in the case of PSF-PPHA. The calculated solubility parameter 'δ', falls in the same order.

Transport characteristics

The permeabilities of solution-cast PSF-PPHA to various gases against driving pressure are plotted in Fig. 4.7. This film had not been previously exposed to CO_2. The permeability values decrease with increasing upstream gas pressure, in qualitative

TABLE 4.6

Dual-sorption parameters for CO_2 and CH_4 for solution-cast PSF-PPHA, PES and PSF at 35°C

Polymer/Gas Parameter	PES[a] CO_2	PES[a] CH_4	PSF[b] CO_2	PSF[b] CH_4	PSF-PPHA CO_2	PSF-PPHA CH_4
k_D (cc(STP)/cc.atm)	0.631	0.168	0.728	0.257	1.103	0.2487 (0.2147)
c_H' (cc(STP)/cc)	29.78	10.80	19.60	6.58	17.33	6.6061 (7.8737)
b (atm^{-1})	0.313	0.123	0.260	0.0901	0.9031	0.1513 (0.1491)
$c_H'b$ (cc(STP)/cc.atm)	9.321	1.328	5.09	0.593	15.65	0.9995 (1.1739)
$k_D CO_2/k_D CH_4$	3.75		2.83		4.43	
$c_H'b/k_D$	14.77	7.90	6.99	2.30	14.18	4.01 (5.46)

Values in the bracket are for the sample treated with 20 atm CO_2 for 8 days.

a. Reference Sanders (1988).

b. Reference McHattie et al (1991).
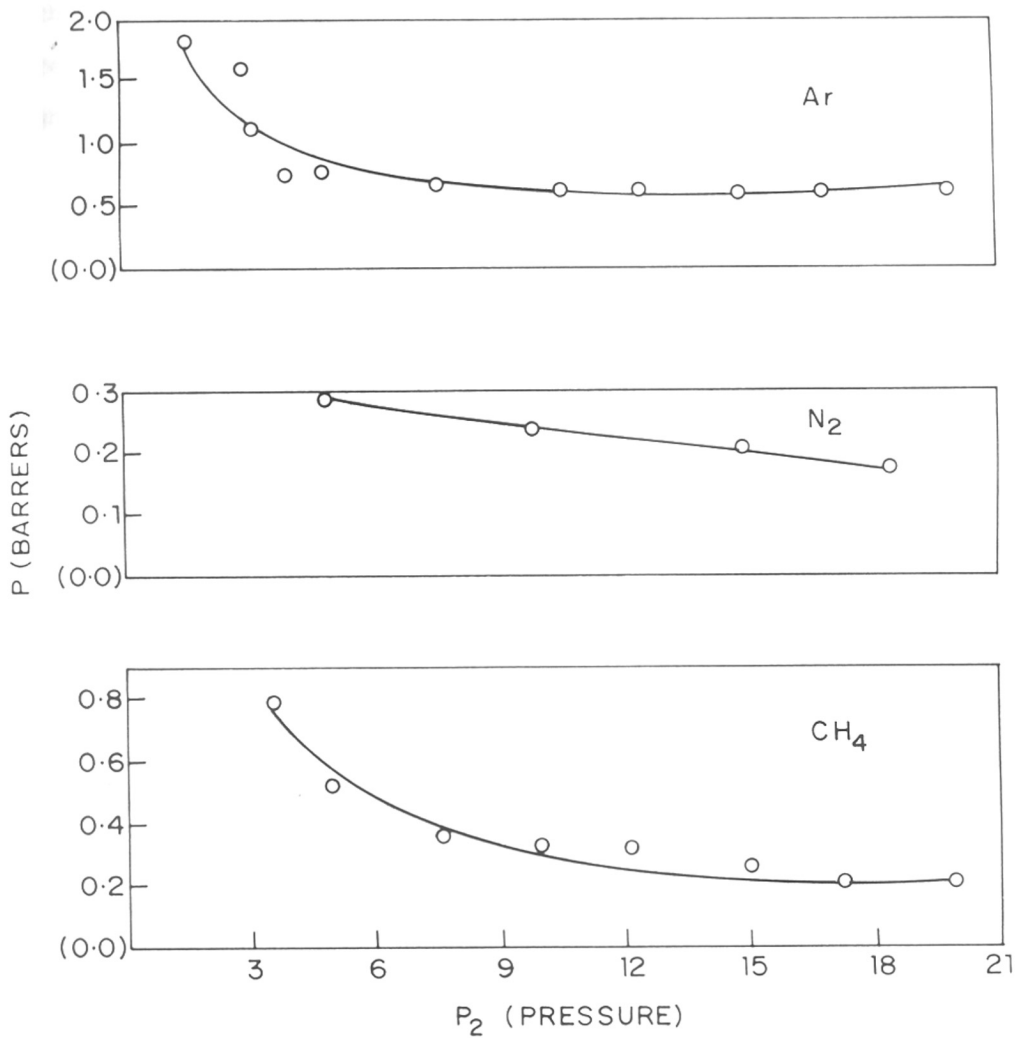
FIG. 4·7 : PRESSURE DEPENDENCE OF PERMEABILITY OF
Ar, N₂ AND CH₄ IN SOLUTION-CAST PSF-PPHA
AT 35°C

111

agreement with the predictions of the dual-sorption model. In general the permeability of PSF-PPHA is almost 1.5 to 2 times higher than that of the polysulfone based on bisphenol-A (PSF) (Erb and Paul 1981, McHattie et al 1991). This trend is in agreement with the results of Sheu et al (1988) who reported higher permeabilities for phenolphthalein based polyarylates than as compared to bisphenol-A based aromatic polyesters.

A dual mobility model has been shown to describe the transport of gases in glassy polymers (Paul 1979). The apparent permeability is given by,

$$P = k_D D_D + D_H c'_H b / (1 + b p_2) \qquad (32)$$

where p_2, is the upstream gas pressure, and D_D and D_H are diffusion coefficients for the Henry's law and Langmuir populations, respectively. The transport parameters, D_D, D_H and F, reported in Table 4.7, were determined by a linear least squares fit of the steady state permeability values against $1/(1+bp_2)$. Since the sorption parameters were independently determined, D and F could be calculated from the intercept and slope of the plot. The lines drawn in Figs. 4.8a and 4.8b for CO_2 and CH_4 respectively, are the least squares fits of the data, and provide a satisfactory description of the pressure dependencies.

The CO_2 and CH_4 diffusivity of the Langmuir type species, D_H, is higher in PSF-PPHA than in the case of PSF. However, the diffusivities for CO_2 or CH_4 dissolved in the Henry's law mode are relatively similar in both polymers (+/- 20-30 %). The D_D values for individual gases correlate well with their respective kinetic diameters. The diffusivities of these samples correlate

112

TABLE 4.7

Transport parameters for CO_2 and CH_4 for solution-cast PSF-PPHA and PSF at $35^{\circ}C$

Polymer/Gas Parameter	PSF (Udel)[*]		PSF-PPHA	
	CO_2	CH_4	CO_2	CH_4
D_D $(10^8 \; cm^2/sec)$	4.40	0.444	3.34	0.522 (2.11)
D_H $(10^8 \; cm^2/sec)$	0.462	0.155	1.04	0.28 (0.444)
$F = D_H/D_D$	0.105	0.349	0.3103	0.5359 (0.2107)

Values in the bracket are for the sample treated with 20 atm CO_2 for 8 days.

* Reference McHattie et al 1991.
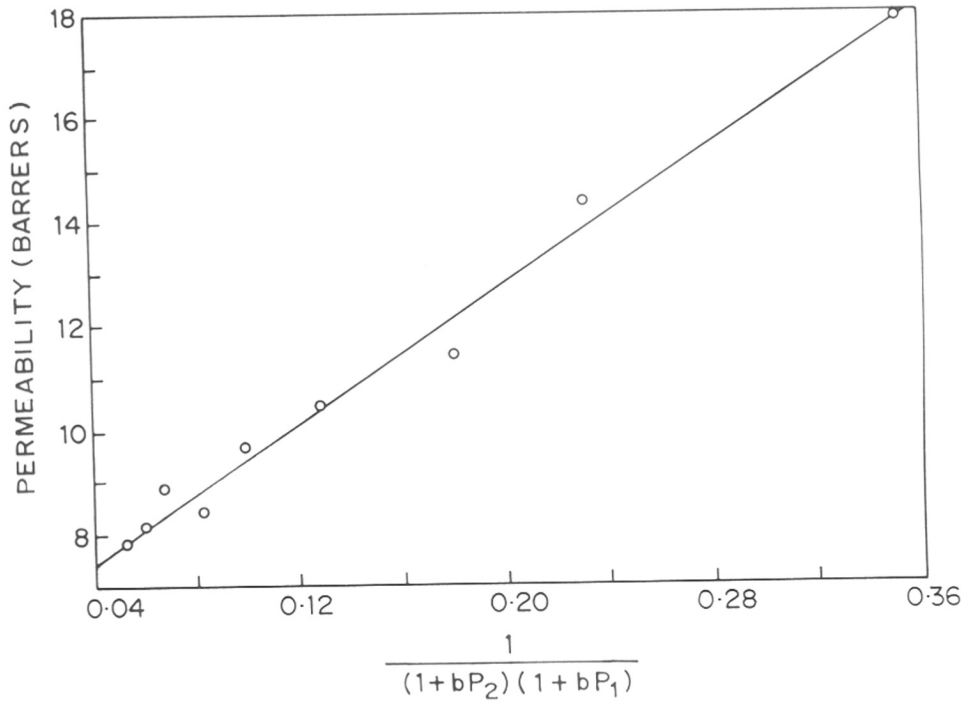
FIG. 4·8a : PERMEABILITY PLOTS FOR CO_2 IN SOLUTION-
CAST PSF-PPHA AT $35°C$. LINES DENOTE
PREDICTIONS FROM DUAL-SORPTION MODEL
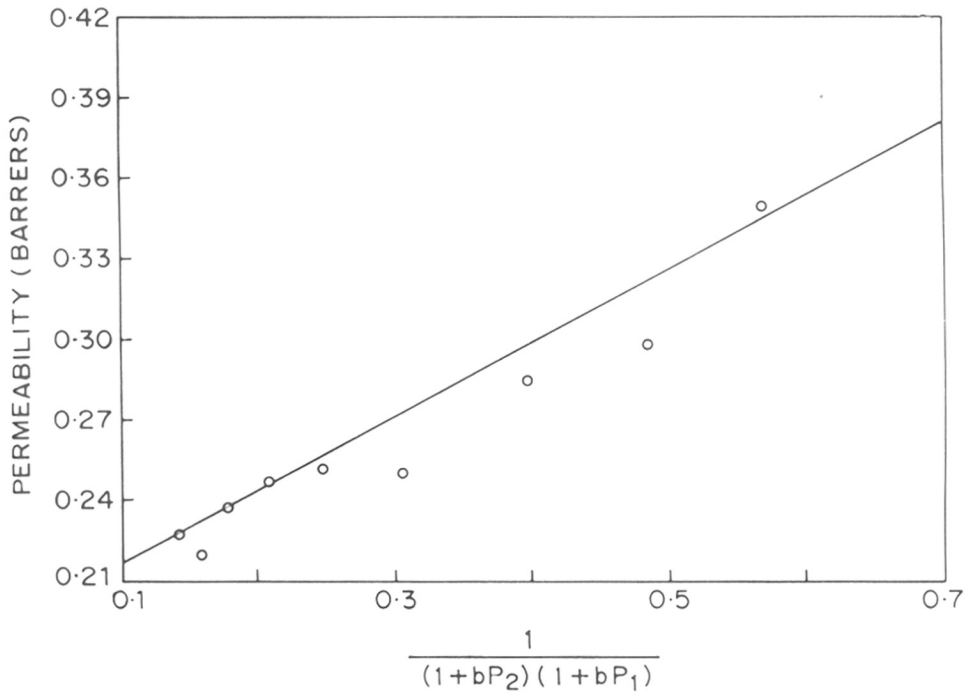
FIG. 4·8b : PERMEABILITY PLOTS FOR CH_4 IN SOLUTION-
CAST PSF-PPHA AT $35°C$. LINES DENOTE
PREDICTIONS FROM DUAL-SORPTION MODEL

well with the d_{sp} rather than the fractional free volume.

The ratios of permeability, concentration-averaged diffusivity, and apparent solubility coefficients, for CO_2/CH_4 determined at 10 atm and 35^oC, are summarized in Table 4.8. The slightly higher solubility selectivity in PSF-PPHA does not completely compensate for the poor diffusivity selectivity compared to PES. The replacement of the isopropylidene group in PSF by the phthalide ring in PSF-PPHA, results in higher permeability for CO_2 without any deterioration in permselectivity over CH_4.

4.2.0 Effect of CO_2 conditioning on properties of phenolphthalein based polysulfone (PSF-PPHA)

It has been recognized for several years that the sorption of condensible gases like CO_2 results in the plasticization of several polymers. This is manifested in the i) depression in glass transition temperature (Chiou et al 1985[a], Fried et al 1989, Hachisuka et al 1990), ii) decrease in modulus or increase in creep compliance (Wang et al 1982, Sanders 1988, Fried et al 1990) and iii) volume dilation (Enscore et al 1977, Berens and Hopfenberg 1978, Stern and Kulkarni 1982, Pope et al 1990). The conditioning effect also results in a significant increase in penetrant sorption and permeation parameters (Chan and Paul 1979, Wonders and Paul 1979, Stern and Kulkarni 1982, Jordan et al 1989).

The effects of high pressure CO_2 conditioning on sorption and transport properties of gases in phenolphthalein based polysulfone (PSF-PPHA) alongwith the changes in thermal and

116

TABLE 4.8

Permeability and permselectivity for the system CO_2/CH_4 in solution-cast PSF-PPHA at 10 atm and $35^\circ C$

Polymer Property	PES[a] (VICTREX)	PSF[b] (UDEL)	PSF-PPHA
PCO_2	3.36	5.6	6.5
PCO_2/PCH_4	28	22	23
SCO_2/SCH_4	3.91	3.7	4.12
DCO_2/DCH_4	7.15	5.9	5.6

a. Reference Sanders (1988).

b. Reference McHattie et al (1991).

volumetric behavior are discussed in this section.

4.2.1 Thermal and volumetric changes

In order to evaluate the magnitude of plasticization, it is of interest to quantify the decrease in T_g of the polymer as a result of sorption of CO_2. Wonders and Paul (1979) using a special differential thermal analyzer, showed that the T_g of polycarbonate containing CO_2 sorbed at 6.8 atm was 8-9°C lower than of the untreated polymer. Wang et al (1982) have also observed reduction in the T_g of polystyrene in the presence of CO_2 by the change in mechanical relaxation behavior. Chiou et al (1985)[b], monitored the reduction in the T_g of various glassy polymers caused by sorbed CO_2 (25 atm) by DSC. Since the transport properties of gases in polymers are significantly influenced by the secondary relaxations, it is important to investigate the effect of plasticization on secondary relaxation processes. However, not many studies have been reported.

The effects of plasticization on the sub T_g relaxations of PSF-PPHA caused by CO_2 exposure have been investigated using dynamic mechanical analysis (DMA). Dilatometric studies have also been carried out. Characterization by the two methods can be used probe changes in polymer rigidity and packing for a better understanding of the mechanism of plasticization.

The DMA data for 1.5 mm thick solution-cast specimens are shown in Fig. 4.9. The solution-cast virgin sample does not show a clear transition at the expected T_g (see Fig. 4.9a). However, the same specimen when rerun after thermal annealing, shows a prominent peak at 291°C (see Fig. 4.9b) which corresponds to the
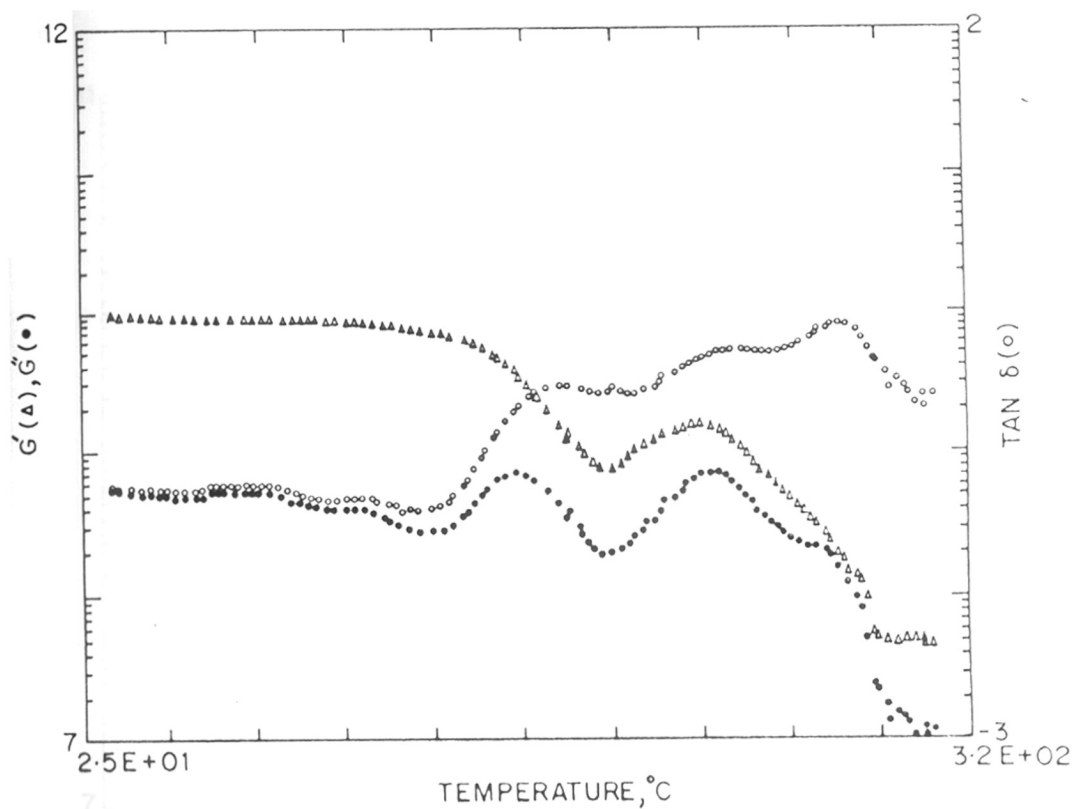
FIG.4·9a: DMA SPECTRA FOR PSF-PPHA (SOLUTION-CAST)
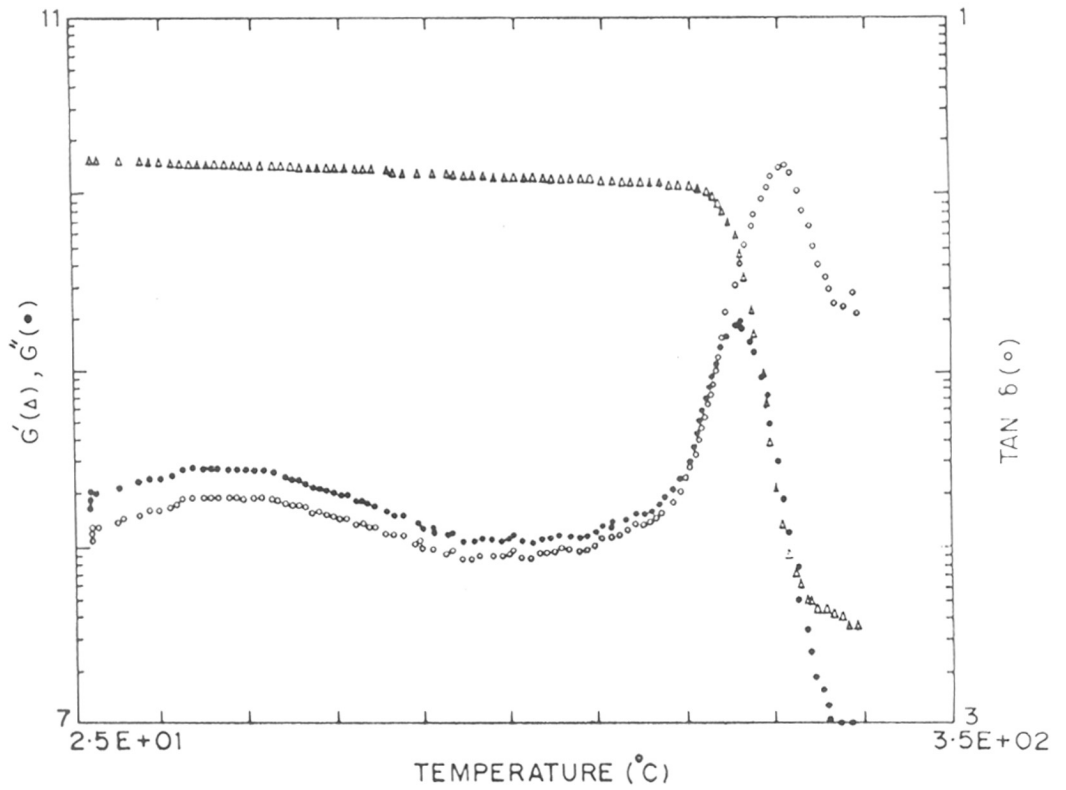
FIG.4·9b: DMA SPECTRA FOR PSF-PPHA (ANNEALED)
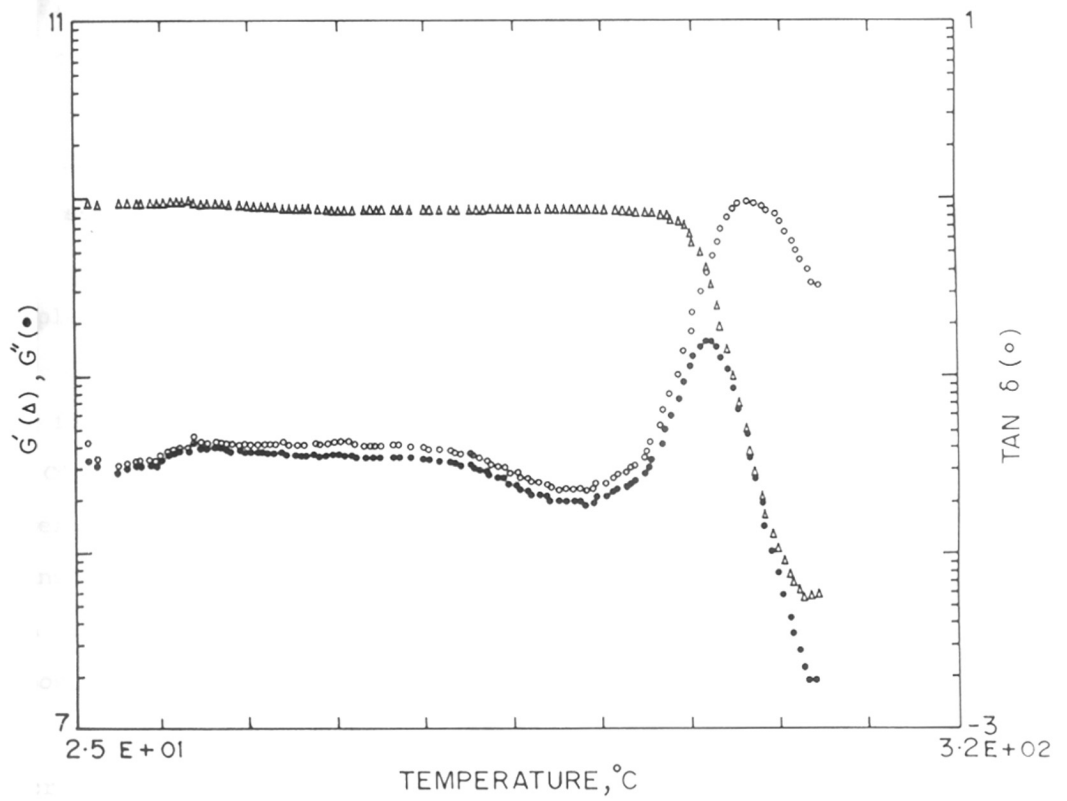
FIG.4·9c : DMA SPECTRA FOR PSF-PPHA EXPOSED TO
20 atm CO$_2$ FOR TWO DAYS

T_g. This value agrees with the glass transition temperature reported by Nurmukhametov et al (1976) using DMA. Additionally, a small and broad transition at $135^{\circ}C$ (β transition) can be seen in Fig. 4.9b. This has been ascribed to non-equilibrium packing defects created during quenching the sample below the glass transition temperature (Goldstein 1972). Its origin has been attributed to the orientational stresses introduced during processing (Illers and Breuer 1963, LeGrand 1969). Clearly the location of 'β' transition is highly dependent on the method, sample preparation and history.

Analysis of the sample used in Fig. 4.9b exposed to 20 atm CO_2 for two days indicates that PSF-PPHA is strongly plasticized by CO_2. The T_g peak is broadened and the peak temperature is lowered from $291^{\circ}C$ to $260^{\circ}C$ (see Fig. 4.9c). Further, the 'β' transition observed at $135^{\circ}C$ for the untreated sample disappears. DMA results indicates the plasticization of the matrix on exposure to high pressure CO_2.

It is reasonable to expect that sorbed CO_2 would lead to increased chain separation and thereby reduce intermolecular barriers to phenyl group rotations. However, The average intersegmental chain spacing (d_{sp}), determined from the WAXD spectra for the PSF-PPHA specimen, before and after exposure to 20 atm CO_2 shows no change in d_{sp}. Dilatometry does show a small decrease in density from 1.3395 g/cc to 1.3305 g/cc. Recently Fleming and Koros (1990) reported a similar decrease in density of polycarbonate (PC) on dilation with CO_2. The changes in T_g and β transitions on exposure to high pressure CO_2 can therefore be

attributed to the change in the polymer conformation without changes in the average intersegmental chain spacing, during conditioning. This is also the case with PSF and PES (Kulkarni et al 1990).

4.2.2 Sorption behavior

Sorption results for methane are shown in Fig. 4.6b. The curves 1 and 2 represent the values for virgin PSF-PPHA and the conditioned sample respectively. Conditioning involved exposure of the virgin polymer to CO_2 at 20 atm for two days, depressurization over a time period of 6-8 hrs and exposure to vacuum for 48 hrs before exposure to CH_4. The virgin polymer was evacuated at 10^{-2} Torr for two days before sorption measurements.

The conditioned sample exhibits higher sorption levels (30 %) than the unconditioned one (see Fig. 4.6b). Similar history dependent sorption results are reported for polycarbonate (Wonders and Paul 1979), polysulfone (Erb and Paul 1981), CA (Stern and Kulkarni 1982). The sorption isotherm of CH_4 in the sample exposed to high-pressure CO_2 is also well described by dual-sorption model. However, the values of dual-sorption parameters differ from those for the virgin sample (see Table 4.6). It is clear from the results shown in Table 4.6 that the increase in overall sorption level stems from enhanced sorption capacity in glassy matrix. This can be seen clearly by comparing the ratio $C_H'b/k_D$ which represents the relative fraction of gas sorbed in the two modes. A possible reason for the increase in C_H' could be the failure of the glassy polymer to regain its original state after evacuation of CO_2 because of long relaxation times

involved. This would incorporate extra frozen void volume in the polymer and result in the increased sorption capacity.

4.2.3 Permeation of CO_2 and CH_4 in pure and mixed gas system

The results of permeability for CO_2 in PSF-PPHA are discussed in the section 4.3.4 in the context of diverse pressure dependence of permeability of CO_2 in various glassy polymers.

CH_4 permeabilities at 10 atm were measured (i) on virgin polymer (0.26 Barrers) and after CO_2 exposure (ii) at 20 atm for one day (0.38 Barrers) and (iii) 40 atm for two days (0.63 Barrers). As a result of CO_2 conditioning, the concentration averaged diffusion coefficient D has increased by 3 times. In particular D_D has increased by 4 times and D_H by a factor of 1.6 (Table 4.7). This is due to the increased mobility of segments as reflected in decreased T_g on dilation.

The experimental results on permeation of a binary mixture of CO_2/CH_4 (55/45, mole ratio) through virgin PSF-PPHA film are represented in Fig. 4.10. Selectivities in PSF-PPHA are relatively less affected compared to other commonly used membrane materials like CA, PC and PSF (Udel).

The permeabilities for CO_2 and CH_4 against the partial pressures of respective gases in the feed stream are plotted in Fig. 4.11a and 4.11b respectively. The solid lines (theoretical) are drawn using the sorption and transport parameters of the respective pure gases shown in Table 4.6 and 4.7.

$$P_A = K_{DA} \cdot D_{DA} \left(1 + F_A K_A / (1 + b_A p_A + b_B p_B)\right) \tag{32}$$

The calculated values agree well with experimental results.
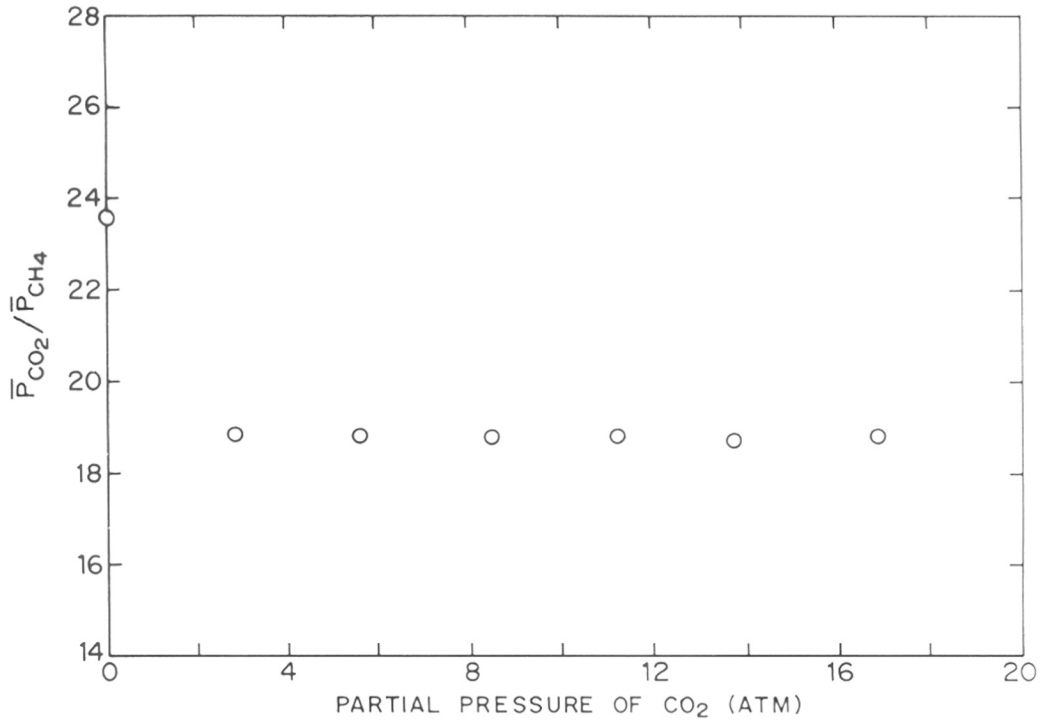
FIG.4·10 : PRESSURE DEPENDENCE OF INTRINSIC SEPARATION
FACTOR FOR CO_2/CH_4 IN SOLUTION-CAST PSF-PPHA
AT $35°C$ (MIXED GAS SYSTEM)
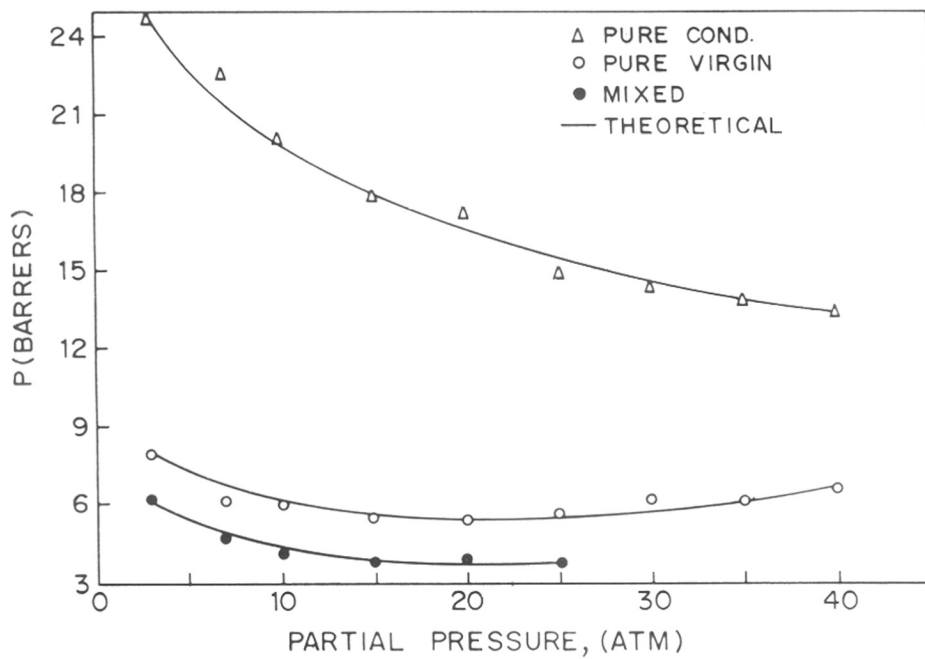
FIG. 4·11a : PURE AND MIXED GAS PERMEABILITY OF CO_2
IN THE SOLUTION-CAST PSF-PPHA AT 35°C
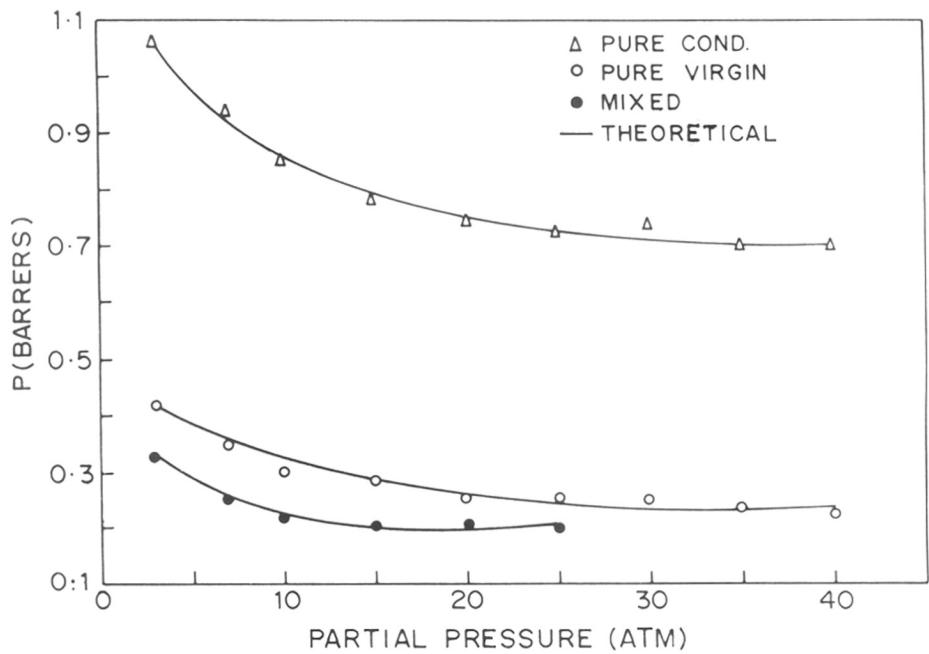
FIG. 4·11b : PURE AND MIXED GAS PERMEABILITY OF CH_4
IN THE SOLUTION-CAST PSF-PPHA AT 35°C

The permeabilities of both CO_2 and CH_4 are lowered in comparison to pure component values. This behavior is in accordance with the transport model for mixed gas system (eqn. 32). Thus in the present case plasticization has small effect on membrane selectivity for the gas pair CO_2/CH_4.

4.2.4 Permeability and permselectivity of various gases

As discussed in the previous section, compared to commercial PSF, phenolphthalein based polysulfone (PSF-PPHA) exhibits higher flux for CO_2. Yet permselectivity for CO_2/CH_4 in pure as well as mixed gas system is not significantly affected. This phase of work was undertaken to study potential for other industrially useful gas separations such as O_2/N_2, He/CH_4.

The permeability values for solution-cast PSF-PPHA at $35^{\circ}C$ and 10 atm for several gases are listed in Table 4.9. The values in the second column were generated for the sample exposed to 40 atm CO_2 for two days. The permeability coefficient for untreated film was measured in the order, He, Ar, O_2, N_2 and CH_4. The measurements were carried out in the reverse order for the samples exposed to CO_2. The observed increase in permeability coefficient as a result of this treatment varied between 5 % for O_2 to 210 % for CO_2. Higher permeabilities for these gases on exposure to CO_2 at high pressures could result from both high solubility as well as higher diffusivity as in the case of CH_4. However, further evaluation of transport parameters will be required..

Exposure to high-pressure CO_2, results increased permeability and decrease in selectivity in glassy polymers such

128

TABLE 4.9

Change in permeability of various gases on exposure to CO_2 in solution-cast PSF-PPHA at 10 atm and $35^{\circ}C$

Prop. Gas	ϵ/k $(^{\circ}K)$	T_C $(^{\circ}C)$	k.d $(\overset{\circ}{A})$	P (Barrers) (Uncond)	(Cond.)[*]	P_r
He	10	− 268	2.55	14.00	22.29	1.59
Ar	125	− 122.5	3.54	0.61	0.74	1.21
O_2	106	− 118.4	3.46	2.00	2.11	1.05
N_2	90	− 147	3.8	0.25	0.32	1.28
CH_4	140	− 82.1	3.76	0.26	0.63	2.42
CO_2	190	31	3.94	6.50	20.11	3.09

$P_r = P_{cond} / P_{uncond}$

[*] 40 atm. CO_2, 2 days.

as polycarbonate (Jordan et al 1987), cellulose acetate (Donohue et al 1989), polyimide (Colemann and Koros 1990). Similar trends are seen here for the gas pairs He/CH_4, N_2/CH_4 and O_2/N_2 CO_2/CH_4. Yet an increase in permeability is accompanied by an increase in permselectivity of CO_2/N_2 (see Table 4.10). This needs to be substantiated by studies on mixed gas system.

The permeability ratio ($P_{conditioned}/P_{virgin}$) (Pr), tends to increase with increase in critical temperature and kinetic diameter of the penetrant gas. The exception is He which has the lowest T_c and (see Table 4.9) yet it has a P_r value greater than that for Ar, N_2 or O_2.

Jordan et al (1989) recently concluded that exposure of polycarbonate to high pressure CO_2 and subsequent exchange with He brings the matrix to its original state as reflected in changes in permeabilities (within +/- 5 % level). However, our results for He indicate that the PSF-PPHA retains its dilated state to some extent even after exposure to He. The time required to complete the experiment after conditioning was 12-14 hrs. Also, the polymer PSF-PPHA is more rigid ($T_g = 291^\circ C$) than PC ($149^\circ C$). It is reasonable to expect that PSF-PPHA will take a longer time to return its original state than that required for PC under similar conditions. Similar results are observed for Helium in case of ring and bridge substituted aromatic polyesters on exposure to high pressure CO_2. Details are discussed in the section 4.4.3.

TABLE 4.10

Effect of CO_2 exposure on selectivity of various gas pairs in solution-cast PSF-PPHA at 10 atm and 35°C

System	Unconditioned	Conditioned[*]
He/CH_4	53.8	35.4
CO_2/CH_4	23	32
CO_2/N_2	24	63
N_2/CH_4	0.96	0.51
O_2/N_2	8.0	6.6

* 40 atm. CO_2, 2 days

4.3.0 Permeation and conditioning effect in glassy polymers

4.3.1 Pressure permeability behavior in glassy polymers

The increase of permeability and diffusivity with increasing pressure is commonly seen for rubbery polymers. The situation in the case of glassy polymers is more complicated in that permeability usually decreases and diffusivity increases with increasing pressure. This type of pressure-dependence has been well explained within the frame-work of the dual-sorption model. However, in some cases involving strongly soluble penetrants such as CO_2, glassy polymers show behavior more typical to rubbery polymers.

The permeation characteristics of glassy polymers with respect to pressure can be classified as follows.

Type 1. On plasticization, the Tg of the glassy polymer decreases below the temperature of the permeation experiment. The polymer then behaves like a typical rubbery polymer e.g. poly(ethyl methacrylate) (PEMA) (Chiou and Paul 1989).

Type 2. The polymer remains in the glassy state; however, its permeability profile resembles that of a rubbery polymer e.g. CA, PMMA and PVC (Sada et al 1990, Donohue et al 1989, Chiou and Paul 1986, Hibri et al 1985).

Type 3. The permeability decreases with increasing pressure (as predicted by the dual sorption theory) upto a critical pressure. Subsequent increase in pressure results in an increase in permeability e.g. polycarbonate (Jordan et al 1989) and polyimides (Kim 1988, Okamato et al 1990).

Type 4. The permeability characteristics vary in accordance with

the predictions of dual-sorption theory. However, permeability is influenced by the exposure of the polymer to highly soluble gas such as CO_2 at high pressures (the "conditioning" effect) (Pope et al 1990, Jordan and Koros 1990, Erb and Paul 1981, Houde et al 1991).

The plasticization of glassy polymers has been modelled by postulating an exponential dependence of (i) diffusivity on solute concentration (Stern and Saxena 1980), (ii) Henry's law constant on concentration (Mauze and Stern 1983) or (iii) a decrease in the microvoid sorption saturation constant (Kamiya et al 1986)[a] as a result of lowered T_g. The change in polymer properties (T_g) as a result of plasticization was first demonstrated by Chiou et al (1985)[a] using DSC. A similar technique has been used by Fried et al (1989). Volume dilation has also been observed in various gas-polymer pairs. Sefcik and Schaefer (1983) have shown by NMR that gas exposure increases the frequency of main chain motions.

We have used WAXD to probe the structural changes in plasticized and virgin polymer samples. The increased polymer chain mobility indicated by DSC, DMA and NMR measurements could also result from increased interchain spacing. The intersegmental spacing, d_{sp}, can be estimated by applying Bragg's equation to amorphous polymer maximum. The d_{sp} values correlate well with diffusivity in various families of glassy polymers. Thus in polymers where permeability increases primarily through an increase in diffusivity, we expected to see an increase in d_{sp} could be expected.

4.3.2 Polymer plasticization : WAXD investigation

WAXD measurements have been extensively used in the past to measure the average intersegmental spacing in amorphous polymers. Permeabilities and diffusivities of gases in polyimides (Stern et al 1989, Kim et al 1987), polycarbonates (Hellums et al 1989) and polyarylates (Charati et al 1991) have been satisfactorily correlated on the basis of the intersegmental spacing (d_{sp}). The effect of sorbed gases on the transition temperatures of bisphenol-A based glassy polymers has been attributed to the possible enhancement in the intersegmental spacing (Fried et al 1989). However, no experimental validation was reported.

In order to verify if the observed enhancement in the diffusivity / permeability of gases results from an increase in the intersegmental spacing, the effect of sorbed gases on the intersegmental spacing was investigated. The results would also help to discern if plasticization is brought about by an increase in the intersegmental spacing and / or modification of the interchain potential energy.

The values of the intersegmental spacing (d_{sp}) for various polymer films prior to and after exposure for 48 hours to (i) a highly soluble gas, CO_2, (ii) a weakly soluble gas, N_2, and (iii) a non polar solvent, n-hexane are summarized in Table 4.11. Typical spectra for 50 μm thick PMMA sample before and after exposure to CO_2 / n-hexane are shown in Fig. 4.12. Thus, dilation of a 50 μm thick PMMA film by CO_2 leads to an enhancement of the intersegmental spacing by 0.18 $\overset{\circ}{A}$. The increase in the intersegmental spacing is highest for CA and PMMA. Polystyrene

TABLE 4.11

Intersegmental spacings (d_{sp}) measured by WAXD for various glassy polymers.

Polymer	d_{sp} (Å)			
	Virgin	CO_2-cond[a].	n-Hexane-cond[b].	N_2-cond[a].
PMMA	6.14	6.32	6.55	6.05
CA	4.84	4.98	4.74	4.74
PSt	4.64	4.64	4.59[c]	– –
PC	5.09	5.18	5.18	5.06
PES	4.95	4.92	5.09	– –
PSF	4.92	4.95	– –	– –
PSF-PPHA	5.03	5.00	5.01	– –

a. 40 atm., room temp., 2 days (42-48 hrs.)

b. Room temp., 2 days

c. Sample turned opaque.
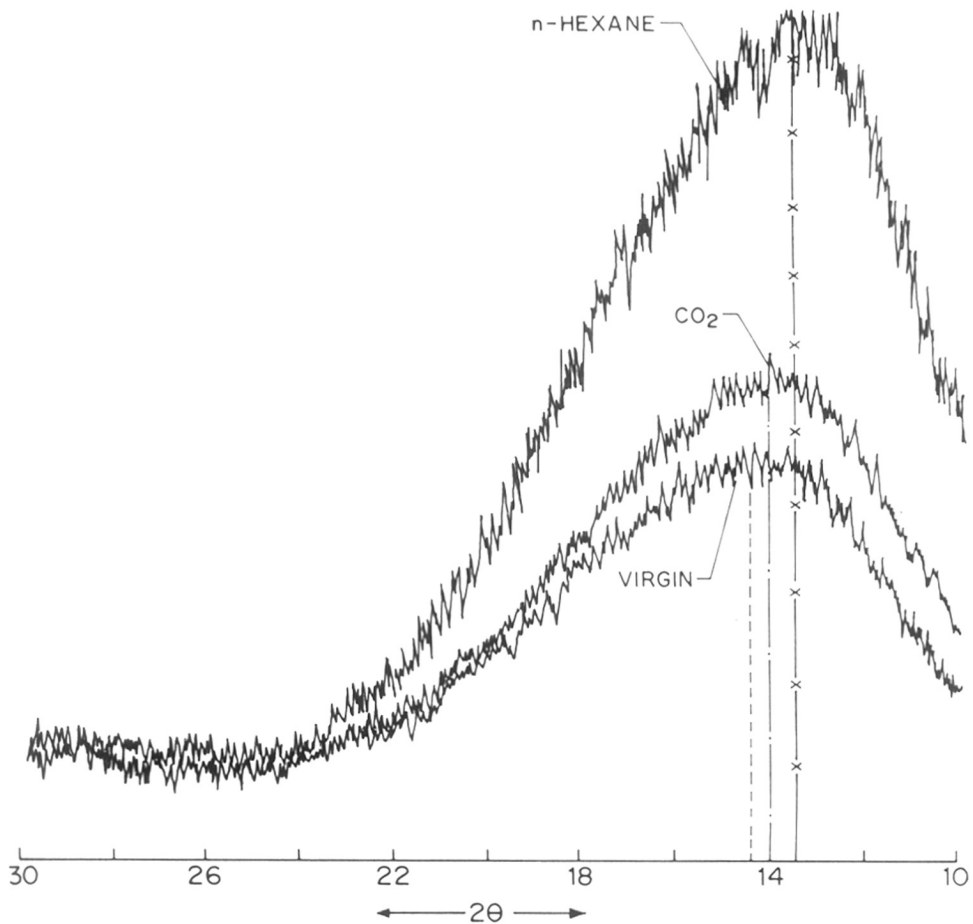
FIG. 4·12 : WAXD   SPECTRA FOR 50 μm THICK SOLUTION-
        CAST PMMA : a) VIRGIN POLYMER, b) EXPOSED TO CO_2
        AT 40 atm FOR 2 DAYS, c) SUBMERGED IN
        n-HEXANE FOR 2 DAYS

and the polysulfones are practically unaffected. The results for polycarbonate lie in between the two extremes.

In order to establish if the presence or otherwise of the gas which brings about dilation has any effect on subsequent changes in intersegmental spacing as a function of time, the effect of dilation by CO_2 on the intersegmental chain spacing of a 2 mm thick PMMA sample was also investigated (see Fig. 4.13). Calculations show that more than 90 % of CO_2 is desorbed from the 50 μm thick film before the WAXD scan is initiated, whereas only 6 % of the gas is desorbed from the 2 mm thick PMMA film till the WAXD measurement is completed. The increase in the intersegmental chain spacing in the case of the 2 mm thick PMMA sample was also 0.18 $\overset{\circ}{A}$. This experiment, therefore, demonstrates that the increase in the intersegmental spacing is the same irrespective of whether CO_2 is present or otherwise during the scan. This can be attributed to the slow rate of relaxation of the polymer chains.

The above conclusion is further substantiated by following experiments. A sample of polycarbonate (50 μm thick) on exposure to CO_2 at 40 atm. for two days showed an increase in d_{sp}. by 0.09 $\overset{\circ}{A}$. The increased d_{sp} was maintained when the sample was evacuated at 10^{-2} Torr and room temperature upto eight days. However, during the same time span, the d_{sp} regained the original value when the film was annealed at $120^{\circ}C$. These results are summarized in Fig. 4.14.

With the exception of polystyrene, the solubility of CO_2 in the various polymers listed in Table 4.11 is in the range of 30-40 cc(STP)/cc(polym).atm. In polystyrene, the solubility of CO_2

137
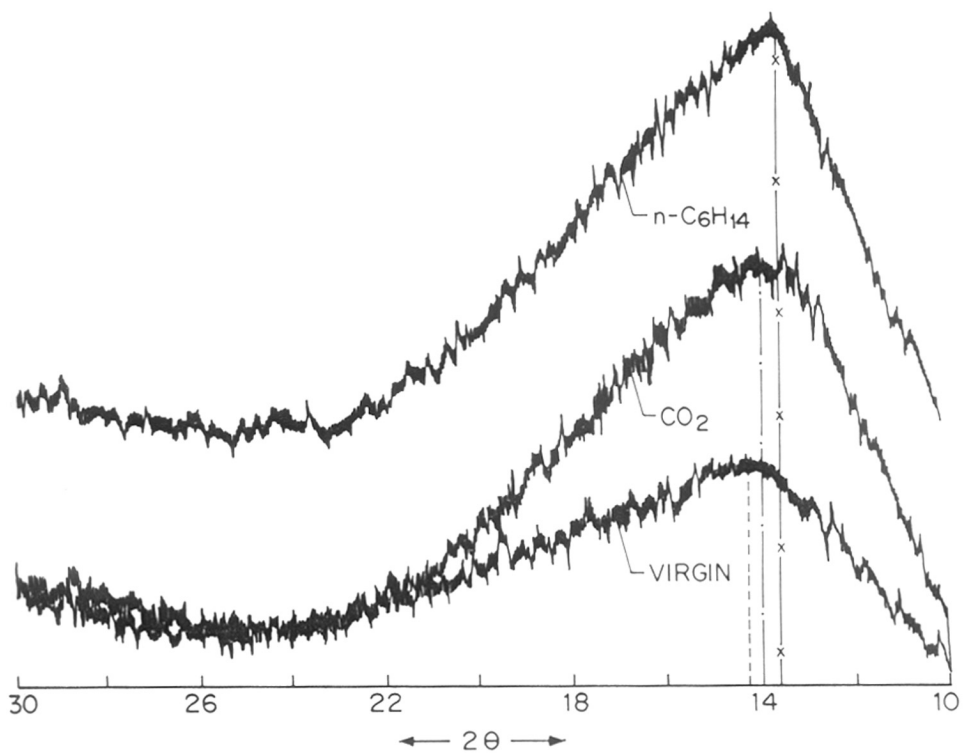
FIG.4·13 : WAXD SPECTRA FOR 2mm THICK SOLUTION-CAST
PMMA: a) VIRGIN POLYMER, b) EXPOSED TO CO_2 AT
40 atm FOR 2 DAYS, c) SUBMERGED IN n-HEXANE
FOR 2 DAYS

PC CO_2, 40 atm   Dilated   Vac., 10^{-2} Torr.   Evacuated
2 mil $\xrightarrow{\hspace{2cm}}$ sample $\xrightarrow{\hspace{2cm}}$ sample
Virgin   R.T., Two days   R.T., Eight days

(5.09 Å)   (5.18 Å)   (5.18 Å)

                            120 °C │ Annealing
                         Eight days │
                                    ↓

                         Annealed sample

                            (5.09 Å)
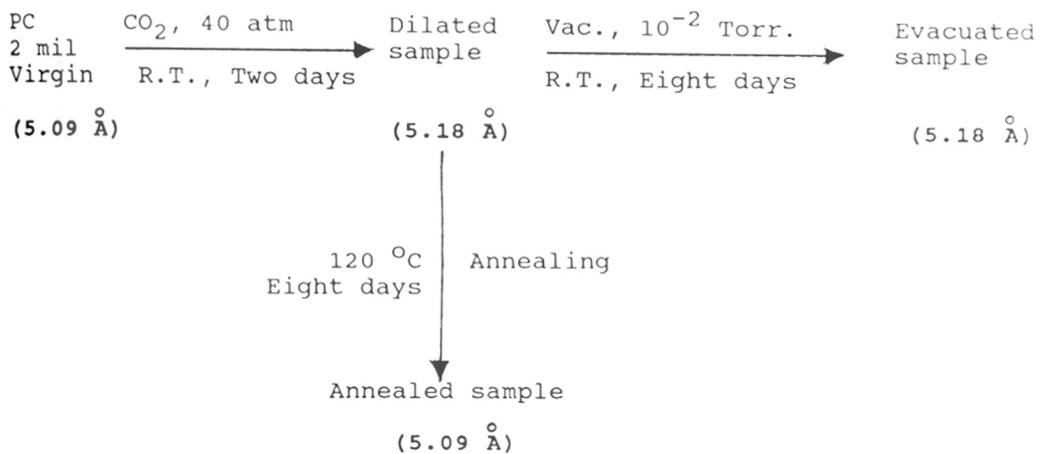
FIG.4·14: CHANGE IN dsp OF 50 μm THICK POLYCARBONATE (PC)
         ON EXPOSURE TO CO_2 AND SUBSEQUENT
         EVACUATION AND THERMAL ANNEALING

is approximately 50 % lower (see Table 4.14). The magnitude of plasticization depends on the amount of the gas sorbed (Sanders 1988, Hachisuka et al 1990). In the case of the polymers in which the solubility of CO_2 is reasonably constant, the increase in d_{sp} is highest for the polymers which exhibit type 2 permeation characteristics (CA, PMMA), constant within experimental error for polymers which exhibit type 4 permeation characteristic (polysulfones) and lies in between for the polymers which exhibit type 3 behavior (polycarbonate).

The effect of exposure time and medium were also investigated. Polymer specimens were exposed to CO_2, N_2 or n-hexane. Exposure to CO_2 upto eight days revealed that in the case of PMMA, the intersegmental chain spacing increased with the period of exposure. However, no further increase was observed after two days in the case of polycarbonate (see Table 4.12).

The solubility of N_2 is low its interaction with the polymer is also very weak. DSC measurements confirm that exposure of polymers such as polyethersulfone to N_2 has no effect on T_g. On the other hand, exposure to CO_2 at pressures as low as 7-8 atm. brings about a decrease in T_g by $76^{o}C$ (Sanders 1988). WAXD investigations, reveal that exposure of CA and PMMA to N_2 at high pressures results in a slight decrease in the intersegmental spacing (see Table 4.11). Since glassy polymers are considered to be incompressible, a decrease in d_{sp} is not anticipated. Although no explanation can be given for this observation at this stage, the decrease in d_{sp} has been observed reproducibly.

TABLE 4.12

Effect of gas and exposure time (days) on d_{sp} of poly(methyl methacrylate) (PMMA) and polycarbonate (PC).

Polymer	Exposure Conditions* days, Gas	Change in d_{sp}. $(\overset{\circ}{A})$ (Exposed - Original)
PMMA	2D CO_2	0.18
	8D CO_2	0.59
	2D N_2	- 0.12
	8D N_2	- 0.20
PC	2D CO_2	0.09
	8D CO_2	0.09
	2D N_2	- 0.03

* 40 atm., room temp.

It is also interesting to compare the effect of the nonpolar solvent, hexane, with that of the high-pressure "polar" gas CO_2. The increase in the intersegmental chain spacing on exposure of the films to n-hexane is identical to or greater than that brought about on exposure to CO_2. The only exception is CA. WAXD spectra of virgin and hexane exposed CA samples are shown in Fig. 4.15. WAXD spectrum of CA exhibits two peaks, at 4.84 Å and at 9.33 Å respectively. The larger dimension (9.33 Å) is of the same magnitude as the fiber axis dimension of the unit crystalline cell in cellulose triacetate (Miller 1975); the lower value represents the intersegmental distance, d_{sp}. Exposure to either n-hexane or CO_2 results in a decrease in the peak height at 9.33 Å (see Fig. 4.15), while exposure to N_2 has no effect. Exposure to CO_2 leads to an increase in the intersegmental spacing whereas n-hexane causes a shift towards lower d_{sp}. This indicates a possible antiplasticizing effect of n-hexane on CA. This hypothesis needs to be verified further.

4.3.3 Polymer plasticization: Correlation of pressure dependence of permeability

Some insight into the plasticization process can be obtained by comparing the WAXD data with the results of transition temperature measurements obtained from DSC and DMA (Chiou and Paul 1987, Sanders 1988, Fried et al 1989). It is reasonable to expect the changes in d_{sp} induced by CO_2 to correlate with the corresponding decrease in Tg since both are measures of polymer plasticization. However, a comparison of the data in Table 4.11 with that in Table 4.13 indicates that the two do not correlate
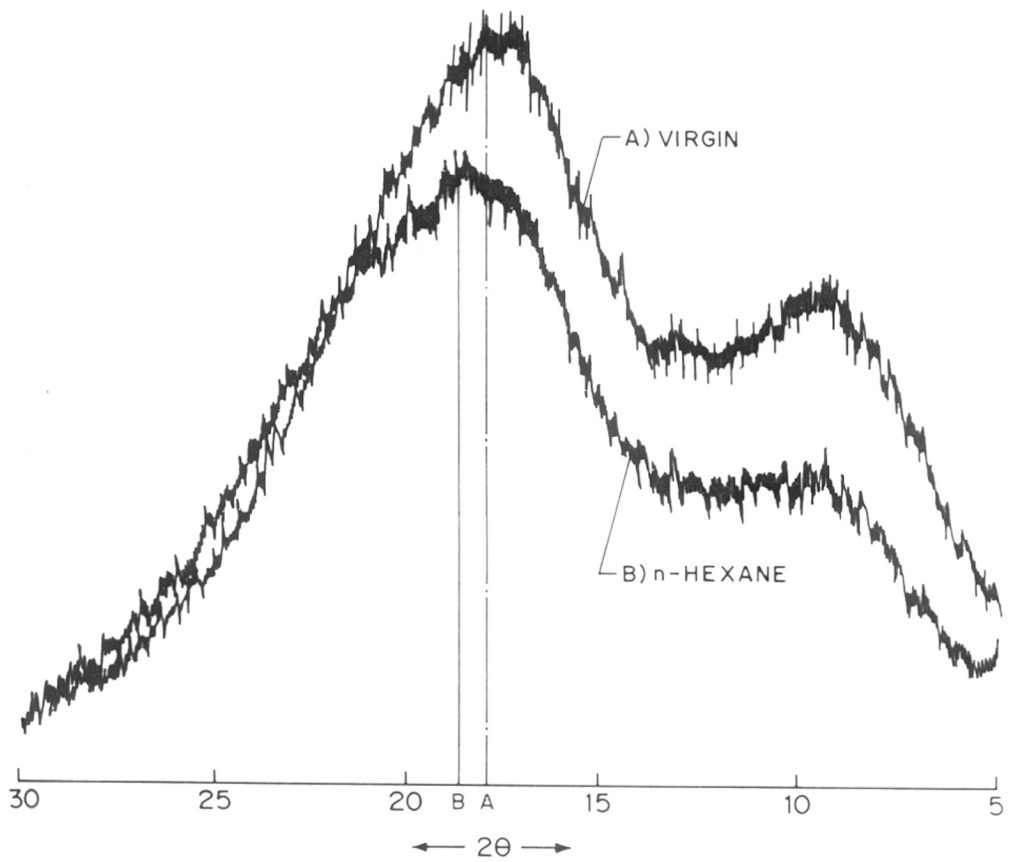
FIG. 4·15: WAXD SPECTRA FOR CA: a) VIRGIN POLYMER,
b) SUBMERGED IN n-HEXANE FOR 2 DAYS

TABLE 4.13

Change in glass transition temperature on exposure to CO_2 for various polymers studied.

Polymer	Virgin	Tg$^\circ$C Cond.[a]	Ref.
PMMA	105	67	Chiou and Paul (1987)
CA	175	120[b]	Sanders (1988)
PSt	100	78	Sefcik (1986)[b]
PC	148	97	Fried et al (1989)
PSF	197	179[c]	Fried et al (1989)
PES	235	135[d]	Sanders (1988)
PSF-PPHA	286	260	This work

a. Glass transition temperature after 20 atm. CO_2 exposure.

b. Calculated from Fig.7 of Ref. Sanders (1988).

c. At 30 atm.

d. At 35 atm.

well. This may be attributed to the fact that WAXD measurements provide a measure of the average intersegmental chain spacing in the polymer, whereas the decrease in Tg and / or increase in chain mobility may arise from the modification of the interchain energy interaction by the penetrant as well. It is thus possible to differentiate between the effect of the sorbed gas on the intersegmental chain spacing and / or on the interchain energy interaction.

Sanders (1988) showed that although the decrease in Tg induced by CO_2 was the same in the case of all the polymers investigated, only PMMA and CA exhibited CO_2 permeation characteristics similar to those of the rubbery polymers. The permeability profile of CA and PMMA was attributed to the enhanced mobility of the pendent ester groups due to the presence of sorbed CO_2 (Sanders 1988). The WAXD measurements reported herein indicate that the increase in the permeability of CO_2 with pressure in the case of CA and PMMA (type 2 behavior), could also be due to the fact that exposure of these polymers to CO_2 results in a significant enhancement in the intersegmental spacing. In contrast, in the case of the polymers, such as the polysulfones, which exhibit type 4 behavior, there is no increase in intersegmental chain spacing.

This conclusion is supported by the plasticization behavior of polycarbonate which exhibits type 3 permeation characteristics. The permeability of CO_2 initially decreases in accordance with the dual sorption theory. However, at pressures greater than 40 atm., permeability increases with pressure (Jordan et al 1989). Correspondingly, a polycarbonate film

exposed to 40 atmospheres pressure of CO_2 for two days, also exhibits a significant increase in the intersegmental chain spacing (0.09 Å) whereas the increase in d_{sp} on exposure to CO_2 at 20 atm is within experimental limits (0.03 Å). Thus an increase in permeability with pressure can result from a significant increase in the d_{sp} irrespective of the presence or otherwise of pendent groups in the polymer.

4.3.4 Permeability : Hysteresis effects

Although the pressure dependence of permeability of CO_2 in polymers such as polysulfones, conforms to the predictions of the dual sorption theory, these polymers exhibit a significant conditioning effect (Houde et al 1991). In these polymers, the d_{sp} does not change significantly on exposure to CO_2. The effect of CO_2 conditioning on the permeability of CO_2 in PSF-PPHA is shown in Fig. 4.16. Curve A is obtained by measuring the permeability at pressures incrementally increasing up to 20 atm. The membrane was then exposed to CO_2 at 20 atm for two days. Permeability of the film to CO_2 was then measured as a function of decreasing pressure (curve B). In each case the membrane was maintained at the test pressure for one hour before measurement. Curves C and D represent the results of a similar experiment carried out on another PSF - PPHA sample conditioned at 40 atm. for two days. Curve D (film conditioned at 40 atm) is flatter than curve B (film conditioned at 20 atm) which is indicative of a decreased Langmuir component in terms of the dual-sorption model. Thus,
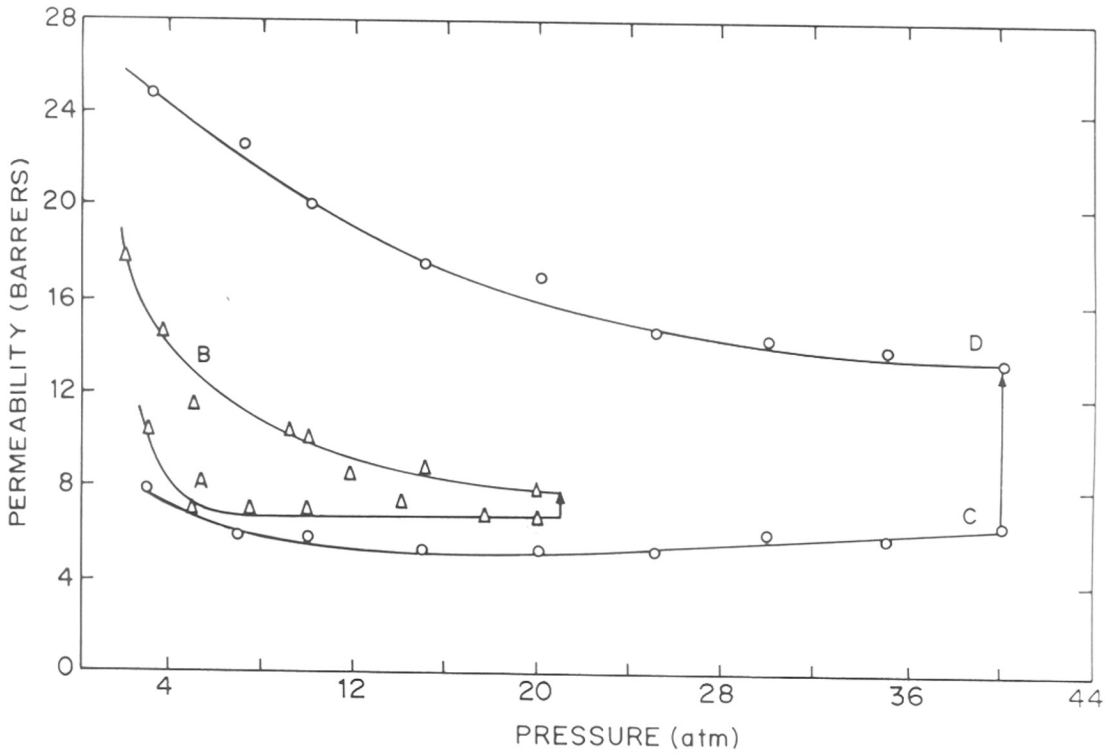
FIG.4·16:CO₂ PERMEABILITIES IN PHENOLPHTHALEIN BASED POLYSULFONE (PSF-PPHA) AT 35°C : CONDITIONING EFFECT

$$\partial \bar{P} / \partial p = -D_H \cdot C_H' b^2 / (1 + bp)^2 \qquad (43)$$

A smaller value of the slope ($\partial \bar{P}/\partial p$) for curve D could result from lower C_H' value. This is consistent with the decrease in Tg observed in all polymers including PSF-PPHA (Table 5.13). Thus, while an increase in permeability with pressure in the polymers exhibiting type 2 behavior (CA and PMMA) appears to be due to increased intersegmental spacing, the conditioning effect in polymers such as PSF - PPHA which exhibit type 4 behavior could be attributed to increased chain flexibility or chain rearrangement at constant d_{sp}. This is because in addition to intersegmental chain spacing, permeation and diffusion in glassy polymers are also affected by mobility considerations. This hypothesis needs to be further verified using techniques such as solid state NMR.

4.3.5 Effect of sorbed gas concentration

From the data plotted in Fig. 4.17, it appears that in the case of a series of glassy polymers in which the solubility of CO_2 is of the same order, the magnitude of increase in intersegmental chain spacing decreases as the glass transition temperature of the polymer increases. The effect of dissolved CO_2 concentration in the polymer (e.g. polystyrene) would bring about smaller changes in d_{sp} similar to the effect on Tg (Sanders 1988). The case of polycarbonate which shows an increase in d_{sp} of 0.09 Å at 40 atm and 0.03 Å at 20 atm has also been mentioned in the last section. Other factors (heat of sorption, original d_{sp} etc.) may also influence the changes in d_{sp} on gas exposure.

Values of concentrations of dissolved CO_2 in various
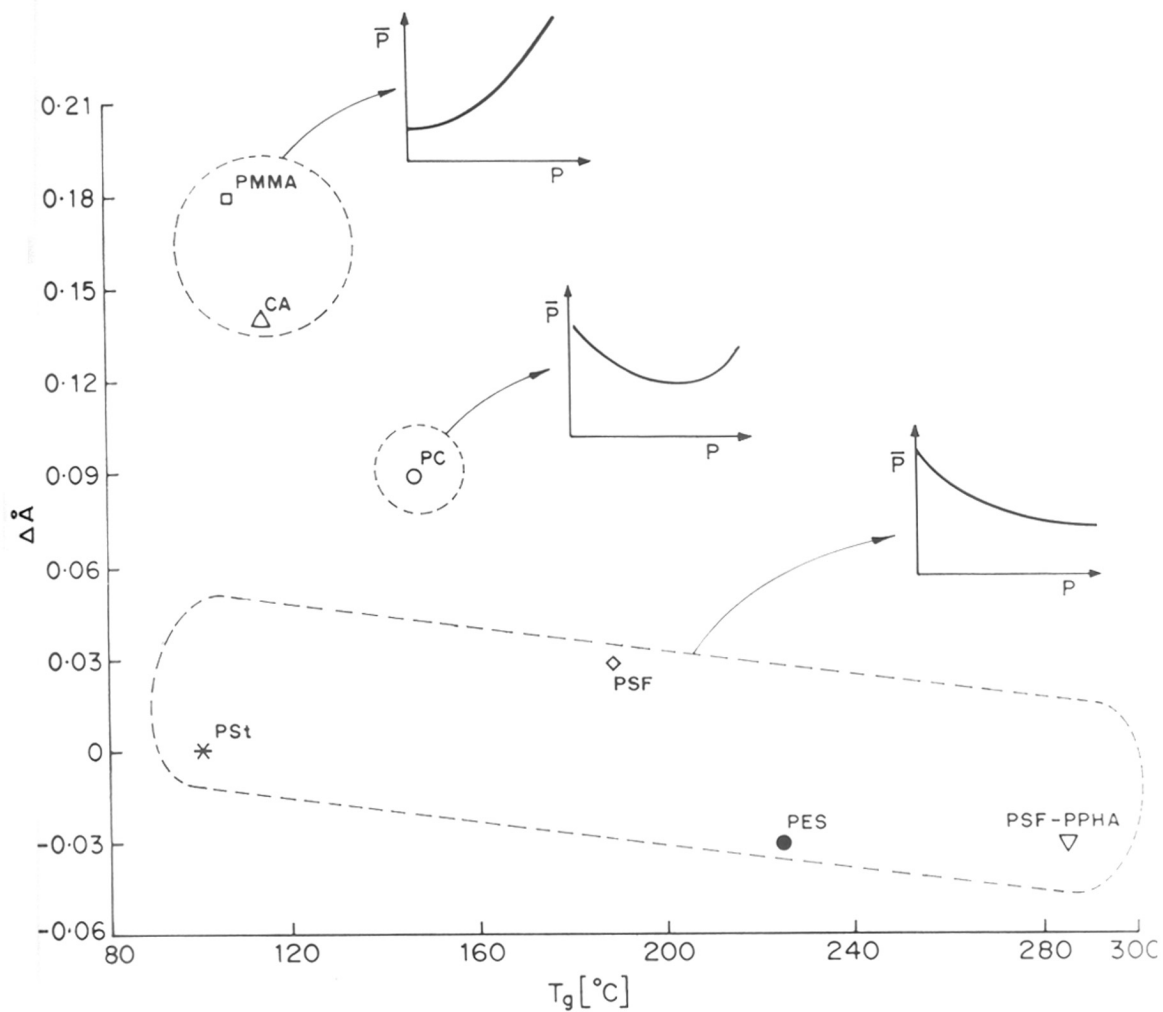
FIG.4·17:CHANGE IN AVERAGE INTERSEGMENTAL SPACING (d_{sp}) AS
A FUNCTION OF THE ORIGINAL GLASS TRANSITION
TEMPERATURE OF THE POLYMER. NOTE LOW SOLUBILITY
OF CO_2 IN POLYSTYRENE (PSt)

polymers are summarized in Table 4.14. Most of these data are at 20 atm and 35°C, with the exception of CA and polystyrene for which the data are reported at 30°C and 25°C respectively. The sorption behavior in each case has been analyzed in terms of the dual - sorption model. The total concentration c_T is divided into the components c_D (matrix dissolution) and c_H (microvoid filling). The increase in d_{sp} (Table 4.11) correlates qualitatively with c_D for all polymers with the exception of PSF-PPHA (Table 4.14). This is in agreement with the results of Fleming and Koros (1990) that volume dilation is caused only by the fraction of the sorbed gas which is associated with the Henry's law mode.

4.4.0 Permeation and hysteresis behavior in aromatic polyesters

In the preceding section the effect of pressure on the permeability of gases in glassy polymers has been classified into four categories. It has been shown that the permeability versus pressure characteristics can be correlated with the changes in d_{sp}. In this section, we attempt to investigate the molecular origin of the pressure dependence of permeability by measuring these properties using a well characterized family of aromatic polyesters based on the bridge and ring substituted bisphenol-A.

The molecular structures and important physical property data for the series of aromatic polyesters used in this study are shown in Fig. 4.18 and Table 4.15 respectively.

4.4.1 Permeability behavior of CO_2

The dependence of permeability of CO_2 on the driving

TABLE 4.14

Solubility of CO_2 in polymers studied.

Polymer	CO_2 sorbed[a] cc(STP)/cc(polym)			Reference
	Total [C_T]	'Matrix'[C_D]	'Sites'[C_H]	
PMMA	34.9	27.2	7.7	Sanders et al (1983)
CA[b]	41.1	21.0	20.1	Stern and DeMeringo (1978)
PSt[c]	18.2	11.4	6.8	Vieth et al (1966)
PC	29.5	13.7	15.8	Erb and Paul (1981)
PSF	28.8	13.3	15.5	Erb and Paul (1981)
PES	38.3	12.6	25.7	Sanders (1988)
PSF-PPHA	37.5	18.8	18.7	This work

a. At 20 atm. and 35°C.

b. At 30°C.

c. At 25°C.
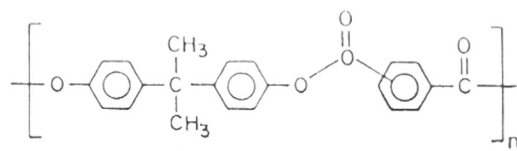
BIS-A-I/T
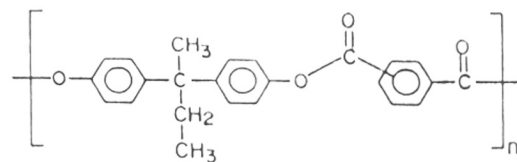
BIS(MEK)-I/T
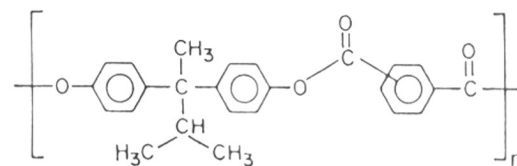
BIS(MIBK)-I/T
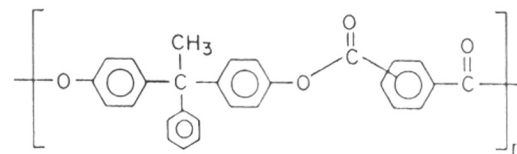
BIS(ACETO)-I/T
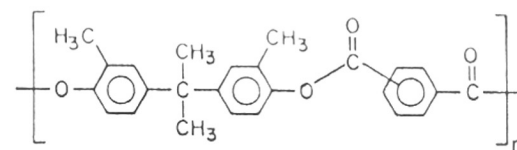
DMBIS-I/T
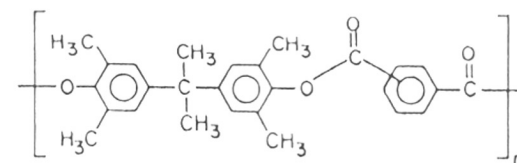
TMBIS-I/T
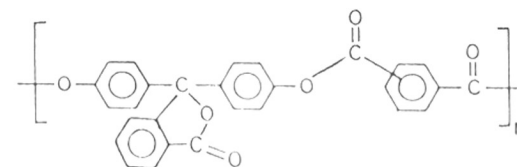
PPHA-I/T

FIG.4·18: REPEAT UNIT STRUCTURE OF POLYESTERS

152

TABLE 4.15

Physical properties of bridge and ring substituted aromatic polyesters

Property	Transitions ($^{\circ}$C)[a]			d_{sp}[b]
Polymer	T_{α}	T_{β}	T_{γ}	($\overset{\circ}{\text{A}}$)
BIS-A-I/T	198	84	$-$ 85	5.15
BIS(MEK)-I/T	190	--	$-$ 73	5.18
BIS(MIBK)-I/T	216	94	$-$ 72	5.21
BIS(ACETO)-I/T	247	--	$-$ 80	5.09
DMBIS-I/T	234	--	30	5.21
TMBIS-I/T	272	129	45	5.74
PPHA-25I/75T	285	--	--	4.98
PPHA-I/T	279	--	--	4.76

a. Determined by DMA at 100 Hz, heating rate 20°C/min.

b. Determined by wide angle X-ray diffraction (WAXD) using Bragg's equation, $n\lambda = 2d \sin \theta$

pressure for the virgin film (solution-cast) as well as the films exposed to 30 atm CO_2 for 24 hrs. is plotted and compared in Fig. 4.19- 4.25. The results are summarized in Table 4.16. This series shows two types of behavior 1) the permeability of CO_2 initially decreases with increasing the pressure and levels off with further increase in pressure (Figs. 4.19, 4.20, 4.22, 4.25 and 4.26) (type 4) 2) alternatively permeability increases with pressure (Figs. 4.21, 4.23 and 4.24) (type 3).

The permeability of CO_2 in aromatic polyesters which has a relatively mobile group substituted on the bridge carbon atom viz., BIS-A-I/T, BIS(MEK)-I/T, BIS(AETO)-I/T and phenolphthalein based polyarylates viz., PPHA-I/T and PPHA-25I/75T exhibit type 4 behavior. This behavior is in accordance with the dual-sorption theory. The samples BIS(MIBK)-I/T, DMBIS-I/T and TMBIS-I/T exhibit type 3 behavior. These are some of the few glassy polymers known presently in which permeability of CO_2 increases with driving pressure (Jordan et al 1989, Okamato et al 1990) after a critical pressure. The increase in permeability of CO_2 in these polymers can be attributed to the significant plasticization by CO_2 causing an increase in diffusion coefficient as a result of increase in intersegmental chain spacing. Although an increase in intersegmental chain spacing has been demonstrated (Table 4.17) the resultant increase in diffusion coefficient needs to be experimentally verified.

The increase in permeability of CO_2 with increase in pressure in the case of a structurally modified polyimide was attributed to the presence of the methyl group substituted on the phenyl ring (Okamato et al 1990). However, the permeability of

TABLE 4.16

Summary of the CO_2 permeability responses for solution-cast aromatic polyesters at 35°C

Polymer	Change in CO_2 permeability with increased driving pressure	
	Unconditioned	Conditioned[*]
BIS-A-I/T	Decrease	Decrease
BIS(MEK)-I/T	Decrease	Decrease
BIS(MIBK)-I/T	Increase then decrease	Increase then decrease
BIS(ACETO)-I/T	Decrease	Decrease
DMBIS-I/T	Increase then decrease	Increase then decrease
TMBIS-I/T	Increase then decrease	Increase then decrease
PPHA-25I/75T	Decrease	Decrease
PPHA-I/T	Decrease	Decrease

[*] 30 atm. CO_2, 24 hrs, room temperature.
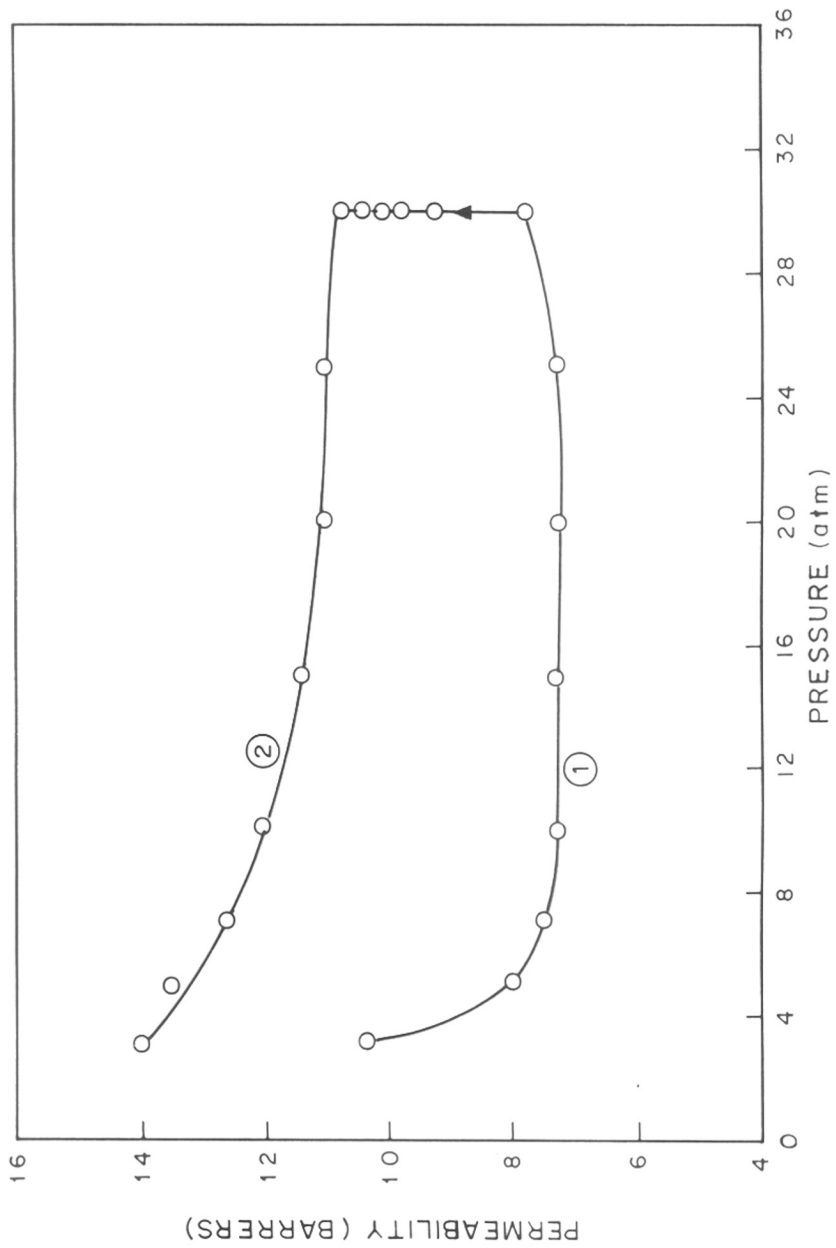
FIG.4·19:PERMEABILITY OF CO₂ IN SOLUTION-CAST BIS-A-I/T AT 35°C:
HYSTERESIS EFFECT
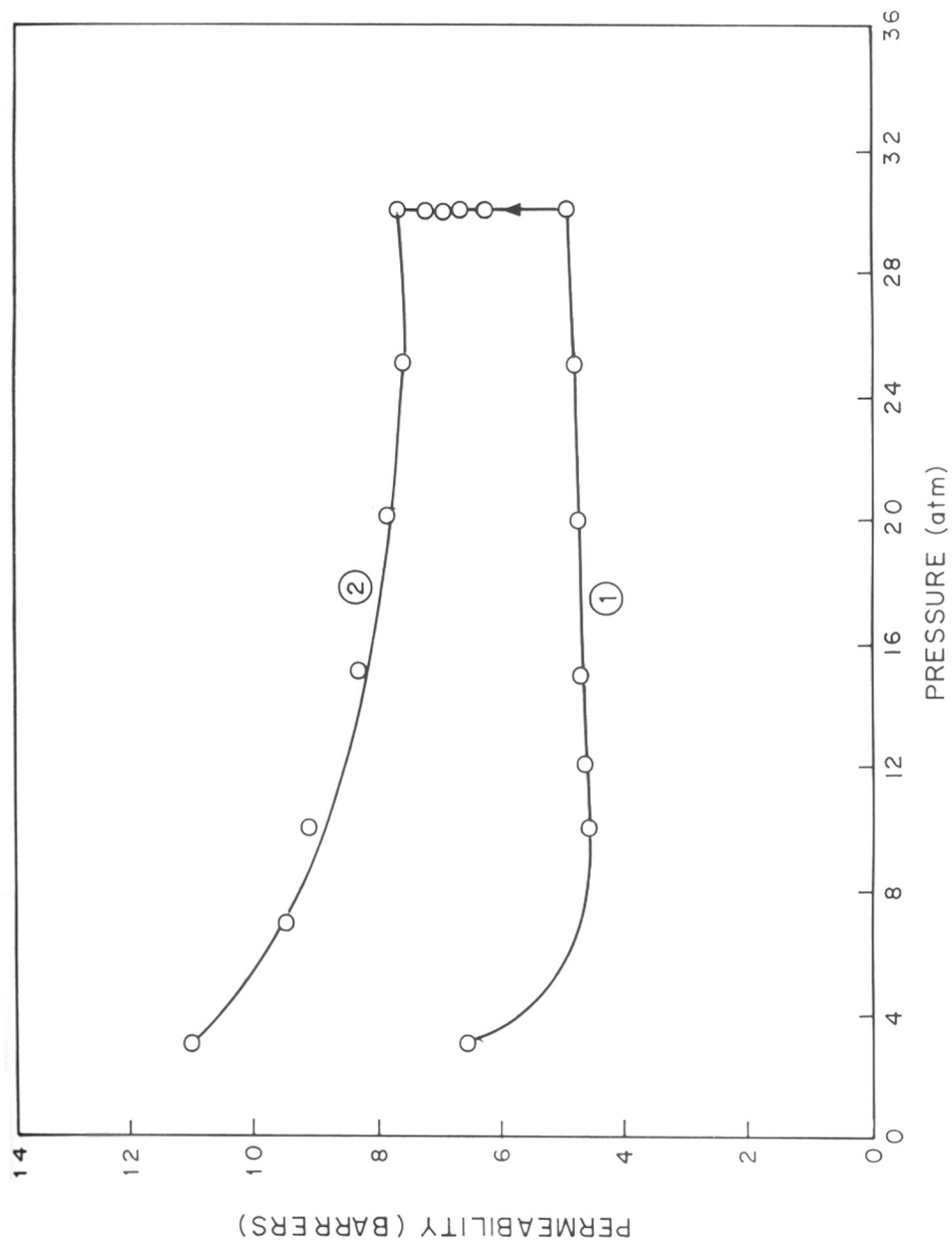
FIG.4·20:PERMEABILITY OF CO$_2$ IN SOLUTION-CAST BIS(MEK)-I/T AT 35°C : HYSTERESIS EFFECT
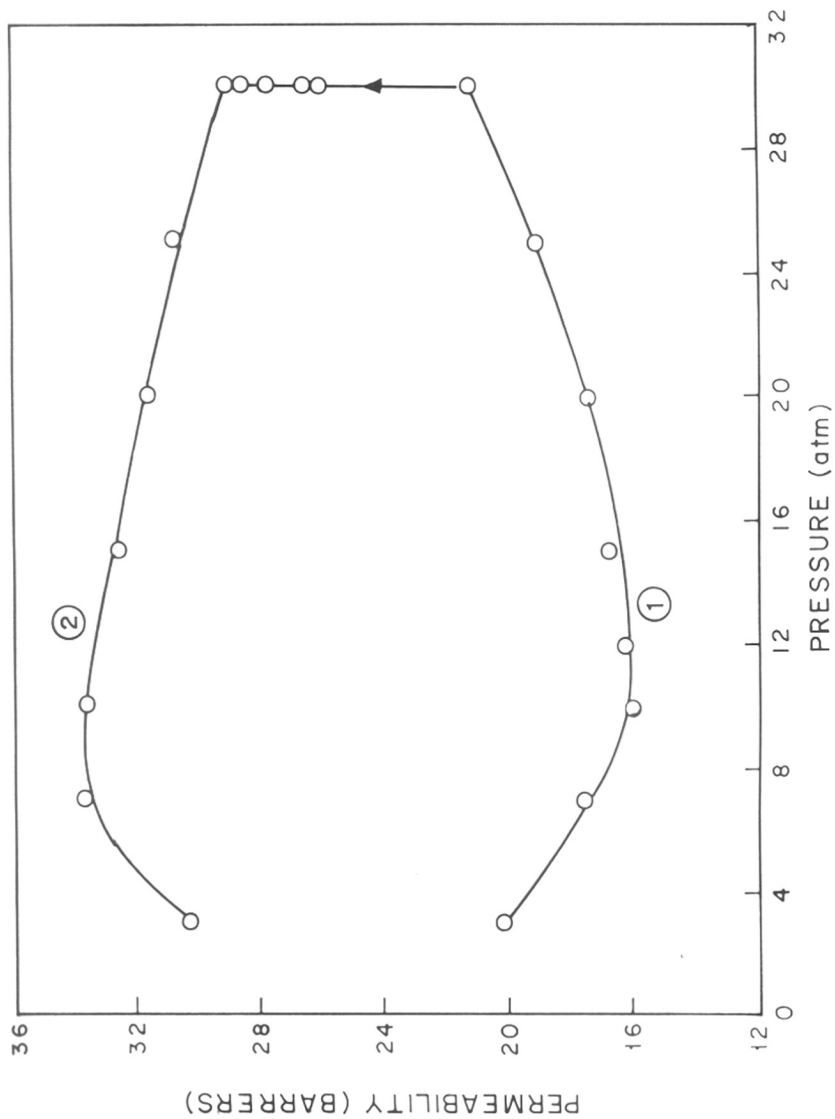
FIG.4·21:PERMEABILITY OF CO_2 IN SOLUTION-CAST BIS(MIBK)-I/T
AT 35°C :HYSTERESIS EFFECT.
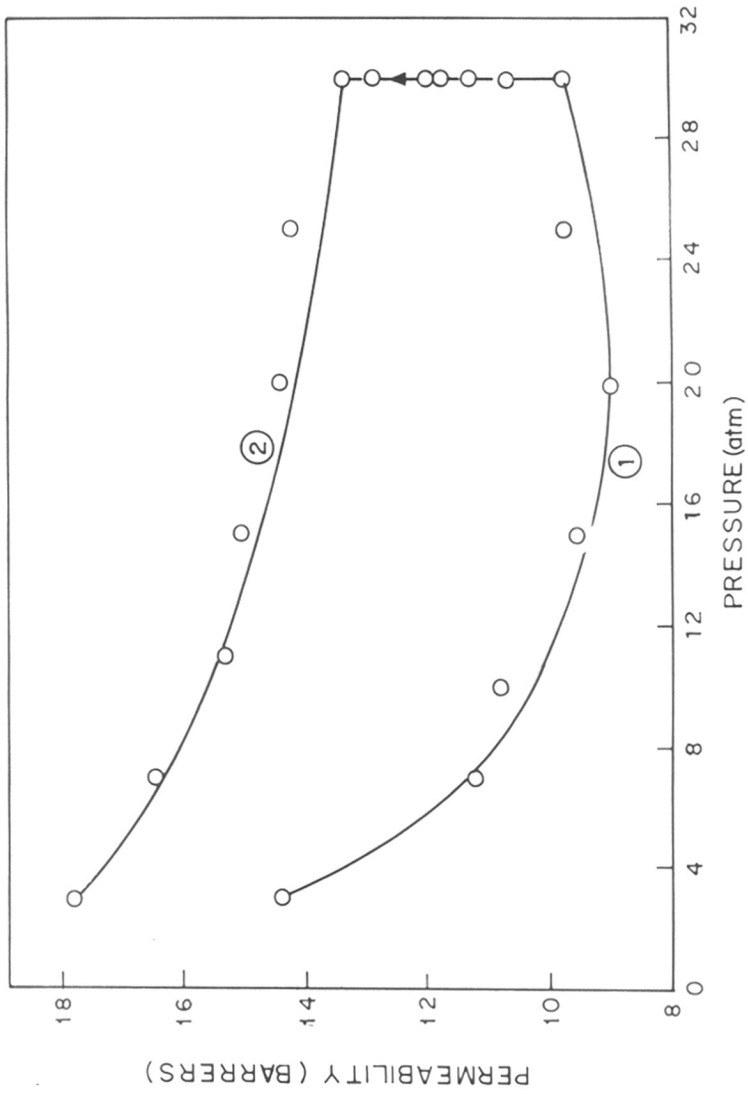
FIG. 4·22 : PERMEABILITY OF CO_2 IN SOLUTION-CAST BIS(ACETO)-I/T AT 35°C : HYSTERESIS EFFECT
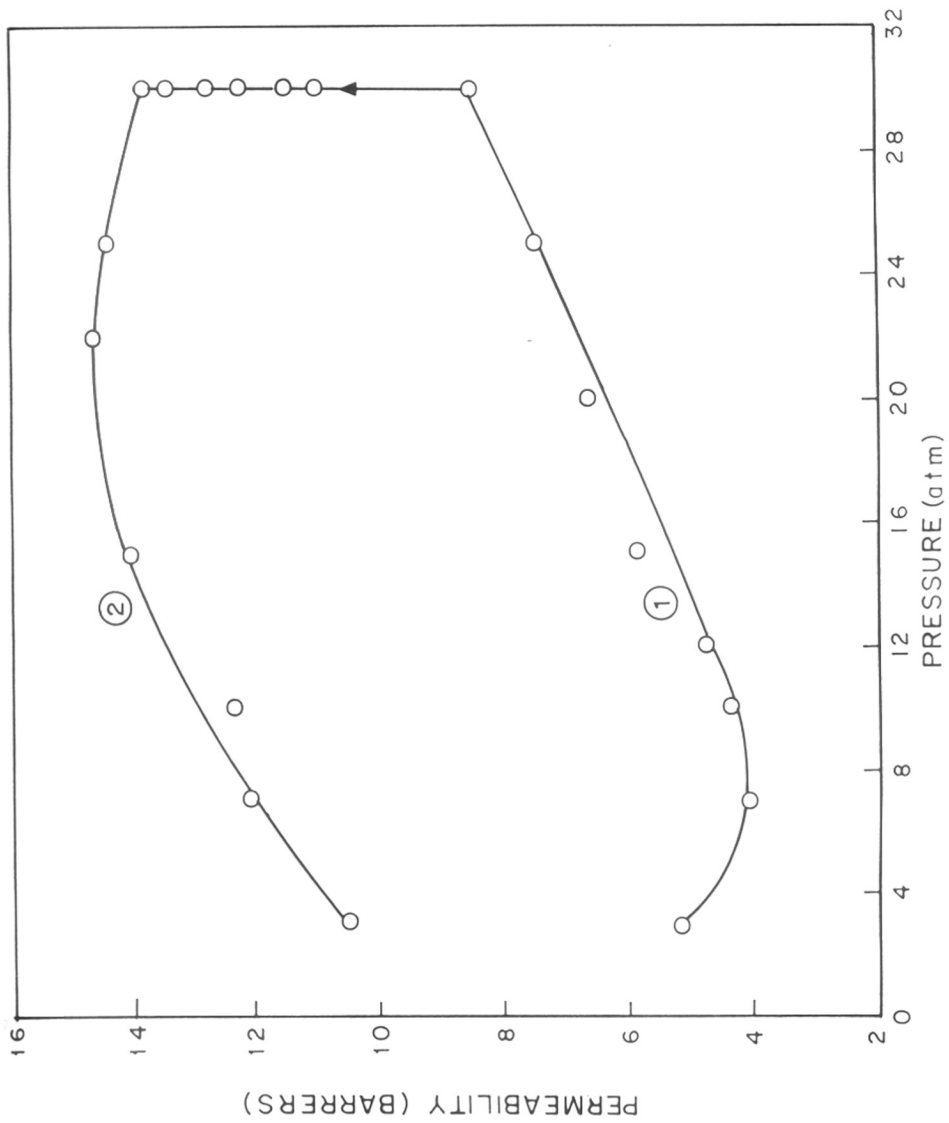
FIG.4·23 :PERMEABILITY OF CO$_2$ IN SOLUTION-CAST DMBIS - I/T
AT 35°C : HYSTERESIS EFFECT
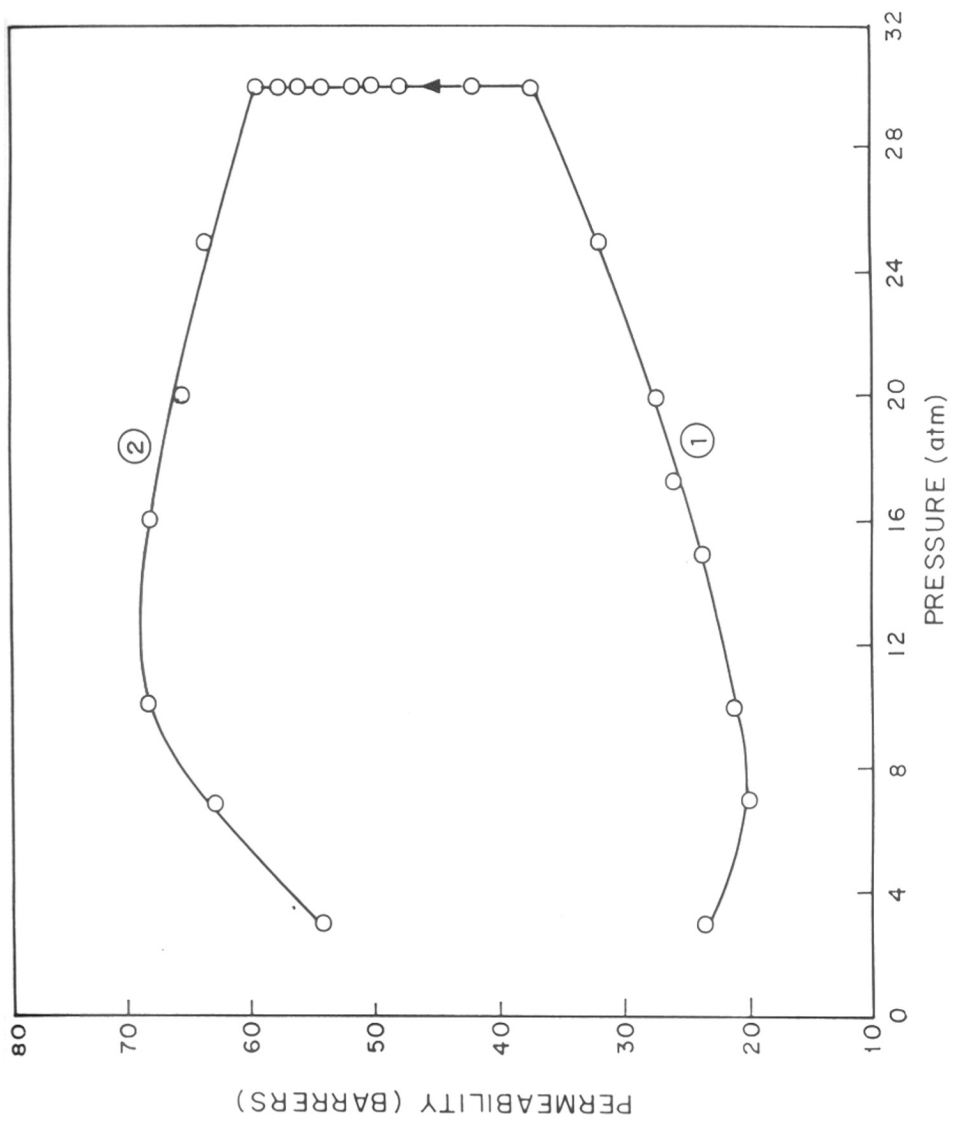
FIG.4.24 : PERMEABILITY OF CO$_2$ IN SOLUTION-CAST TMBIS-I/T
AT 35°C : HYSTERESIS EFFECT

161
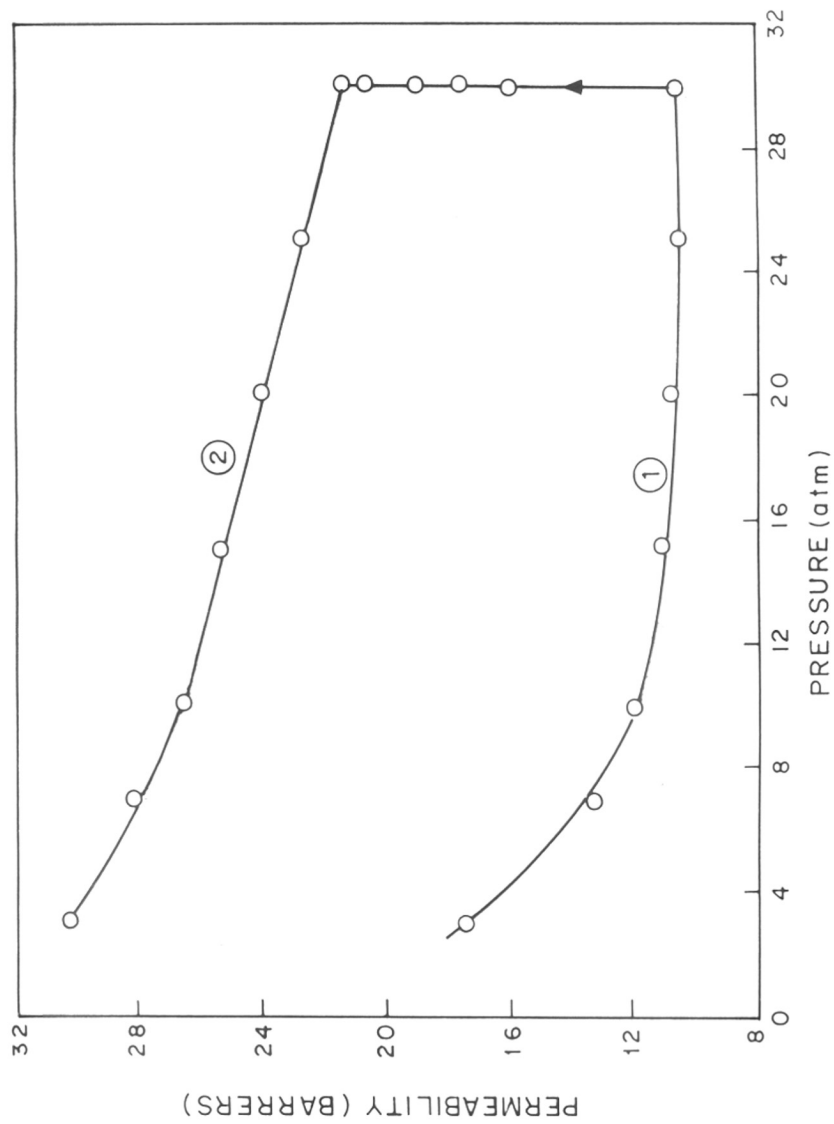
FIG. 4·25 : PERMEABILITY OF CO_2 IN SOLUTION-CAST PPHA-25I/75T AT 35°C : HYSTERESIS EFFECT
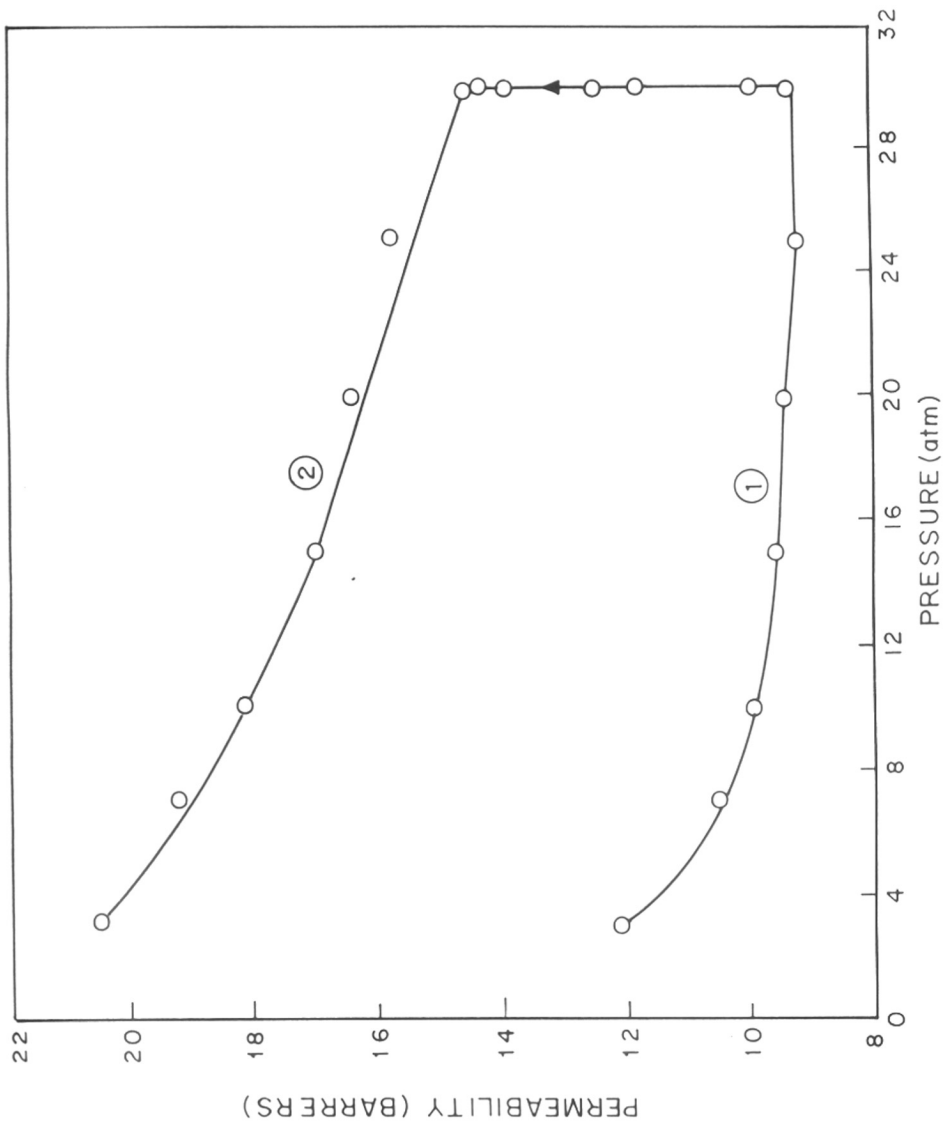
FIG 4.26: PERMEABILITY OF CO_2 IN SOLUTION-CAST PPHA-I/T AT 35° C : HYSTERESIS EFFECT

TABLE 4.17

Effect of CO_2-exposure on d_{sp} of aromatic polyesters

Polymer	d_{sp} ($\overset{\circ}{A}$)		
	Virgin	CO_2-Cond.[*]	(Cond - Virgin)
BIS-A-I/T	5.15	5.18	0.03
BIS(MEK)-I/T	5.18	5.21	0.03
BIS(MIBK)-I/T	5.21	5.57	0.36
BIS(ACETO)-I/T	5.09	5.13	0.04
DMBIS-I/T	5.21	5.33	0.12
TMBIS-I/T	5.74	6.06	0.32
PPHA-25I/75T	4.98	5.00	0.02
PPHA-I/T	4.76	4.79	0.03

[*] 30 atm. CO_2, 24 hrs, room temperature.

CO_2 in the case of PPO (Chern et al 1987) which has the similar structure resembles type 4 behavior. Although the variation in d_{sp} on exposure to CO_2 can explain the increase in permeability why a change in d_{sp} is observed only in certain polymers while the decrease in T_g results for all polymers, needs to be investigated further.

The pressure dependence of permeability results for the structuraly modified aromatic polyesters used in this investigation reveal that, the presence of mobile group accompanied by the change in d_{sp} could lead to the increase in permeability with pressure.

4.4.2 Hysteresis behavior

The permeability values of CO_2 for the polymers listed in Table 4.15 before and after exposure to CO_2 at 30 atm for one day are summarized in Figs. 4.19 - 4.26. Curve 1 in all the cases was obtained by measuring the permeability at incrementally increasing pressure upto 30 atm. The membrane was then exposed to CO_2 at 30 atm for 24 hrs. The permeability of the film to CO_2 was then measured as a function of decreasing pressure (curve 2). In each case the membrane was maintained at the test pressures for one hour prior to measurement.

The mobility in glassy polymers is very low. Besides depending upon the its history, it is far from equilibrium. Polymeric chains require a certain time to achieve a new organizational state. Thus the magnitude of effect of exposure to CO_2 depends on the time period (Erb and Paul 1981) and conditioning pressure (Fleming and Koros 1990). In this series of

experiments, the upstream pressure was kept constant at 30 atm and the permeability was periodically measured over a period of 24 hrs. Permeability coefficients initially increased rapidly but leveled off after about 20 hrs (see Fig. 4.27 and 4.28). These samples were selected as model polymers, representing the bridge and ring substituted aromatic polyesters used in this investigation respectively. Polymers used in Fig. 4.27 and 4.28 exhibit type 4 and type 3 permeability bahavior respectively. These results demonstrate that the polymers have attained an apparent equilibrium state after 24 hrs.

During plasticization, the CO_2 dissolved in the glassy polymer perturbs the local segmental organization. Desorption of CO_2 is followed by a slow relaxation of the dilated state. This process depends mainly on the relaxation time for the polymeric chains under experimental conditions.

The polymers which exhibit type 3 and type 4 behavior also exhibit qualitatively different hysteresis curves. The polymers BIS-A-I/T, BIS(MEK)-I/T, Bis(ACETO)-I/T, PPHA-25I/75T and PPHA-I/T exhibit continuous increase in permeability with decreasing pressure during depressurization. This indicates that these samples require a longer time to regain their unperturbed glassy state upon removal of CO_2. In these cases, curve 2 is flatter than curve 1 (see Figs. 4.19, 4.20, 4.22, 4.25 and 4.26 low pressure range), which is indicative of a decrease in the Langmuir sorption capacity. The second type of hysteresis curve is observed for BIS(MIBK)-I/T, DMBIS-I/T and TMBIS-I/T, Figs. 4.21, 4.23 and 4.24 respectively. Initially the permeability of
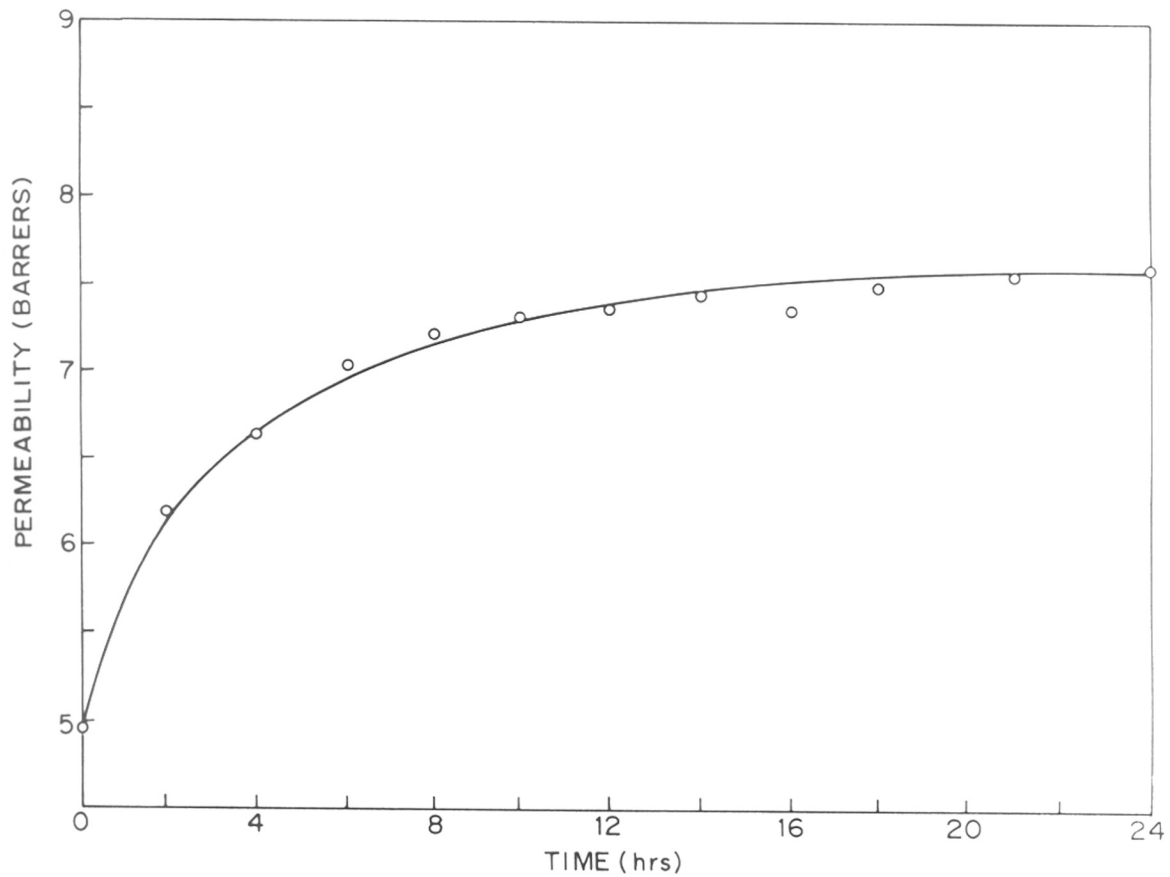
FIG.4·27:PERMEABILITY OF CO_2 AS A FUNCTION OF TIME FOR
SOLUTION-CAST BIS(MEK)-I/T AT 35°C , 30 atm
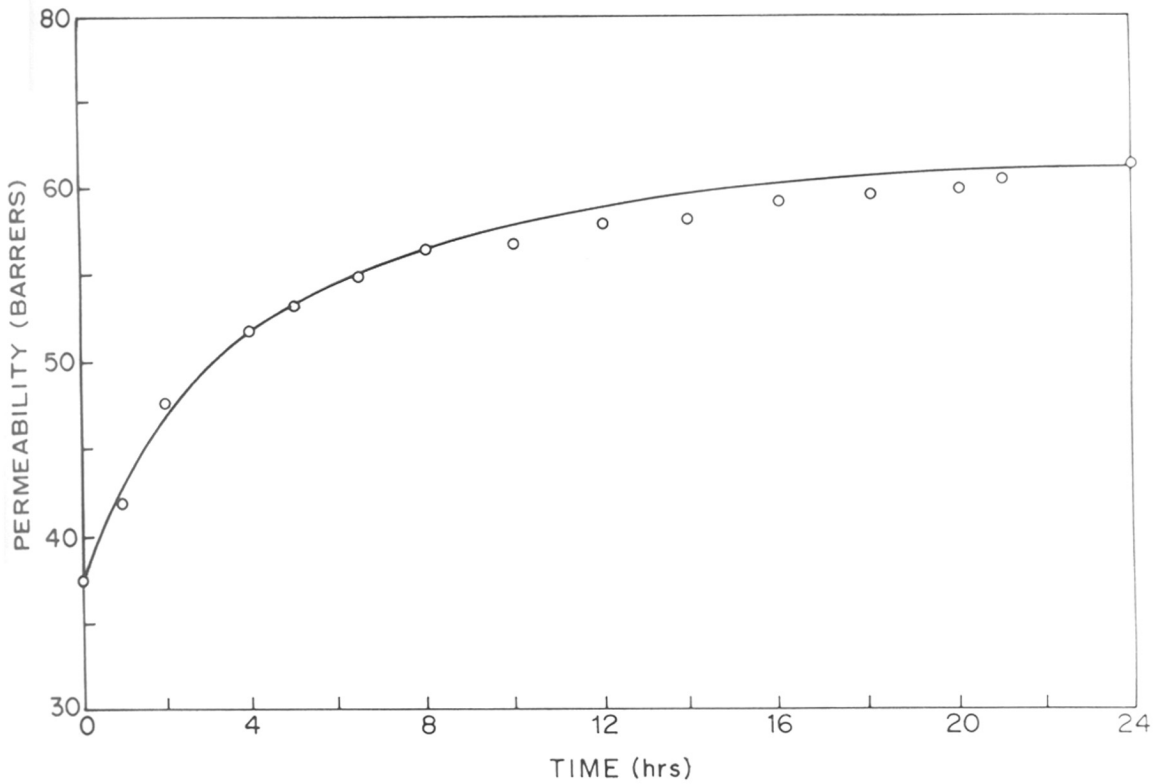
FIG.4·28:PERMEABILITY OF CO₂ AS A FUNCTION OF TIME FOR
SOLUTION-CAST TMBIS-I/T AT 35°C , 30 atm

CO_2 increases with decreasing pressure as expected. After a certain critical pressure, the permeability decreases indicating a collapse of the void volume.

Relative increase in permeability (Pr) of various gases for conditioned and virgin film is shown in Table 4.18. The value of Pr for CO_2 at 10 atm is plotted against the respective d_{sp} values in Fig. 4.29. It is clear that, Pr increases with the increase in d_{sp} for the highly rigid polymers PPHA-25I/75T, PPHA-I/T, DMBIS-I/T and TMBIS-I/T with high Tg. However, in the case of the bridge substituted polymers the variation in intersegmental chain spacings are too small to draw any conclusions.

4.4.3 Effect of CO_2 conditioning on permeability of non polar gases

The permeabilities for Helium (He), Argon (Ar), Oxygen (O_2), Nitrogen (N_2) and Methane (CH_4) were measured in that order at 10 atm and $35^{O}C$ for the unconditioned film. After these measurements, the films were exposed to CO_2. Then the permeability for these gases was measured in the reverse order. The time required for the completion of this study was 20-24 hrs after CO_2 conditioning was over. The results are summarized in Table 4.18.

Permeabilities of gases measured subsequent to CO_2 conditioning are strongly influenced by the extent to which the polymer returns to its undilated state (Jordan et al 1989). For example, at ambient conditions, a polycarbonate sample took 6-8 weeks to regain its original state (Jordan et al 1989). A similarly dilated sample returned to its original state within

169

Table 4.18

Comparison of permeability and relative permeability $(P_r)^b$ for various gases in solution-cast aromatic polyester films at 10 atm and 35°C

Polymer	He		Ar		O_2		N_2		CH_4		CO_2	
	Vir	P_r	Vir	P_r	Vir	P_r	Vir	P_r	Vir	P_r	Vir	P_r
BIS-A-I/T	16.0	1.15	0.56	1.84	1.39	1.48	0.33	1.88	0.40	1.68	7.31	1.65
BIS(MEK)-I/T	12.8	1.14	0.57	1.28	0.90	2.44	0.236	2.29	0.166	2.95	4.55	2.00
BIS(MIBK)-I/T	29.0	1.07	1.71	1.21	3.52	1.06	0.53	1.89	0.61	2.42	15.93	2.11
BIS(ACETP)-I/T	15.9	1.15	0.74	1.18	2.13	1.10	0.32	1.38	0.46	1.63	10.83	1.42
DMBIS-I/T	14.0	1.24	0.66	2.28	0.52	2.83	0.19	3.05	0.17	3.24	4.36	2.83
TMBIS-I/T	36.6	1.44	1.95	1.62	4.28	1.74	0.86	2.16	0.75	2.75	20.86	3.27
PPHA- 25I/75T	15.5	1.61	1.18	1.62	2.19	1.57	0.44	1.95	0.475	2.32	12.0	2.21
PPHA-I/T	12.7	1.54	0.94	1.66	2.05	1.34	0.37	1.85	0.398	2.41	18.17	1.82

a $P \times 10^{10}$ [cc(STP).cm / cm^2.Sec.cmHg]

b $P_r = P_{conditioned}^c / P_{virgin}$

c 30 atm CO_2, 24 hrs, room temperature
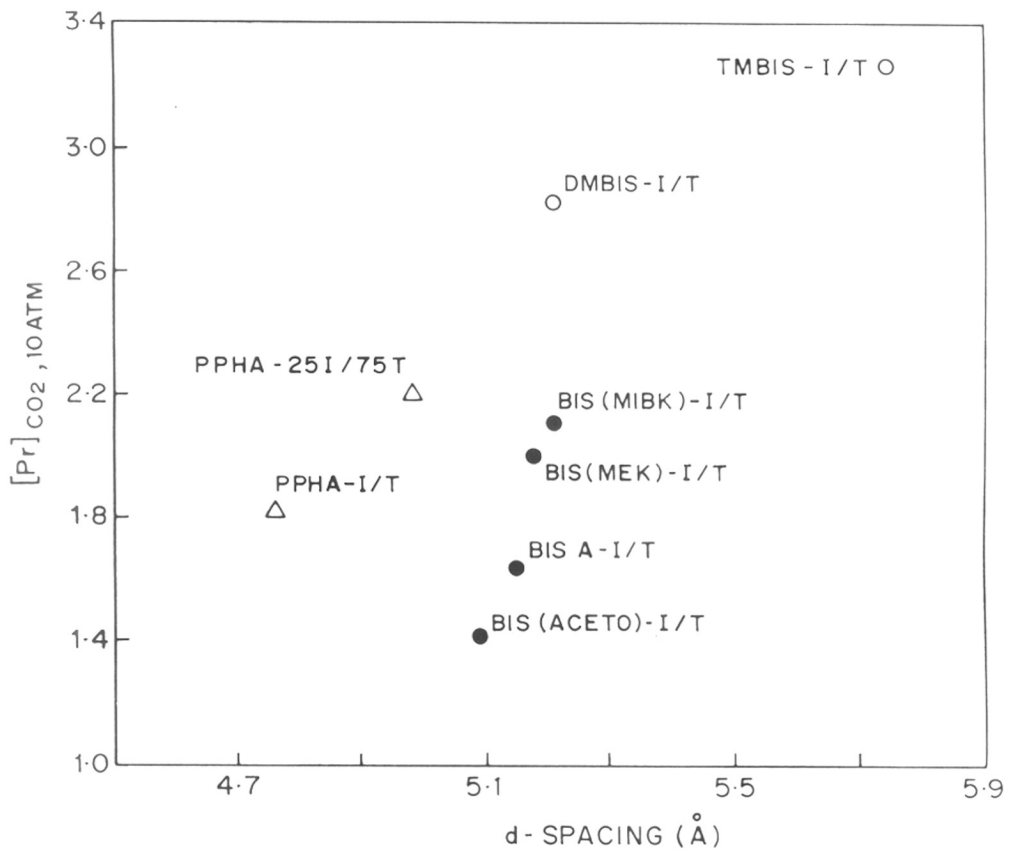
FIG.4·29:RELATIVE PERMEABILITY OF CO_2 AT 10 atm
AGAINST d_{sp}

one week on thermal annealing at $120^{\circ}C$ (see section 4.3.2). These results demonstrate that glassy polymers with high T_g remain in the dilated state for a longer time at ambient conditions due to their long relaxation times. Thus, the observed range of Pr values for He 1.07 [BIS(MIBK)-I/T] and 1.61 [TMBIS-I/T] appears reasonable.

The relative change in permeability (Pr) caused by exposure to CO_2 increases with the molecular size of the penetrant gas in the case of more rigid polymers viz. PPHA-25I/75T, PPHA-I/T, DMBIS-I/T and TMBIS-I/T (see Fig. 4.30 and 4.31). However, no correlation could be found in the case of the bridge substituted polymers (Fig. 4.32). The results for DMBIS-I/T, TMBIS-I/T,PPHA-25I/75T and PPHA-50I/50T show that, the enhancement in void volume and its distribution caused by dilation is favorable for the permeation of larger penetrants (see Fig. 4.30 and 4.31) similar to that observed in the case of PSF-PPHA (see section 4.2.4).
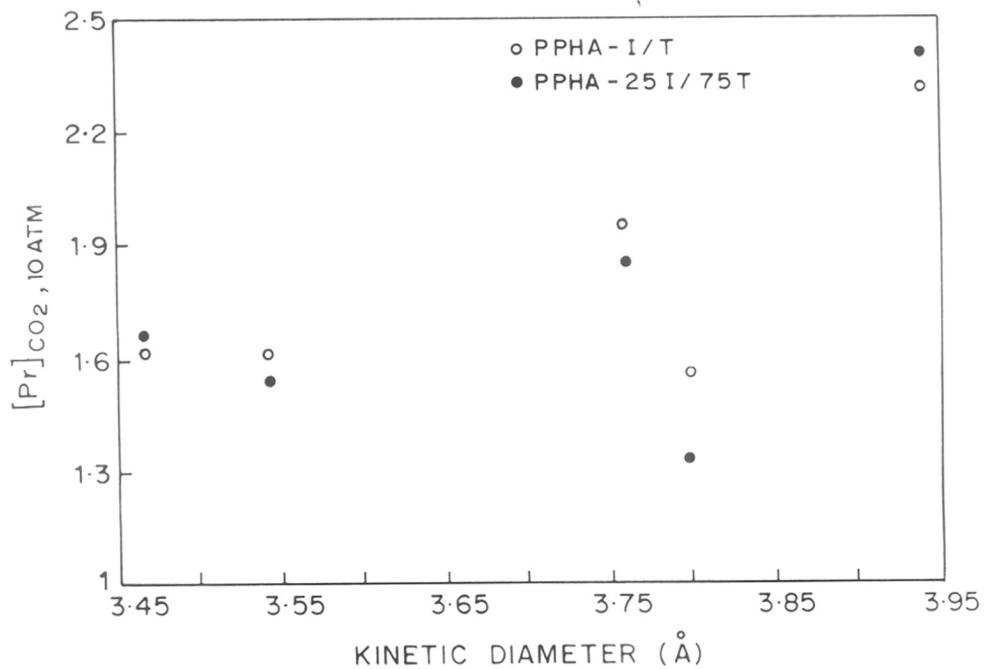
FIG.4·30:RELATIVE PERMEABILITY IN CO_2-CONDITIONED
PPHA-25I/75 T AND PPHA-I/T
AT 35°C AGAINST KINETIC DIAMETER OF GAS
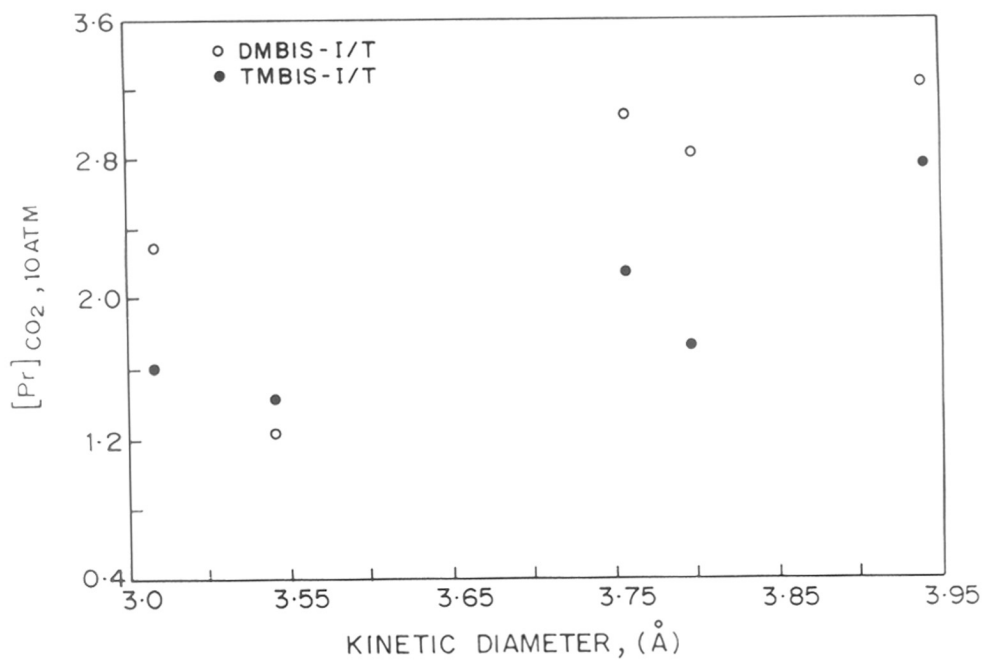
FIG.4·31:RELATIVE PERMEABILITY IN CO_2-CONDITIONED DMBIS-I/T AND TMBIS-I/T AT 35°C AGAINST KINETIC DIAMETER OF GAS
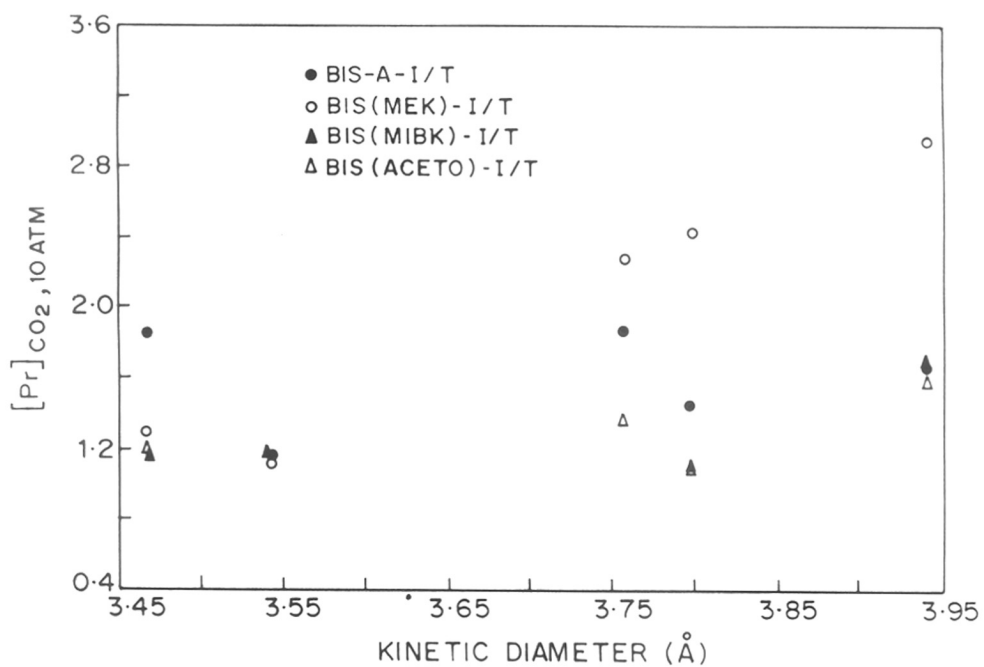
FIG. 4·32: RELATIVE PERMEABILITY IN CO_2-CONDITIONED
BRIDGE SUBSTITUTED AROMATIC POLYESTER AT 35°C
AGAINST KINETIC DIAMETER OF GAS

CHAPTER - V

CONCLUSIONS

CONCLUSIONS

Effect of ester and ether linkages on physical and transport properties of polysulfones

Direct substitution of the ether linkage in PSF with an ester linkage as in PAES leads to an enhancement in both the rigidity (T_g) and openness (d_{sp}) of the polymer. However, incorporation of an additional ether linkage in the case of PA1 did not result in further enhancement. In comparison to PSF, PA1 has similar rigidity and openness.

In comparison to PSF, both PAES and PA1 are more permeable to polar gases such as CO_2 and less permeable to non condensable (low T_c) gases viz. Ar, N_2. The permeability value for CH_4 remains relatively unaltered. As a result, the permselectivity for polar gases such as CO_2 over CH_4 or N_2 is increased in PAES and PA1. However, the permselectivity for the system O_2/N_2 is lowest in the case of PAES having more open structure. The permselectivity for the systems He/CH_4 is not drastically affected. The increased permeability and permselectivity of CO_2 arises from the fact that the presence of the additional ester group in the case of PAES and PA1 increases the polymer-penetrant interaction and thereby the solubility of CO_2. The solubility of CH_4 is not affected and the solubility of Ar and N_2 is actually decreased. The diffusivity of various gases in the three polymers viz. PAES, PA1 and PSF does not bear a simple correlation with the intersegmental chain spacing.

Effect of isomerism

Replacement of the para linkage (PA1) in the diacid chloride of the repeat unit by meta substituted diacid chloride (PA2) leads to a decrease in T_g as well as d_{sp}. The values for the polymer containing both para/meta linkages lie within the two limits. The permeability of CO_2 in PA1 is more than 3.5 times that of PA2, while, the permselectivities for CO_2/CH_4 are similar (within 13 %). The permeability values for other non polar gases are also lower in the case of PA2 than in PA1. The permeabilities of gases in the polysulfone synthesized from mixed acid chloride isomers (PA3), lie within the limiting values for the two polymers PA1 and PA2.

Since PA2 has a lower d_{sp} value than that of PA1, one would expect lower permeabilities and higher permselectivity values for PA2. As the d_{sp} is decreased from 5.33 $\overset{\circ}{A}$ (PAES) to 4.76 $\overset{\circ}{A}$ (PA2), there are marked changes in the diffusivity selectivity. Diffusivity is more dramatically affected for larger molecules such as CH_4 or N_2 than for smaller molecules such as He. This has significant effects on both permeability and permselectivity. The resulting changes in permeabilities and permselectivities of various polysulfones are seen most dramatically for the system He/CH_4. Initially, both permeability and permselectivity increase slightly with an increase in the value of d_{sp} from 4.76 $\overset{\circ}{A}$ (PA2) to 4.92 $\overset{\circ}{A}$ (PA3). A sudden change is observed at d_{sp} = 4.95 $\overset{\circ}{A}$ (PSF, PA1) when He/CH_4 selectivity drops dramatically as the permeability of CH_4 is enhanced significantly. Subsequent increases in d_{sp} lead to relatively constant permeability and permselectivity values.

177

Another unusual effect is the variation in permselectivity for CO_2/N_2 in the isomer series PA1-PA3. As expected, PA2 (d_{sp} = 4.76 Å) and PA3 (d_{sp} = 4.92 Å) exhibit lower permeabilities for both CO_2 and N_2. In PA1 (d_{sp} = 4.98 Å), the permeability of CO_2 has increased markedly while the corresponding increase in the case of N_2 was far less significant. As a result the selectivity value for CO_2/N_2 in PA1 is higher than that in PA2.

Sorption and transport of various gases in phenolphthalein based polysulfone (PSF-PPHA)

This work was undertaken to investigate the effect of substitution of the isopropylidine unit in bisphenol-A by a bulky phthalide ring. The corresponding polysulfone was synthesized by the condensation of phenolphthalein (PPHA) and difluro diphenylsulfone. PSF-PPHA is more polar, has a higher T_g and a more open structure than either PSF or PES. Compared to PSF, PSF-PPHA exhibits 50 - 100 % higher permeabilities for CO_2, CH_4, N_2, and Ar. The presence of additional ester group in the phthalide moiety in the case of PSF-PPHA also leads to higher (20-25 %) solubilities for both CO_2 and CH_4. The pure gas sorption and permeation results for pure as well as mixed gas systems are in accordance with the dual-sorption model. Inspite of the higher glass-transition temperature of PSF-PPHA, the value for C_H is ~ 40 % lower than that for PES and similar to that for PSF. However, the total solubility in the Langmuir mode of sorption ($\sim C_H'b$) is ~ 150 - 300 % higher than that for PSF and PES. The D_H values for CO_2 and CH_4 are also ~ 100 % higher in PSF-PPHA as compared to the corresponding values for PSF. However, the D_D

178

values for these gases are similar in both the polymers. The permeability of gases through the fixed sites (Langmuir mode) is a more significant mode of transport in PSF-PPHA compared to PSF or PES.

Effect of CO_2 conditioning on properties of phenolphthalein based polysulfone (PSF-PPHA)

"Conditioning" of the polymer in the case of PSF-PPHA exposed to high pressure CO_2 was studied using WAXD, DMA, dilatometry and direct sorption and permeation measurements. The conditioning phenomenon in PSF-PPHA appears to arise from increased chain flexibility or from chain rearrangement without significant effect on intersegmental chain spacing. By comparing CH_4 sorption isotherms in conditioned and virgin PSF-PPHA samples it was observed that the conditioned PSF-PPHA specimen exhibits ~ 6 % higher sorption levels for CH_4 than the virgin one. The increase in overall sorption level stems from an enhanced sorption capacity in the glassy matrix. The amount of gas sorbed in the Henry's law mode is relatively constant and may even decrease (< 13 %). The increase in C_H' can be attributed to the failure of the glassy polymer to regain its original state after evacuation of the CO_2 because of the long relaxation time of the polymer. Selectivities for the system CO_2/CH_4 in PSF-PPHA are relatively less affected as compared to polysulfone based on bisphenol-A being used as membrane material commercially.

An increase in permeability is observed for all the gases studied as a result of prior CO_2 treatment. As in the case of CH_4, this enhancement in permeabilities could be due to both

179

higher solubility as well as higher diffusivity. The value of Pr ($Pr = P_{cond} / P_{virgin}$) tends to increase with increase in the critical temperature (T_c) and kinetic diameter (σ) of the penetrant gas, Helium however was an exception to this trend.

The molecular origin of the conditioning process requires further study.

Pressure permeability behavior in glassy polymers

WAXD has been used as a probe to quantify the effect of gas-polymer interaction on the average intersegmental spacing in glassy polymers. The permeability versus pressure profiles of glassy polymers can be classified into four distinct categories.

Type 1. On plasticization, the Tg of the glassy polymer decreases below the temperature of the permeation experiment. The polymer then behaves like a typical rubbery polymer.

Type 2. The polymer remains in the glassy state; however, its permeability profile resembles that of a rubbery polymer.

Type 3. The permeability decreases with increasing pressure upto a critical pressure. Subsequent increase in pressure results in an increase in permeability.

Type 4. The permeability characteristics vary in accordance with the predictions of dual-sorption theory. However, permeability is influenced by the exposure of the polymer to highly soluble gas such as CO_2 at high pressures (the "conditioning" effect).

While permeability profiles in these polymers are very different, the decrease in glass transition temperature, brought

about by exposure to CO_2 is of the same order of magnitude. However, the observed increase in the intersegmental chain spacing follows a definite trend which can be correlated with the experimentally observed permeation profiles. The increase in d_{sp} is highest for polymers such as CA and PMMA which exhibit type 2 behavior. The polymers which exhibit type 4 behavior (polysulfones) do not show any significant change in d_{sp} while the changes brought about in polycarbonate which exhibits type 3 behavior lie within these two extremes.

Permeation and hysteresis behavior in aromatic polyesters

In order to illustrate the role of polymer structural attributes of the polymer on permeation and conditioning behavior, a series of bridge and ring substituted aromatic polyesters were investigated. The ring substituted polymers viz., DMBIS-I/T and TMBIS-I/T and the bridge substituted polymer [BIS(MIBK)-I/T] exhibit type 3 behavior. The other bridge substituted polymers viz., BIS-A-I/T, BIS(MEK)-I/T, BIS(ACETO)-I/T, and phenolphthalein based polyarylates, PPHA-I/T AND PPHA-25I/75T, exhibit type 4 behavior. These results can be correlated with the corresponding changes in the d_{sp} values of these polymers on exposure to high pressure CO_2. This illustrates that the presence of the mobile group accompanied by the increase in d_{sp} on exposure to high pressure CO_2 leads to the increase in permeability with increase in pressure.

The effect of high pressure CO_2 was further investigated by measuring the permeabilities at gradually increasing and then gradually decreasing pressures. A permeability hysteresis curve

was thus constructed. The pressure dependence of permeabilities shown by these hysteresis studies can be attributed to the differences in the recovery of additional frozen free volumes in the dilated specimens.

CHAPTER - VI

SUGGESTIONS FOR FUTURE WORK

6.0.0   SUGGESTIONS FOR FUTURE WORK

The present investigation illustrates how newer membrane materials which would offer higher flux and permselectivity for the desired gas can be synthesized. The role of chemical composition on the sorption and transport properties of polysulfones has been highlighted. In addition to these primary effects of structural variation on transport properties, effects of exposure to high pressure CO_2 are also discussed.

1) It was shown that the affinity for CO_2 over CH_4 in the polysulfone series could be enhanced by incorporating ester groups in the backbone as well as by substituting a phthalide ring at the bridge carbon atom. It would be worthwhile to validate the utility of this approach by incorporating such groups in other bisphenol-A based polymers.

2) On the basis of their intrinsic permeation and separation properties, polymers PAES, PA1 and PSF-PPHA have been found to be superior to bisphenol-A based polysulfone. Additionally the permeation / separation characteristics of phenolphthalein based polysulfone (PSF-PPHA) have been found not to be adversely affected on exposure to CO_2. It will be interesting to cast these in the form of asymmetric membranes and evaluate the performance of asymmetric membranes.

3) It was shown that the CO_2 treated PSF-PPHA exhibits 210 % higher permeability for CO_2 than in the solution-cast specimen. The validity of using carefully controlled penetrant conditioning procedures as an additional means of

tailoring the membrane materials for gas separation needs to be further investigated.

4) Conditioning effects in the glassy polymers have been systematically categorized on the basis of the pressure dependence of CO_2 permeability and WAXD measurements. In the case of phenolphthalein based polysulfone (PSF-PPHA), although exposure of the polymer to high pressure CO_2 resulted in an enhancement in the permeability of the polymer, intersegmental chain spacing remained unchanged. The change in the permeability therefore appears to be the result of increase in the segmental mobility. This needs to be further confirmed by mobility measurements using solid state NMR techniques.

APPENDICES

APPENDIX - III.1

Source and purities of chemicals used for synthesis

Chemical	Grade or Purity	Supplier
Tosoyl chloride	AR Grade (99.7 %)	M/S Aldrich, USA
Toluene	AR Grade	M/S Loba Chemie., Bombay.
Aluminium tri chloride ($AlCl_3$ (Anhydrous)	LR Grade	M/S S.D. Fine Chemicals Bombay.
1,2-dichloro-ethane (EDC)	LR Grade	M/S S.D. Fine Chemicals Bombay.
Glacial Acetic Acid (GAA)	AR Grade	M/S S.D. Fine Chemicals Bombay.
Chromium-trioxide (CrO_3)	AR Grade	M/S S.D. Fine Chemicals Bombay.
Sulfuric acid (H_2SO_4)	LR Grade	M/S S.D. Fine Chemicals Bombay.
Hydrochloric acid (HCl)	LR Grade	M/S S.D. Fine Chemicals Bombay.
Sodium hydroxide (NaOH)	AR Grade	M/S S.D. Fine Chemicals Bombay.
Sodium carbonate (Na_2CO_3)	AR Grade	M/S S.D. Fine Chemicals Bombay.
Thionyl chloride ($SOCl_2$)	AR Grade	M/S Loba Chemie., Bombay.
4,4'-Difluo-diphenyl sulfone (DFDPS)	99.8 %	M/S Aldrich, USA.
Phenolphtha-lein (PPHA)	ACS Reagent	M/S Loba chemie., Bombay.
N,N'-dimethyl-acetamide (DMAc)	LR Grade	M/S Loba Chemie., Bombay.
Potassium carbo-nate (K_2CO_3)	AR Grade	M/S Loba Chemie., Bombay.

Bisphenol-A (BIS-A)	99.9 %	M/S Aldrich, USA.
Benzyl triethyl-ammonium chloride (BTEAC)	99.9 %	M/S Aldrich, USA.

Source and specifications of commercial polymers used

Polymer	Commercial name & grade	Source	Casting solvent
Polymethyl-methacrylate (PMMA)	Acrypole 932 HR	GSFC India	Chloroform
Cellulose-acetate (CA)	CA 398-30	Eastman Kodak	Acetone
Polycarbonate (PC)	Lexan	General Electric	Dichloromethane
Polysulfone (PSF)	Udel P-1700	Union Carbide	Chloroform
Polyether-sulfone (PES)	Victrex	ICI	Chloroform
Polystyrene (PSt)	Polystron MCG-100	Polychem Ltd. India	Toluene

APPENDIX - III.3

Purity and supplier of gases

Gas	Specificationn	Supplier
Helium (He)	IOLAR-2 (99.9 %)	M/S Indian Oxygen Ltd., Bombay.
Argon (Ar)	IOLAR-2 (99.9 %)	M/S Indian Oxygen Ltd., Bombay.
Oxygen (O_2)	IOLAR-2 (99.9 %)	M/S Indian Oxygen Ltd., Bombay.
Nitrogen (N_2)	IOLAR-2 (99.9 %)	M/S Indian Oxygen Ltd., Bombay.
Methane (CH_4)	Speciality Mixture (99.2 %)	M/S Indian Oxygen Ltd., Bombay.
Carbondioxide (CO_2)	Research grade (99.5 %)	M/S Bombay Carbondioxide Corpn., Bombay.
$CO_2 : CH_4$ Mixture	55 : 45 (mole ratio)	M/S Indian Oxygen Ltd., Bombay.

Source and specifications of components used for sorption and permeation apparatus

Item	Specifications	Supplier
Transducer	Range - 0-500 psia 0-1000 psia Model - TH-1	M/S T-Hydronics, USA
Transducer indicator	5 1/2 digit Model - 1028	M/S T-Hydronics, USA
Bourdon pressure gauze	Range - 0-1000 psia Heise make Model - CM 43641	M/S Dressor Ind., USA
Bellow seal valve	SS 316, End conn. - 1/8" NPT Type - SS 2H	M/S Creximco, USA
Needle valve	SS 316, End conn. - 1/8" NPT	M/S Astek, Bombay India
Three way ball valve	SS 316, End conn. - 1/8" NPT	M/S Astek, Bombay India
Union Tee & Cross, Male and Female connectors	SS 316, End conn. - 1/8" NPT	M/S Chromato-pak Bombay, India
Tubing	SS 316, O.D - 1/8"	M/S Chromato-pak Bombay, India
Porous plate	SS 316, 5 μ	M/S Kumar Process Bombay, India
Cathetometer	L.C.- 0.005 mm	M/S Electrofones, Ambala Cant, India.

APPENDIX - III.5

Summary of volume calibration results

Expt. No.	Volume (cc)			% Deviation from mean		
	V_A	V_B	V_R	V_A	V_B	V_R
A	20.9041	19.2056	100.9111	+ 0.35	+ 0.45	+ 1.38
B	20.9336	19.1840	100.2729	+ 0.49	+ 0.34	+ 0.74
C	20.7565	19.1255	100.9923	− 0.35	+ 0.03	+ 0.56
D	20.7661	19.1474	99.6143	− 0.31	+ 0.15	+ 0.08
E	20.5199	18.9492	97.5962	− 1.49	− 0.88	− 1.94
F	21.1032	19.0979	98.7189	+ 1.31	− 0.10	− 0.82
G	20.9925	18.9607	99.7337	+ 0.77	− 0.82	+ 0.20
Mean	20.8306	19.1183	99.5343			

APPENDIX - III.6

Complex method of Box

The optimization method of Box -- complex method -- is capable of handling a large polygon of more than $n+1$ vertices, where n is the number of parameters to be estimated. This figure generated can expand and contract in any or all directions and can extend round "corners." It is a simple and straightforward procedure and can be easily programmed for convex regions. Vertices are generated as in the case of Simplex method, however, no attempt is made to preserve a regular figure in which each vertex is equidistant from all other points.

The complex method requires use of $k \geq n + 1$ vertices, each one satisfying all the imposed constraints. The algorithm for this method is described below, and a listing of the computer code is also given.

Algorithm:

1. Initially using random guesses, $n + 1$ vertices can be generated, and the sum of squares of the differences between experimental and calculated values can be stored as an additional variable in the program structure. Also, user can have a choice of screen-input of guess values or can use previously generated guesses from a file.

2. To generate the next point, the point with poorest maximum sum of squares is identified. Using this value, the centroid (M) of the figure for the rest n points is computed using a formula,

$$X_{i, M} = \frac{1}{k - 1} \left(\sum_{j=1}^{k} X_{i,j} - X_{i, R} \right) \qquad (a)$$

where, k is the number of guess points, n is unknown variables denoted by $X_{i,j} = 1,2,...,n$.

3. Using the coordinates of centroid M, the coordinates of a new point N is generated using following formula,

$$X_{i, N} = (1 + \alpha) X_{i, M} - \alpha X_{i, R} \qquad (b)$$

4. After this step, steps 2 and 3 are repeated until a satisfactory sum of squares is obtained.

In all this process of optimization, to ensure convergence of the objective function to be minimized, following set of rules are followed:

Rule 1: If a constraint violation occurs, the trial point is moved half-way in towards the centroid of the vertices already determined.

Rule 2: The objective function is computed at each vertex, and the poorest estimate is rejected and replaced by a point, which is located at a distance α ($\alpha \geq 1$) times as far from the centroid of the remaining points as the distance of this rejected vertex, but in a direction defined by a vector pointing from the rejected point to the centroid. This is embedded in the formula given by equation (b), used in step 3.

Rule 3: If the new point has the worst value in the set of vertices, its location is moved half-way towards the previous centroid. Thus, this new point (N) is generated using the equation,

$$X_{i, N} = \frac{1}{2} (X_{i, N} + X_{i, M}) \qquad (c)$$

Rule 4: If an algebraic constraints on the feasible region, $g_k \leq 0$ is at any time violated, the vertex is again moved half-way towards the centroid. If this constraint is still violated, the retreat is continued until a valid point is obtained.

Rule 5:   Additionally, if a generated point does not satisfy one of the explicit inequalities imposed on a particular variable, X_i, it is reset at a suitable small distance inside the appropriate boundary to get a feasible point.

The normally recommended value for α is 1.3, and the number of the guesses (k) used should be about $2n$. During a search, the complex roles over and over, expands and contracts, and finally collapses into the generated centroid.

Computer program used for dual-sorption parameter estimation[*]

```
DECLARE SUB COND (LP, NV, X#(), XLOW#(), XUPP#(), F#, J!, IFLAG!)
DECLARE SUB FUNC (K, J, NV, NP, X#(), XLOW#(), XUPP#(), R#(), XE#(), YE#(),
F#)
DEFDBL A-H, O-Z
REM    .................................................
REM    OPTIMIZATION PROGRAM FOR DUAL-SORPTION MODEL
REM     FOR GLASSY MEMBRANES
REM    METHOD EMPLOYED : COMPLEX METHOD OF BOX
REM    REF. : OPTIMIZATION: THEORY AND PRACTICE
REM     by BEVERIDGE & SCHECHTER
REM    .................................................
REM
      DIM X(50, 3), R(30, 3), XE(40), YE(40), XLOW(1, 3), XUPP(1, 3)
      DIM IR(50), FF(50), XM(1, 3), XR(1, 3), XAVG(1, 10)
      COMMON SHARED /OPT/ ALPHA
      CLS : CLEAR : RESET
REM    .................................................
REM    .................... HEART OF THE PROGRAM........................
REM    .......................INITIALIZATION............................
REM    ......... INITIAL VALUES OF PARAMETERS TO BE ESTIMATED ...........
REM
REM    NV : NUMBER OF PARAMETERS TO BE ESTIMATED.
REM    NP : NUMBER OF SETS OF POINTS FROM EXPERIMENT.
REM    NG : NUMBER OF INITIAL VERTICES TO BE GENERATED.
REM    .................................................
```

```
OPEN "COMPLEX.DAT" FOR INPUT AS #2
INPUT #2, NV, NP: PRINT NV, NP: PRINT
FOR KK = 1 TO NV: INPUT #2, XLOW(1, KK), XUPP(1, KK)
    PRINT XLOW(1,   KK), XUPP(1, KK)
    NEXT KK
PRINT
FOR KK = 1 TO NP: INPUT #2, XE(KK), YE(KK): PRINT XE(KK), YE(KK)
    NEXT KK
PRINT
CLOSE #2
LOCATE 23, 5: PRINT "Press any key continue...": A$ = INPUT$(1)
REM    ....................................................
REM    ..................INITIALIZATION SECTION........................
NG = 3
ALPHA = 1.2#
NTRIAL = 50
X(1, 1) = *****#: X(1, 2) = *****#: X(1, 3) = *****#
REM    ....................................................
REM    .............SELECTION MODE OF INITIAL POINTS....................
39    CLS
        LOCATE 10, 15: INPUT "INPUT GUESS VALUES FROM SCREEN OR
        GENERATE (S/G)"; YN$
    IF YN$ = "S" OR YN$ = "s" THEN GOTO 19
    IF YN$ = "G" OR YN$ = "g" THEN GOTO 29
    LOCATE 20, 10: PRINT "Wrong input. Input S/s for screen
        or G/g to generate. Press any key to continue..."
    A$ = INPUT$(1)
    GOTO 39
REM    ....................................................
29    OPEN "RND.NUM" FOR INPUT AS #1
    FOR L = 1 TO 23: FOR K = 1 TO 3: INPUT #1, R(L, K): NEXT K: NEXT L
    CLOSE #1
REM    ....................................................
```

```
REM    ................. GENERATION OF INITIAL VERTICES................
       J = 1
       FOR K = 1 TO NG
10     CALL FUNC(K, J, NV, NP, X#(), XLOW#(), XUPP#(), R#(), XE#(), YE#(), F#)
       PRINT K, X(K, 1), X(K, 2), X(K, 3), "F ="; F
       FF(K) = F
       IFLAG = 0: LP = K
       CALL COND(LP, NV, X#(), XLOW#(), XUPP#(), F#, J, IFLAG)
       'PRINT IFLAG
       IF IFLAG = 1 THEN J = J + 1: GOTO 10
       J = J + 1
       NEXT K
       GOTO 49
REM    ................................................
REM    ..............SCREEN INPUT OF INITIAL GUESS VALUES..............
19     CLS
       LOCATE 10, 10: INPUT "ARE THE GUESS POINTS IN A FILE?(Y/N)", XN$
       IF XN$ = "Y" OR XN$ = "y" THEN GOTO 13
       IF XN$ = "N" OR XN$ = "n" THEN GOTO 23
       LOCATE 20, 10: PRINT "Wrong input. Input Y/N OR y/n.
           Press any key to continue..."
       A$ = INPUT$(1)
       GOTO 19
13     OPEN "GUESS.DAT" FOR INPUT AS #3
       FOR IO = 1 TO NG
       INPUT #3, X(IO, 1), X(IO, 2), X(IO, 3), FF(IO)
       NEXT IO
       CLOSE #3
       GOTO 49
REM    ................................................
REM    ................................................
23     OPEN "C:GUESS.DAT" FOR OUTPUT AS #3
       J = 999
```

```
        FOR IAS = 1 TO NG
47      FOR JAS = 1 TO NV
        PRINT "GUESS NO. "; IAS
        PRINT "PARAMETER ("; JAS; ") ="; : INPUT X(IAS, JAS)
        NEXT JAS
        K = IAS
        CALL FUNC(K, J, NV, NP, X#(), XLOW#(), XUPP#(), R#(), XE#(), YE#(), F#)
        PRINT "SUM OF SQUARE OF ERROR ="; F
        FF(IAS) = F
        PRINT "*********************************************"
REM     ................................................................
REM     ....................STORING THE GUESS VALUES....................
37      PRINT : INPUT "STORE THE SET OF GUESS VALUES?(Y/N)", XN$
        IF XN$ = "Y" OR XN$ = "y" THEN GOTO 17
        IF XN$ = "N" OR XN$ = "n" THEN GOTO 27
        LOCATE 20, 10: PRINT "Wrong input. Input Y/N OR y/n.
            Press any key to continue..."
        A$ = INPUT$(1)
        GOTO 37
27      GOTO 47
17      WRITE #3, X(IAS, 1), X(IAS, 2), X(IAS, 3), FF(IAS)
        NEXT IAS
        CLOSE #3
REM     ................................................................
        GOTO 49
REM     ................................................................
REM     ................ FINAL PROCEDURE OF OPTIMIZATION ...............
REM
REM     THIS FINAL PART OF THE PROCEDURE FINDS THE CENTROID
REM      OF THE POLYGON AND FINDS THE BEST GUESSTIMATE
REM      USING CERTAIN RULES FOR REJECTING THE POINTS IN CASE
REM      OF POOR ESTIMATE OF FUNCTION TO BE MINIMIZED.
REM
```

```
49    NACPT = NG: KFLAG = 1
      FOR INAM = 1 TO NTRIAL: IR(INAM) = 0: NEXT INAM
      FOR KK = (NG + 1) TO NTRIAL
      IF (KK > NG + 1) THEN KFLAG = 5
      PRINT : FOR ITT = 1 TO 80: PRINT "*"; : NEXT ITT
      PRINT "*********************ITERATION NO.";
         " "; KK; " ********************"
REM   .................REJECTION OF POOREST ESTIMATE...................
9009  NFLAG = 0: J = 999: FMAX = 0
      PRINT "PRESENT KK VALUE IS :"; KK
      FOR IX = 1 TO KK - 1
      IF KFLAG = 1 AND NFLAG = 0 THEN
        FMAX = FF(1): PRINT "FMAX ="; FMAX: NFLAG = 1: IL = 1
      END IF
      IF (FF(IX) > FMAX) AND (IR(IX) = 0) THEN
        IL = IX: FMAX = FF(IX)
         PRINT "IL ="; IL; " FMAX ="; FMAX
      END IF
      NEXT IX
      IR(IL) = 1: 'PRINT "POINT "; IL; " IS REJECTED": PRINT
      PRINT X(IL, 1), X(IL, 2), X(IL, 3), FF(IL)
      FOR IOP = 1 TO NV: XR(1, IOP) = X(IL, IOP): NEXT IOP: FR = FF(IL)
      PRINT "CO-ORDINATES OF REJECTED POINT ARE :"
      PRINT XR(1, 1), XR(1, 2), XR(1, 3), FR
REM   ................................................................
REM   ................................................................
REM   .................CALCULATION OF CENTROID........................
REM   ................................................................
REM
      PRINT "RULE 2 FOLLOWED FOR OPTIMIZATION PROCEDURE."
REM   ................................................................
REM   THESE RESULTS WILL BE TESTED FOR NEWLY GENERATED POINT
REM    USING OTHER RULES VIZ. : 1, 3, 4, 5.
```

```
REM    ...................................................
    NNN = 0
    IF (KFLAG = 1) THEN NITER = NG ELSE NITER = KK - 1
    FOR IRR = 1 TO NITER
    IF IR(IRR) = 0 THEN NNN = NNN + 1
    'PRINT "POINT NO. "; IRR; " ERROR FLAG ="; IR(IRR)
    NEXT IRR
    PRINT "NO. OF POINTS USED IN CALCULATION OF CENTROID ARE :"; NNN
    IF (NNN < > (NG - 1)) AND (KFLAG < > 1) THEN PRINT
        "ERROR:  NP TO BE USED ="; NG - 1; " NP ACCEPTED "; NNN: STOP
    FOR LL = 1 TO NV: SSUM = 0#
    FOR JK = 1 TO NITER
    TERM = X(JK, LL)
    IF IR(JK) = 0 THEN SSUM = SSUM + TERM
    NEXT JK
    XM(1, LL) = 1# / (NG - 1#) * SSUM
    NEXT LL
    PRINT "****************************************************************"
    PRINT
    PRINT "CO-ORDINATES OF CENTROID ARE :"
    FOR INN = 1 TO NV: PRINT USING " ##.####"; XM(1, INN); : NEXT INN
        PRINT
59  FOR INN = 1 TO NV
    X(KK, INN) = (1# + ALPHA) * XM(1, INN) - ALPHA * X(IL, INN)
    NEXT INN
9002  K = KK
    CALL FUNC(K, J, NV, NP, X#(), XLOW#(), XUPP#(), R#(), XE#(), YE#(), F#)
    PRINT "CO-ORDINATES OF NEW POINT GENERATED ARE :"
    PRINT USING " ##.####"; X(KK, 1); X(KK, 2); X(KK, 3);
    PRINT USING " #.####^^^^"; F: PRINT
    FF(KK) = F
REM    ................................................
REM    ..........COMPARING REJECTED POINT AND GENERATED POINT..........
```

```
        IRULE3 = 0
        PRINT "NEW F ="; F, "F REJECTED ="; FR
        IF (F > FR) THEN
            PRINT "RULE 3 TO BE APPLIED..."
            IRULE3 = 3: GOTO 9001
        END IF
REM     ..............................................
REM     ..........................................
9004    PRINT "CHECKING RULE 5": GOTO 9003
9007    IF IFLAG = 1 THEN IFLAG = 0: GOTO 9004
REM     ..............................................
REM     ....................PRINTING ACCEPTED POINTS...................
        IR(IL) = 1
        FOR IBI = 1 TO KK
        'PRINT "ERROR FLAG ="; IR(IBI)
        IF IR(IBI) = 0 THEN
        PRINT USING "## "; IBI; : PRINT " ";
        PRINT USING " ##.####"; X(IBI, 1); X(IBI, 2); X(IBI, 3);
        PRINT "  F= "; : PRINT USING " #.####^^^^"; FF(IBI)
        END IF
        NEXT IBI
REM     ..............................................
REM     ...............SET OF RULES FOR POOR ESTIMATES..................
REM     ...................RULE ONE...................
REM     IF THE CONSTRAINT IS VIOLATED ON THE BOUNDS ON PARAMETERS
THEN
REM     THE POINT IS MOVED HALF-WAY TOWARDS THE CENTROID.
REM
        IFLAG = 0: LP = KK
        CALL COND(LP, NV, X#(), XLOW#(), XUPP#(), F#, J, IFLAG)
        IF IFLAG = 1 THEN
            PRINT "RULE 1 VIOLATED": PRINT
            FOR IXY = 1 TO NV
```

```
    X(KK, IXY) = X(KK, IXY) / 2#
    NEXT IXY
  GOTO 59
  END IF
REM    ...................RULE TWO.................................
REM    IT DEALS WITH THE COMPUTATION OF THE CENTROID TO GENERATE
NEW PT.
REM      ALREADY EMBEDDED IN THE OPTIMIZATION ALGORITHM.
REM    ................................................................
REM    ...................RULE THREE................................
9001  IF IRULE3 = 3 THEN
    FOR IPP = 1 TO NV: X(KK, IPP) = .5# * (X(KK, IPP) + XM(1, IPP))
      NEXT IPP
  GOTO 9002
  END IF
REM    ................................................................
REM    ................................................................
REM    ...................RULE FOUR................................
REM    ................................................................
REM    ................................................................
  PRINT "NO. OF POINTS ACCEPTED ARE : "; NACPT
  PRINT "AT THE END OF ITERATION "; KK; "NO. OF POINTS
      ACCEPTED ARE "; NACPT
  NEXT KK
REM    ................................................................
REM    .............PRINTING FINAL RESULTS............................
  CLS
  LOCATE 2, 20: PRINT "RESULTS OF OPTIMIZATION"
  PRINT : PRINT
  FOR LL = 1 TO NV: XAVG(1, LL) = 0#: NEXT LL
  FOR II = 1 TO NV
  FOR JJ = NTRIAL TO NTRIAL - NG + 1 STEP -1
  XAVG(1, II) = XAVG(1, II) + X(JJ, II)
```

```
NEXT JJ
XAVG(1, II) = XAVG(1, II) / NG
PRINT TAB(10); "PARAMETER "; II; "= "; XAVG(1, II)
NEXT II
PRINT : PRINT
PRINT "          EXPT. P   EXPT. C   CALC. C   DIFF."
PRINT : PRINT
K = 1
FOR I = 1 TO NV: X(1, I) = XAVG(1, I): NEXT I
FOR II = 1 TO NP
K = 1
F = XE(II) * X(K, 1) + (X(K, 2) * X(K, 3) * XE(II)) /
    (1# + X(K, 3) * XE(II))
PRINT "No. "; : PRINT USING " ##"; II; : PRINT " ";
PRINT USING " ###.####"; XE(II); YE(II); F;
PRINT USING " #.###^^^^"; (YE(II) - F)
NEXT II
LOCATE 1, 5: PRINT "Press any key to continue...": A$ = INPUT$(1)

REM    ............SENDING DATA TO PRINTER.................................
1039   CLS
LOCATE 10, 15: INPUT "SEND REPORT TO PRINTER (Y/N)"; YN$
IF YN$ = "Y" OR YN$ = "y" THEN GOTO 1019
IF YN$ = "N" OR YN$ = "n" THEN GOTO 1029
LOCATE 20, 10: PRINT "Wrong input. Input Y/N.
    Press any key to continue..."
A$ = INPUT$(1)
GOTO 1039
REM    .................................................................
1019  IF YN$ = "Y" OR YN$ = "y" THEN
LPRINT TAB(20); "CONVERGED RESULTS"
FOR II = 1 TO NV
FOR JJ = NTRIAL TO NTRIAL - NG + 1 STEP -1
```

```
      LPRINT USING "  ##.#####"; X(JJ, II); FF(JJ)
      NEXT JJ: NEXT II
      LPRINT : LPRINT "*****************************************************"
      LPRINT : LPRINT
      LPRINT TAB(20); "RESULTS OF OPTIMIZATION"
      LPRINT : LPRINT
      FOR II = 1 TO NV
      LPRINT TAB(10); "PARAMETER "; II; "= "; XAVG(1, II)
      NEXT II
      LPRINT : LPRINT
      LPRINT "          EXPT. P   EXPT. C   CALC. C   DIFF."
      LPRINT : LPRINT
      K = 1
      FOR I = 1 TO NV: X(1, I) = XAVG(1, I): NEXT I
      FOR II = 1 TO NP
      K = 1
      F = XE(II) * X(K, 1) + (X(K, 2) * X(K, 3) * XE(II)) /
          (1# + X(K, 3) * XE(II))
      LPRINT "No. "; : LPRINT USING " ##"; II; : LPRINT " ";
      LPRINT USING "  ###.####"; XE(II); YE(II); F;
      LPRINT USING "  #.###^^^^"; (YE(II) - F)
      NEXT II
      END IF
1029  END
REM   ...............................................
REM   ...............RULE FIVE...................
9003  IFLAG = 0: LP = KK:
      PRINT X(KK, 1), X(KK, 2), X(KK, 3), FF(KK)
      CALL COND(LP, NV, X#(), XLOW#(), XUPP#(), F#, J, IFLAG)
      PRINT IFLAG
      IF IFLAG = 1 THEN
        FOR IE = 1 TO NV
        IF X(KK, IE) > XM(1, IE) THEN X(KK, IE) = X(KK, IE) / 2#
```

```
        IF X(KK, IE) < XM(1, IE) THEN X(KK, IE) = X(KK, IE) * 1.2#
        NEXT IE
      K = KK
      CALL FUNC(K, J, NV, NP, X#(), XLOW#(), XUPP#(), R#(), XE#(), YE#(), F#)
      FF(KK) = F
      PRINT "CO-ORDINATES OF MODIFIED NEW POINT USING RULE 5 ARE :"
      PRINT USING " ##.###"; X(KK, 1); X(KK, 2); X(KK, 3); FF(KK)
      END IF
      GOTO 9007
REM      ...................................................

      SUB COND (LP, NV, X#(), XLOW#(), XUPP#(), F#, J, IFLAG)
      IFLAG = 0
      PRINT X(LP, 1), X(LP, 2), X(LP, 3), F
      PRINT "LOWER LIMIT ARE :"
      PRINT XLOW(1, 1), XLOW(1, 2), XLOW(1, 3)
      PRINT XUPP(1, 1), XUPP(1, 2), XUPP(1, 3)
      FOR LAX = 1 TO NV
      IF (X(LP, LAX) < XLOW(1, LAX)) THEN
        PRINT "LOWER LIMIT CONDITION VIOLATED"
        IFLAG = 1
      END IF
      IF (X(LP, LAX) > XUPP(1, LAX)) THEN
        PRINT "UPPER LIMIT CONDITION VIOLATED"
        IFLAG = 1
      END IF
      NEXT LAX
      END SUB

      SUB FUNC (K, J, NV, NP, X#(), XLOW#(), XUPP#(), R#(), XE#(), YE#(), F#)
REM      ...................................................
      IF J = 999 THEN GOTO 101
      IF K = 1 THEN GOTO 101
      FOR I = 1 TO NV
```

```
      X(K, I) = XLOW(I) + R(J, I) * (XUPP(I) - XLOW(I))
      NEXT I
      SUM = 0#
101   FOR I = 1 TO NP
      GOSUB 1000
      SUM = SUM + (YE(I) - F) ^ 2#
      'PRINT "YE(I),F"; YE(I), F; "DIFF ="; (YE(I) - F); "SUM ="; SUM
      NEXT I
      F = SUM
      GOTO 2000
1000  F = XE(I) * X(K, 1) + (X(K, 2) * X(K, 3) * XE(I)) /
         (1# + X(K, 3) * XE(I))
1099  RETURN
2000  END SUB
```

Preliminary permeability results for mixed gas system (CO_2/CH_4)

for solution-cast PC(Lexan) at $35^{\circ}C$

Sample - Polycarbonate (Lexan)
        (solution-cast, vacuum dried)

Gas   - CO_2 : CH_4 (55 : 45 mole ratio)

Temp. - $35^{\circ}C$

p_2	$J_T\ 10^3$	CO_2		CH_4		α
		p_2	P	p_2	P	
(atm)	(cc/sec)	(atm)	(Barrers)	(atm)	(Barrers)	CO_2/CH_4
9	0.3273	5.1	3.9283	3.9	0.2066	19
15	0.5695	8.4	3.7919	6.6	0.2050	18.5
20	0.7692	11.5	3.6471	8.5	0.2031	17.96
25	0.9472	14.1	3.6009	9.9	0.2036	17.68

REFERENCES

REFERENCES

* Aitken C L, Paul D R and Koros W J (1990), Gas transport properties of new polysulfone membrane materials, Proceedings of 'ICOM 90', Chicago, IL, USA, August 21-25, Pg. 821.

* Assink R A (1975), Investigation of the dual-mode sorption of ammonia in Polystyrene by NMR, J. Polym. Sci., Polym. Phys. Ed., 13 : 1665.

* Baker R W and Blume I (1986), Permselective membranes separate gases, Chem. Tech., April : 232.

* Barbari T A, Koros W J and Paul D R (1989), Polymeric membranes based on bisphenol-A for gas separations, J. Memb. Sci., 42 : 69.

* Barrer R M (1939), Permeation and solution of gases in organic polymers, Trans Faraday Soc., 35 : 628.

* Barrer R M (1957), Some properties of diffusion coefficients in polymers, J. Phys. Chem., 61 : 178 and references therein.

* Barrer R M, Barrie J A and Slatter J (1958), Sorption and diffusion in ethyl cellulose, Part III. Comparison between ethyl cellulose and rubber, J. Polym. Sci., 27 : 177.

* Barrer R M (1984), Diffusivities in glassy polymers for the dual-mode sorption model, J. Memb. Sci., 18 : 25.

* Berens A R (1974), The solubility of vinylchloride in poly(vinyl chloride), Am. Chem. Soc., Coatings and Plastics. Prepr., 15(2) : 197.

* Berens A R (1975), The solubility of vinyl chloride in Poly(vinyl chloride), Angew Macromol. Chem., 47 : 97.

* Berens A R and Hopfenberg H B (1978), Diffusion and relaxation in glassy polymer powder : 2. Separation of diffusion and relaxation parameters, Polymer, 19 : 489.

* Bernier G A and Kambour R P (1968), The role of organic agents in the stress crazing and cracking of Poly (2,6-dimethyl-1,4-phenylene oxide), Macromolecules, 1 : 393.

* Berry G C and Fox T G (1968), The viscocity of polymers and their concentrated solutions, Adv. Polym. Sci., 5 : 261.

* Bixler H J and Sweeting O J (1971), Barrier properties of polymers films, in Sweeting O J (Eds.), Sci. & Tech. of Polymer films, Wiley, NY, Vol II : 1.

* Bondi A (1964), Van der Walls volumes and radii, J. Phys. Chem., 68 : 441.

* Bourbon D, Kamiya Y and Mizoguchi K (1990), Sorption and dilation properties of Poly (p-phenylene sulfide) under high-pressure CO_2, J. Poly. Sci., Polym. Phys. Ed., 28 : 2057.

* Brown W E and Sauber W J (1959), Gas transmission by plastic films, Mod. Plastics, 36 (12) : 107.

* Brubaker D W and Kammermeyer K (1953), Apparatus for measuring gas permeability of sheet materials, Anal. Chem., 25 : 424.

* Brunauer S (1977), Physical adsorption of gases and vapors, Oxford University Press, Pg. 150.

* Buechler C A and Masters J E (1939), The identification of aromatic sulfones, J. Org. Chem., 4 : 262.

* Chan A H and Paul D R (1979), Influence of history on the gas sorption, thermal and mechanical properties of glassy polycarbonate, J. Appl. Polym. Sci., 24 : 1539.

* Chan A H and Paul D R (1980), Effect of sub-Tg annealing on CO_2 sorption in polycarbonate, Polym. Eng. Sci., 20 : 87.

* Charati S G, Houde A Y, Kulkarni S S and Kulkarni M G (1991), Transport of gases in aromatic polyesters : correlation with WAXD results, J. Polym. Sci., Polym. Phys. Ed., 29 : 961.

* Chern R T, Koros W J, Hopfenberg H B and Stannett V T (1983)[a], Reversible-isopentene-induced depression of CO_2 permeation through polycarbonate, J. Polym. Sci., Polym. Phys. Ed., 25 : 753.

* Chern R T, Koros W J, Sanders E S, Chen C H, Hopfenberg H B (1983)[b] in T E Whyte Jr., E H Wagener (Eds.), Industrial gas separations, ACS Symp. Ser. 223, American Chemical Society, Washington DC, P. 47.

* Chern R T, Koros W J, Sanders E S and Yui E E (1983)[c], "Second component" effects in sorption and permeation of gases in glassy polymers, J. Memb. Sci., 15 : 157.

* Chern R T, Koros W J, Yui B, Hopfenberg H B and Stannett V T (1984), Selectivite permeation of CO_2 and CH_4 through Kapton[R] polyimide : Effects of penetrant competition and gas phase nonideality, J. Polym. Sci., Polym. Phys. Ed., 22 : 1061.

* Chern R T, Koros W J, Hopfenberg H B and Stannett V T (1985), in D R Lloyd (Ed.), Materials science of synthetic membrane, ACS Symp. Ser. No. 269, American Chemical Society, Washington DC, Pg. 25.

* Chern R T, Sheu F R, Jia L, Stannett V T and Hopfenberg H B (1987), Transport of gases in unmodified and aryl-brominated 2,6-dimethyl-1,4-poly(phenylene oxide), J. Memb. Sci., 35 : 103.

* Chiou J S, Barlow J W and Paul D R (1985)[a], Plasticization of glassy polymers by CO_2, J. Appl. Polym. Sci., 30 : 2633.

* Chiou J S, Barlow J W and Paul D R (1985)[b], Sorption and transport of gases in miscible poly(methyl methacrylate) poly(epichlorohydrin) blends, J. Appl. Polym. Sci., 30 : 1173.

* Chiou J S and Paul D R (1986), Sorption and transport of CO_2 in PVF_2/PMMA blends, J. Appl. Polym. Sci., 32 : 2897.

* Chiou J S, Maeda Y and Paul D R (1987), Gas permeation in polyethersulfone, J. Appl. Polym. Sci., 33 : 1823.

* Chiou J S and Paul D R (1987), Effects of CO_2 exposure on gas transport properties of glassy polymers, J. Memb. Sci., 32 : 195.

* Chiou J S and Paul D R (1989), Gas sorption and permeation in poly(ethyl methacrylate), J. Memb. Sci., 45 : 167.

* Coleman M R and Koros W J (1990), Isomeric polyimides based on fluorinated dianhydrides and diamines for gas separation applications, J. Memb. Sci., 50 : 285.

* Daynes H A (1920), The process of diffusion through a rubber membrane, Proc. Roy. Soc. (London)., A97 : 296.

* Dong J H, Huang C K and Jiang Y Y (1989), Gas permeation in poly[(butyl methacrylate)-co-(4-vinyl pyridine)] membrane containing transition metal ions, J. Macromol. Chem., Rapid Commun., 10 : 145.

* Donohue M D, Minhas B H and Lee S Y (1989), Permeation behavior of CO_2-CH_4 mixtures in cellulose acetate membrane, J. Memb. Sci., 42 : 197.

* Enscore D J, Hopfenberg H B, Stannett V T and Berens A R (1977), The effect of prior sample history on n-hexane sorption in glassy polystyrene microspheres, Polymer, 18 : 1105.

* Erb A J and Paul D R (1981), Gas sorption and transport in Polysulfone, J. Memb. Sci., 8 : 11.

* Ferry J D (1980), The glassy state, in Ferry J D (Eds.), "Viscoelastic properties of polymers", Wiley and Sons, NY, Pg. 437.

* Fleming G K and Koros W J (1990), CO_2 conditioning effects on

sorption and volume dilation behavior for bisphenol-A polycarbonate, Macromolecules, 23 : 1353.

* Fried J R, Liu H C and Chang C (1989), Effect of sorbed CO_2 on the dyanamic mechanical properties of glassy polymers, J. Polym. Sci., Polym. Let. Ed., 27 : 385.

* Fried J R, Zhang C and Liu H-C (1990), Effect of sorbed carbon dioxide on the impact strength of amorphous glassy polymers, J. Polym. Sci., Polym. Lett. Ed., 28 : 7.

* Frisch H L (1980), Sorption and transport in glassy polymers - A review, Polym. Eng. Sci., 20 : 2.

* Fujita H (1961), Diffusion in polymer-diluent systems, Fortschr. Hochpolym. Forsch, 3 : 1.

* Fujita H (1968), Organic vapors above the glass transition temperature, in Crank J and Park G S (Eds.), Diffusion in polymers, Academic press, NY., Pg. 75.

* Goldstein M (1972), 'Amorphous Materials', Wiley-Interscience, London.

* Graham T (1866), Philos. Mag., 32 : 401.

* Hachisuka H, Sato T, Imai T, Tsujita Y, Takizawa A and Kinoshita T (1990), Glass transition temperatures of glassy polymers plasticized by CO_2 gas, Polymer J., 22 : 77.

* Hachisuka H, Tsujita Y, Takizawa A and Kinoshita (1991), Gas transport properties of annealed polyimide films, J. Polym. Sci., Polym. Phys. Ed., 29 : 11.

* Heilman W, Tammela V, Meyer J A, Stannett V and Szwarc M (1956), Permeability of polymer films to H_2S gas, Ind. Eng. Chem., 48 : 821.

* Hellums M W, Koros W J, Husk G R and Paul D R (1989), Fluorinated polycarbonates for gas separation application, J. Memb. Sci., 46 : 93.

* Hibri M J El and Paul D R (1985), Effects of uniaxial drawing and heat treatment on gas sorption and transport in PVC, J. Appl. Polym. Sci., 30 : 3649.

* Hoehn H (1974), Heat treatment of membranes of selected polyimides, polyesters and polyimides, US patent 3,822,202 assigned to DuPont.

* Hoehn H and Richter J W (1974), Semipermeable membranes, US patent, 273,802.

* Hoehn H and Richter J W (1980), Aromatic polyimide, polyester and polyamide separation membranes, US patent Reissue 30,351.

*   Hojo H and Findley W N (1973), Effect of gas diffusion on creep behavior of polycarbonate, Polym. Eng. Sci., 13 : 255.

*   Holt G and Pagdin B (1960), The preparation of diaryl sulfones, J. Chem. Soc., Pg. 2508.

*   Houde A Y, Kulkarni S S and Kulkarni M G (1991), Permeation and conditioning effects in phenolphthalein based polysulfone, Proceedings of 'Polymer's 91' National Chemical Laboratory, Pune, India. Jan. 1-4. Pg. 675.

*   Ichiraku Y, Stern S A and Nakagawa T (1987), An investigation of the high the permeability of poly(1-trimethylsilyl-1-propyne), J. Memb. Sci., 34 : 5.

*   Illers K H and Breuer H J (1963), Molecular motions in poly(ethylene terephthalate), J. Coll. Sci., 18 : 1.

*   Jaques C H M, Hopfenberg H B and Stannett V T (1974) in : Hopfenberg H B (Ed.), "Permeability of plastic films and coatings", Plenum press, NY., Pg. 73.

*   Johnson R N, Farnham A G, Clendinning R A, Hale W F and Merriam C N (1967), Poly(aryl ethers) by nucleophilic aromatic substitution, I. Synthesis and properties, J. Polym. Sci., 5 : 2375.

*   Jolley J E and Hildebrand J H (1958), Solution, entropy, and partial molal volumes in solution of gases in non polar solvents, J. Am. Chem. Soc., 80 : 1050.

*   Jordon S M, Koros W J and Fleming G K (1987), The effect of CO_2 exposure on pure and mixed gas permeation behavior. Comparison of glassy polycarbonate and silicone rubber, J. Memb. Sci., 30 : 191.

*   Jordan S M, Koros W J and Beasley J K (1989), Characterization of CO_2 induced conditioning of polycarbonate films using penetrants with different solubilities, J. Memb. Sci., 49 : 103.

*   Jordan S M and Koros W J (1990), Characterization of CO_2 induced conditioning of substituted polycarbonates using various "Exchange" penetrants, J. Memb. Sci., 51 : 233.

*   Kambour R P, Romagosa E E and Gruner C L (1972), Swelling, crazing, and cracking of an aromatic copolyether-sulfone in organic media, Macromolecules, 5 : 335.

*   Kambour R P, Gruner C L and Romagoso E E (1974), Bisphenol-A polycarbonate immersed in organic media. Swelling and response to stress, Macromolecules, 7 : 248.

*   Kambour R P and Gruner C L (1978), Effects of polar group

incorporation on crazing of glassy polymers : styrene-acrylonitrile co-polymer and dicyano bisphenol polycarbonate, J. Polym. Sci., Polym. Phys. Ed., 16 : 703.

* Kamiya Y, Mizoguchi K, Naito Y and Hinese T (1986)[a], Gas sorption in poly(vinyl benzoate), J. Polym. Sci., Polym. Phys. Ed., 24 : 535.

* Kamiya Y, Hirose T, Mizoguchi K and Naito Y (1986)[b], Gravimetric study of high pressure sorption of gases in polymers, J. Polym. Sci., Polym. Phys. Ed., 24 : 1525.

* Kamiya Y, Hirose T, Nairo Y and Mizoguchi K (1988), Sorptive dilation of polysulfone and PET films by high pressure CO_2, J. Polym. Sci., Polym. Phys. Ed., 26 : 159.

* Kim T H, Koros W J, Husk G R and O'Brien K C (1987), Relationship between gas separation in a series of aromatic polyimides, J. Memb. Sci., 37 : 45.

* Kim T H (1988), Gas sorption and permeation in a series of aromatic polyimides, Ph. D. Dissertation, University of Texas at Austin (TX).

* Koros W J and Paul D R (1976), Design considerations for measurement of gas sorption in polymers by pressure decay, J. Polym. Sci., Polym. Phys. Ed., 14 : 1903.

* Koros W J, Paul D R and Rocha A A (1976), Carbon dioxide sorption and transport in polycarbonate, J. Polym. Sci., Polym. Phys. Ed., 14 : 687.

* Koros W J (1977), Sorption and transport of gases in glassy polymers, Ph.D. Dissertation, The University of Texas at Austin (TX), USA.

* Koros W J, Paul D R, Fuji M, Hopfenberg H B and Stannett V T (1977), Effect of pressure on CO_2 transport in PET, J. Appl. Polym. Sci., 21 : 2899.

* Koros W J, Chan A H and Paul D R (1978), Sorption and transport of various gases in polycarbonate, J. Memb. Sci., 2 : 165.

* Koros W J and Paul D R (1978), CO_2 sorption in poly(ethylene terephthalate) above and below the glass transition, J. Polym. Sci., Polym. Phys. Ed., 16 : 1947.

* Koros W J (1980), Model for sorption of mixed gases in glassy polymers, J. Polym. Sci., Polym. Phys. Ed., 18 : 981.

* Koros W J, Chern R T, Stannett V T and Hopfenberg H B (1981), A model for permeation of mixed gases and vapors in glassy polymers, J. Polym. Sci., Polym. Phys. Ed., 19 : 1513.

212

* Koros W J (1985), Simplified analysis of gas/polymer selective solubility behavior, J. Polym. Sci., Polym. Phys. Ed., 23 : 1611.

* Kulkarni S S and Stern S A (1983), The diffusion of CO_2, CH_4, C_2H_4, and C_3H_8 in polyehtylene at elevated pressures, J. Polym. Sci., Polym. Phys. Ed., 21 : 441.

* Kulkarni S S, Houde A Y and Li N N (1990), Plasticization of glassy polymers, Proceedings of 'ICOM 90', Chicago, IL, USA, August 21-25, Pg. 984.

* Kumins C A and Kwei T K (1968), Free-volume and other theories, in : Crank J and Park G S (Eds.), "Diffusion in polymers", Academic press, NY., Pg. 107.

* Kurz J E and Narayan R S (1986), New developments and applications in membrane technology, AIChE spring National meeting, New Oreans, LA, April 6-9, paper no. 199.

* Landrock A H and Proctor B E (1952), The simultaneous measurement of oxygen and carbon dioxide permeabilities of packing materials, Tappi, 35 : 241.

* Legrand D G (1969), Crazing, yielding and fracture of polymers. I. Ductile brittle transition in polycarbonate, J. Appl. Polym. Sci., 13 : 2129.

* Li N N and Long R N (1969), Permeation through plastic films, AIChE J., 15 : 73.

* Lonsdale H K (1982), The growth of membrane technology, J. Memb. Sci., 10 : 81.

* Maeda Y and Paul D.R (1985), Selective gas transport in miscible PPO-PS blends, Polymer, 26 : 2055.

* Maeda Y and Paul D R (1987)[a], Effect of antiplasticization on gas sorption and transport Part I. Polysulfone, J. Polym. Sci., Polym. Phys. Ed., 25 : 957.

* Maeda Y and Paul D R (1987)[b], Effect of antiplasticization on gas sorption and transport Part II. Poly(phenylene oxide), J. Polym. Sci., Polym. Phys. Ed., 25 : 981.

* Maeda Y and Paul D R (1987)[C], Effect of antiplasticization of selectivity and productivity of gas separation membranes, J. Memb. Sci., 30 : 1.

* Manami H, Nakazawa M, Oishi Y, Kakimoto M and Imai Y (1990), Preparation and properties of aromatic polyamides and aromatic polyesters derived from 4,4'-sulfonyldibenzoic acid, J. Polym. Sci., Polym. Chem. Ed., 28 : 465.

* Masuda T, Isobe E, Higashimura T and Takada K (1983), Poly

[1-(trimethylsilyl)-1-propyne] : A new high polymer synthesized with transition-metal catalyst and characterized by extremely high gas permeability, J. Amer. Chem. Soc., 105 : 7473.

* Mauze G R and Stern S A (1982), The solution and transport of water vapor in poly(acrylonitrile) : A re-examination, J. Memb. Sci., 12 : 51.

* Mauze G R and Stern S A (1983), The dual-mode solution and transport of water in poly(acrylonitrile), Polym. Eng. Sci., 23 : 548.

* McBain J W and Baker A M (1926), A new sorption balance, J. Am. Chem. Soc., 48 : 690.

* McHattie J S, Koros W J and Paul D R (1991), Gas transport properties of polysulfones : 1. Role of symmetry of methyl group placement on bisphenol rings, Polymer, 32 : 840.

* Meares P (1958)[a], The solubilities of gases in poly(vinyl acetate), Trans Faraday Soc., 54(1) : 40.

* Meares P (1958)[b], Diffusion of allyl chloride in poly(vinyl acetate). Part II. The transient state of permeation, J. Polym. Sci., 27 : 405.

* Michaels A S and Bixler H J (1961), Solubility of gases in polyethylene, J. Polym. Sci., 50 : 393.

* Michaels A S, Vieth W R and Barrie J A (1963)[a], Solution of gases in poly(ethylene terephthalate), J. Appl. Phys., 34 : 1.

* Michaels A S, Vieth W R and Barrie J A (1963)[b], Diffusion of gases in poly(ethylene terephthalate) , J. Appl. Phys., 34 : 13.

* Milan A and Jiri N (1960), Preparation of diphenyl sulfone - 4,4'- dicarboxylic acid and its methyl and ethyl esters, CA : 55 : 22205 i.

* Miller R L (1975), Crystallographic data for various polymers, in J. Brandup and E H Immergut (Eds.), Polymer Hand Book, 2nd Ed., J. Wiley and Sons, Pg. III-47.

* Mitchell J Y (1831), On the preparation of fluids, J. Roy. Inst. Great Britain, 2 : 101, 307.

* Mizoguchi K, Hirose T, Naito Y and Kamiya Y (1987), CO_2-induced crystallization of poly(ethylene terephthalate), Polymer, 28 : 1298.

* Muruganandam N, Koros W J and Paul D R (1987), Gas sorption and transport in substituted polycarbonates, J. Polym. Sci.,

Polym. Phys. Ed., 24 : 1999.

* Nishide H, Obyanogi M, Suenaga K and Tsuchida E (1989), Oxygen permeation in silicone-bound cobaltporphyrin membrane, J. Polym. Sci., Polym. Chem., Ed., 27 : 1439.

* Nurmukhametov F N, Askadskii A A, Slonimskii G L, Kroshak V V, Salazkin S N, Vygodskii Ya S and Vinogradova S V (1976), The dynamic mechanical properties of number of aromatic polymers, Vysokomol Soyed., A 18 : 812.

* O'Brien K C, Koros W J and Barbari J A (1986), A new technique for the measurements of multicomponent gas transport through polymeric films, J. Memb. Sci., 29 : 229.

* O'Brien K C, Koros W J and Husk G R (1988), Polymeric materials based on pyromellitic dianhydride for the separation of CO_2 and CH_4 gas mixture, J. Memb. Sci., 35 : 217.

* Okamato K, Tanaka T, Shigematsu T, Kita H, Nakamura A and Kusuki A (1990), Sorption and transport of CO_2 in a polyimide from 3,3',4,4'-biphenyltetracarboxylic dianhydride and dimethyl-3,7-diaminodibenzothiophene-5,5'-dioxide, Polymer, 31 : 673.

* Pace R J and Datyner A (1979), Statistical mechanical model for diffusion of simple penetrants in polymers. I. Theory, J. Polym. Sci., Polym. Phys. Ed., 17 : 437.

* Pace R J and Datyner A (1981), The temperature dependence of the Langmuir capacity factor in glassy polymers, J. Polym. Sci., Polym. Phys. Ed., 19 : 1657.

* Paul D R (1969), Effect of immobilizing adsorption on the diffusion time lag, J. Polym. Sci. Part A-2, 7 : 1811.

* Paul D R and Koros W J (1976), Effect of partially immobilizing sorption on permeability and the diffusion time lag, J. Polym. Sci., Polym. Phys. Ed., 14 : 675.

* Paul D R (1979), Gas sorption and transport in glassy polymers, Ber Bunsenges Phys. Chem., 83 : 294 and references therein.

* Perrin D D and Armarego W L F (1988), Purification of laboratory chemicals, (3rd Ed), Permagon press, NY.

* Petropolous J H (1970), Quantitative analysis of gaseous diffusion in glassy polymers, J. Polym. Sci., Pt. A-2, 8 : 1797.

* Petropolous J H (1985), Membranes with non-homogeneous sorption and transport properties , Adv. Polym. Sci., 64 : 93.

*   Pilato L A, Litz L M, Hargitay B, Osborne R C, Farnham A V, Kawakami J H, Fritze P E and McGrath J E (1975), Polymers for permselective membrane gas separations, A.C.S. Div. Polym. Chem. Polym. Prepr., 16(2) : 41.

*   Pope D S, Fleming G K and Koros W J (1990), Effect of various exposure histories on sorption and dilation in a family of polycarbonate, Macromolecules, 23 : 2988.

*   Prigogine I (1957), The molecular theory of solutions, North Holland Publishing Co. Amsterdam. Ch. 6.

*   Pye D G, Hoehn H H and Panar M (1976)[a], Measurement of gas permeability of polymers I. Permeabilities in constant volume / variable pressure, J. Appl. Polym. Sci., 20 : 1921.

*   Pye D G, Hoehn H H and Panar M (1976)[b], Measurement of gas permeability of polymers II. Apparatus for determination of permeabilities of mixed gases and vapors, J. Appl. Polym. Sci., 20 : 287.

*   Raucher D and Sefcik M D (1983)[a], Gas transport and co-operative main chain motions in glassy polymer, in J E Whyte, Yon C M and Wagner F H (Eds.), ACS Symp. Ser. no. 223, Pg. 89.

*   Raucher D and Sefcik M D (1983)[b], Sorption and transport in glassy polymers, gas-polymer-matrix model, in J E Whyte, Yon C M and Wagner F H (Eds.), ACS Symp. Ser. no. 223, Pg. 111.

*   Riedinger H and Faul W (1988), The focussing of membrane R & D on areas of commercial potential, J. Memb. Sci., 36 : 5.

*   Robenson L M (1969), The effect of antiplasticization on secondary loss transitions and permeability of polymers, Polym. Eng. Sci., 9 : 277.

*   Sada E, Kumazawa H and Xu P (1987), Some considerations on the mechanism of gas transport in glassy polymer films, J. Memb. Sci., 35 : 117.

*   Sada E, Kumazawa H and Xu P (1988)[a], Sorption and diffusion of carbon dioxide in polyimide films, J. Appl. Polym. Sci., 35 : 1497.

*   Sada E, Kumazawa H, Xu P and Nishigaki M (1988)[b], Mechanism of gas permeation through glassy polymer films, J. Memb. Sci., 37 : 165.

*   Sada E, Kumazawa H, Yoshio Y, Wang S T and Xu P (1988)[c], Permeation of carbon dioxide through homogeneous dense and asymmetric cellulose acetate membranes, J. Polym. Sci., Polym. Phys. Ed., 26 : 1035.

216

* Sada E, Kumazawa H, Xu P and Wang S T (1990), Permeation of pure CO_2 and CH_4 and binary mixtures through cellulose acetate membrane, J. Polym. Sci., Polym. Phys. Ed., 28 : 113.

* Sanders E S, Koros W J, Hopfenberg H B and Stannett V T (1983), Mixed gas sorption in glassy polymers : Equipment design considerations and preliminary results, J. Memb. Sci., 13 : 161.

* Sanders E S, Koros W J, Hopfenberg H B and Stannett V T (1984), Pure and mixed gas sorption of carbon dioxide and ethylene in poly(methyl methacrylate), J. Memb. Sci., 18 : 53.

* Sanders E S (1988), Penetrant induced plasticization and gas permeation in glassy polymers, J. Memb. Sci., 37 : 63.

* Schell W J (1985), Commercial application for gas permeation membrane systems, J. Memb. Sci., 22 : 217.

* Schwaar R H (1990), Membranes for gas separations, Proc. Economics Prog., SRI International Report No. 190.

* Sefcik M D and Schaefer J (1983), Solid-state ^{13}C NMR evidence for gas polymer interactions in the carbon dioxide poly(vinyl chloride) system, J. Polym. Sci., Polym. Phys. Ed., 21 : 1055.

* Sefcik M D, Schaefer J, May F C, Raucher D and Rub S M (1983), Diffusivity of gases and main chain co-operative motions in plasticized PVC, J. Polym. Sci., Polym. Phys. Ed., 21 : 1041.

* Sefcik M D (1986)[a], Dilation of polycarbonate by CO_2, J. Polym. Sci., Polym. Phys. Ed., 24 : 935.

* Sefcik M D (1986)[b], Dilation and plasticization of polystyrene by carbon dioxide, J. Polym. Sci., Polym. Phys. Ed., 24 : 957.

* Sheu F R, Chern R T, Stannett V T and Hopfenberg H B (1988), Transport of CO_2 and CH_4 in glassy polyesters, J. Polym. Sci., Polym. Phys. Ed., 26 : 883.

* Sheu F R and Chern R T (1989), Effects of packing density on the gas transport properties of poly (phenolphthalein phthalate)s, J. Polym. Sci., Polym. Phys., Ed., 27 : 1121.

* Stannett V T (1968), Simple gases, in Crank J and Park G S (Eds.), "Diffusion in polymers", Academic Press, NY., Pg. 41.

* Stern S A, Gareis P J, Sinclair T F and Mohr P H (1963), Performance of a versatile variable-volume permeability cell. Comparison of gas permeability measurements by the variable-volume and variable-pressure methods, J. Appl. Polym. Sci., 7

: 2035.

* Stern S A, Malhaupt J T and Gareis P J (1969), The effect of pressure on the permeation of gases and vapors through polyethylene. Usefulness of the corresponding states principle, AIChE J., 15 : 64.

* Stern S A and DeMeringo A H (1978), Solubility of carbon dioxide in cellulose acetate at elevated pressures, J. Polym. Sci., Polym. Phys. Ed., 16 : 735.

* Stern S A and Saxena V (1980), Concentration dependent transport of gases and vapors in glassy polymers, J. Memb. Sci., 7 : 47.

* Stern S A and Frisch H L (1981), Selective permeation of gases through polymers, Ann. Rev. Mater. Sci., 11 : 523.

* Stern S A and Kulkarni S S (1982), Solubility of methane in cellulose acetate - conditioning effect of carbon dioxide, J. Memb. Sci., 10 : 235.

* Stern S A, Kulkarni S S and Frisch H L (1983)[a], Tests of free-volume model of gas permeation through polymer membrane. I. Pure CO_2, CH_4, C_2H_4 and C_3H_8 in polyethylene, J. Polym. Sci., Polym. Phys. Ed., 21 : 467.

* Stern S A, Mauze G R and Frisch H L (1983)[b], Tests of free-volume model for the permeation of gas mixtures through polymer membranes. II. CO_2-C_2H_4, CO_2-C_3H_8 and C_2H_4-C_3H_8 mixtures in polyethylene, J. Polym. Sci., Polym. Phys. Ed., 21 : 1275.

* Stern S A, Mi Y, Yamamato H and Clair A K (1989), Structure/permeability relationships of polyimide membranes. Application to the separation of gas mixtures, J. Polym. Sci., Polym. Phys. Ed., 27 : 1887.

* Story B J and Koros W J (1991), Sorption of CO_2 / CH_4 mixtures in poly(phenylene oxide) and a carboxylated derivative, J. Appl. Polym. Sci., 42 : 2613.

* Strathmann H J (1981), Membrane separation processes, J. Memb. Sci., 9 : 121.

* Svehla R A (1962), NASA Tech. Rep., R-132, Lewis Research Center, Cleveland, Ohio.

* Tyagi O S and Deshpande D D (1989), Simple dilatometer for polymer density and thermal expansivity measurements, J. Appl. Polym. Sci., 37 : 2041.

* Ulhmann D R, Renninger G, Kritchevsky and Vandersands J (1976), Electron microscopy and small angle X-ray studies of amorphous polymers , J. Macromol. Sci. Phys., B 12 : 153.

*   Van Amerongen G J (1964), Diffusion in elastomers, Rubber Chemistry and Technology, 37 : 1065.

*   Van Krevelen D W and Hoftyzer P J (1976), Properties of polymers : Their estimation and correlation with chemical structrue, 2nd Ed., Elsevier, Amsterdam.

*   Vieth W R and Sladek K J (1965), A model for diffusion in glassy polymers, J. Colloid Sci., 20 : 1014.

*   Vieth W R, Tam P M and Michaels A S (1966), Dual-sorption mechanism in glassy polystyrene, J. Coll. and Interface Sci., 22 : 360.

*   Vieth W R, Howell J M and Hsieh J H (1976), Dual-sorption theory, J. Memb. Sci., 1 : 177.

*   Viswanathan R, Johnson B C and McGrath J E (1984), Synthesis, kinetic observations and characteristics of polyaylene ether sulphones prepared via a potassium carbonate DMAC process, Polymer, 25 : 1827.

*   Vrentas J S, Jarzebski C M and Duda J L (1975), A deborah number for diffusion in polymer-solvent systems, AIChE J., 21 : 894.

*   Von Wroblewski, Wiedemanns S (1879), Ann. Physik., 8 : 29. Wang C H, Kramer E J and Sachse W H (1982), Effect of high-pressure CO_2 on the glass transition temperature and mechanical properties of polystyrene, J. Polym. Sci., Polym. Phys. Ed., 20 : 1371.

*   Wonders A G and Paul D R (1979), Effect of CO_2 exposure history on sorption and transport in polycarbonate, J. Memb. Sci., 5 : 63.

*   Yamamato H, Mi Y, Stern S A and Clair A K (1990), Structure/permeability relationships of polyimide membrane. II., J. Polym. Sci., Polym. Phys. Ed., 28 : 2291.

LIST OF PUBLICATIONS

1. S.G. Charati, **A.Y. Houde**, S.S. Kulkarni and M.G. Kulkarni, "Transport of Gases in Aromatic Polyesters : Correlation with the WAXD Investigation", J. Polym. Sci., Poly. Phys., Ed., 29 (1991), Pg. 961.

2. S.G. Charati, **A.Y. Houde**, S.S. Kulkarni and M.G. Kulkarni, "Transport of Gases in Aromatic Polysesters : Corelation with WAXD Studies", presented at '7th National Conference on Membrane Processes and Their Applications', held at Vadodara, India. February 22-23, 1990. Proceedings, Pg. 1.

3. S.S. Kulkarni, **A.Y. Houde** and N.N. Li, "Plasticization of Glassy Polymers", presented at 'International Congress on Membrane and Membrane Processes' (ICOM 90), held at Chicago, IL, U.S.A., August 20-24, 1990. Proceedings, Vol 2, Pg. 984.

4. **A.Y. Houde**, S.S. Kulkarni and M.G. Kulkarni, "Permeation and Conditioning Effects in Phenolphthalein based Polysulfone", presented at 'POLYMERS' 91 Conference, held at National Chemical Laboratory, Pune, India, January 1-4, 1991. Proceedings, Vol 2, Pg. 675.

5. **A.Y. Houde**, S.S. Kulkarni and M.G. Kulkarni, "Permeation and Plasticization Behavior in Glassy Polymers : A WAXD Interpretation", J. Memb. Sci. (in press).

6. **A.Y. Houde**, S.S. Kulkarni and M.G. Kulkarni, "Sorption and Transport of CO_2 and CH_4 in Modified Polysulfone ", Polymer, (communicated).

7. **A.Y. Houde**, S.S. Kulkarni and M.G. Kulkarni, "CO_2 Conditioning Effect on Gas Transport Properties of a Series of Aromatic Polyesters", J. Polym. Sci., Polym. Phys., Ed., (communicated).

8. **A.Y. Houde**, B.B. Idage, S.S. Kulkarni and M.G. Kulkarni, "Effect of Substitution of Flexible Ether and Ester Groups in the Polysulfone Backbone on Gas Transport Properties" , (in preparation).

Introduction

Membrane technology for gas / vapor separation is a relatively new technology. Although diffusion through membranes has been studied for over 100 years, the technology has found industrial acceptance only during the last decade. In order to broaden the scope of the technology, there is a need to tailor membranes which would offer superior performance in terms of permeation and separation characteristics.

Criteria for material selection have been discussed in the literature (1,2). In the recent years increasing efforts have been made to improve the performance of polymeric membranes such as Polycarbonate (3) and Polyimides (4) for gas separation application. We have done the systematic study to understand structure - property - performance relationship in a family of Polysulfones.

Scope of the work

This work was undertaken with the following objectives,

1. To improve the gas transport characteristics of polysulfone based materials particularly for the system CO_2/CH_4 and O_2/N_2. Bisphenol-A polysulfone is being extensively used as a membrane material for gas separation application.

2. To elucidate the effect of additional polar / flexible groups such as -COO- or / and -O- , in the polysulfone backbone on its gas transport behavior.

3. To investigate and elucidate permeation and plasticization behavior in various glassy polymers. The polymers studied

include various materials commonly used for fabricating gas selective membranes as well as a systematically varied family of polyarylates.

Experimental work

The following series of modified polysulfone containing flexible groups viz. (i) ester, (ii) ether or (iii) both ether and ester in the main chain were synthesized and studied :

A) Phenolphthalein based polysulfone was synthesized by condensing phenolphthalein with 4,4' dichlorodiphenylsulfone in N,N'-dimethylacetamide solvent at 160°C.

B) Polysulfone containing ester group in the main chain was synthesized from acid chloride of 4,4'-dicarboxydiphenylsulfone and bisphenol-A by the interfacial polycondensation method at room temperature using benzyl triethyl ammonium chloride as a phase transfer catalyst.

C) A third type of polysulfone was synthesized from the acid chloride of 4,4'- / 3,3'- [sulfonylbis(p-phenyleneoxy)dibenzoic-acid] derivative and bisphenol-A. Polymers were also synthesized from mixed acid chlorides.

All these polymers have higher Tg than conventional polysulfone and are polar; thus they were expected to have better transport characteristics.

The polymers were characterized by wide angle X-ray diffraction spectroscopy (WAXD), differential scanning calorimetry (DSC) dynamical mechanical spectroscopy (DMA).

In order to assess the utility of a polymer as a gas separation membrane, its performance evaluation in terms of

sorption and permeation characteristics is needed. A high pressure permeation apparatus based on the variable volume principle (5) for pure as well as mixed gas permeation studies was constructed and standardised. Similarly a sorption apparatus based on the pressure decay principle (6) was constructed and standardized. The sorption and permeation properties were measured and were correlated with their physical properties.

We also examined the conditioning / plasticization effects on these and other polymers. Based on WAXD studies, a general framework to categorize the various types of plasticization has been constructed.

Results and discussion

It was found that phenolphthalein based polysulfone (A) polymer exhibits nearly 50 % higher permeability for CO_2 than conventional polysulfone based on bisphenol-A. Permeability for CO_2 was further increased by 210 % on "conditioning" the polymer at 40 atm. CO_2 pressure. The permeability of CO_2 decreases up to 25 atm., which can be explained within the framework of the classical dual-sorption theory. Beyond 25 atm., the CO_2 permeability increases with pressure in contrast to the predictions of the dual-sorption theory. The selectivity of phenolphthalein based polysulfone for CO_2 / CH_4 is almost the same as that for polysulfone based on bisphenol-A, while a higher selectivity (8.0) is observed for the O_2 / N_2 system. The higher permeability values for CO_2 and CH_4 in phenolphthalein based polysulfone can be explained on the basis of its sorption and diffusivity characteristics. Separation factors for the mixed gas

system containing 55 % CO_2 and 45 % CH_4 were also determined. It was found that the mixed gas selectivity remains almost unaltered in the pressure range wherein partial pressure of CO_2 varied between 5-20 atm., in contrast to that in cellulose acetate and polysulfone (Udel) where it decreases with the increase in partial pressure of CO_2.

In case of poly aryl ester sulfone (B) it was seen that the permeability value for CO_2 (7.1 Barrers at 10 atm. and 35°C) is almost the same as that for phenolphthalein based polysulfone (6.8 Barrers) under identical conditions. Selectivity value observed for the system CO_2 / CH_4 (30.0) is higher than that for conventional polysulfone based on bisphenol-A (24.0).

Finally in the third category of polysulfones (C) amongst the three polymers studied, the polymer derived from acid chloride of 4,4'-[sulfonyl bis(p-phenyleneoxy) dibenzoic acid] and bisphenol-A has the highest permeability for all six gases viz. He, Ar, N_2, O_2, CH_4 and CO_2, followed by the polymer derived from equimolar mixture of 4,4'- and 3,3'- derivative of acid and 3,3'- derivative with bisphenol-A. These results cannot be explained on the basis of the average intersegmental chain spacing values determined by WAXD measurements. These polymers need to be characterized in terms of their solubility characteristics. This work is currently in progress.

Effect of plasticization on the permeation profiles of various glassy polymers was studied. In rubbery polymers, both diffusivity and permeability of gases increases with increasing pressure (7), the change in CO_2 permeability with pressure in the case of glassy polymers (8-10) can be categorized into four

classes. It is shown that wide angle X-ray diffraction (WAXD) results for the samples exposed to high pressure CO_2 gas can be used to rationalize the various types of CO_2 permeability versus pressure profiles in glassy polymers. The increasing CO_2 permeability with pressure observed in cellulose acetate and poly(methylmethacrylate) arises from the significant increases in the intersegmental spacing of these polymers on exposure to high pressure CO_2. The change in the intersegmental spacing can be correlated with the Tg of the polymer prior to conditioning and also with the penetrant solubility in the polymer.

In order to elucidate the above mentioned results, plasticization phenomenon was studied in a systematically varied family of polyarylates. The influence of various parameters such as carbonyl group density, glass transition temperature and average intersegmental chain spacing of the polymer on the high pressure CO_2 conditioning / plasticization effect was measured in a series of bridge and ring substituted aromatic polyesters. It was observed in some cases that the permeability of CO_2 increases with pressure even at low pressure irrespective of whether the polymer possesses polar side chains. The permeability versus pressure profiles of these polymers show significant hysteresis effects. DSC analysis confirms that all these polymers remain in the glassy state even when exposed to high pressure CO_2. These results can satisfactorily be explained on the basis of WAXD results obtained for the CO_2 treated polymer films.

References

1. H Hoehn and J W Richter, US Patent 30, 351 (1980).

2. R T Chern, W J Koros, H B Hopfenberg and V T Stannet, "Materials selection for membrane-based gas separations", in ACS Symp. Ser. No. 269, Material Science of Synthetic Membranes, D R Loyd Ed., Washington D. C., (1985).

3. M W Hellums, W J Koros, G R Husk and D R Paul, "Fluorinated polycarbonates for gas separation applications", J. Memb., Sci., 46 (1989) 93-112.

4. S A Stern, Y Mi, H Yamato and A K St. Clair, "Structure / permeability relationship of polyimide membranes : Application to the separation of gas mixtures", J. Polym. Sci., Polym. Phys. Ed., 27 (1989) 1887-1909.

5. S A Stern, P J Gareis, T F Sinclair and P H Mohr, "Performance of versatile variable-volume permeability cell. comparison of gas permeability measurements by the variable-volume and variable-pressure methods", J. Appl. Polym. Sci., 7 (1963) 2035-2051.

6. S A Stern and De Meringo, "Solubility of carbon dioxide in cellulose acetate at elevated pressures", J. Polym. Sci., Polym. Phys., 16 (1978) 735-751.

7. S A Stern, S S Kulkarni and H L Frisch, "Tests of 'free-volume' model of gas permeation through polymer membranes. I Pure CO_2, CH_4, C_2H_4 and C_3H_8 in polyethylene," J. Polym. Sci., Polym. Phys. Ed., 21 (1983) 467-481.

8. E S Sanders, "Penetrant-induced plasticization and gas permeation in glassy polymers", J. Memb. Sci., 37 (1988) 63-

80.

9.   A J Erb and   D R Paul, "Gas sorption and transport in polysulfone", J. Memb. Sci., 8 (1981) 11-22.

10. K Okamato, K Tanaka, T Shigematsu, H Kita, A Nakumura and A Kusuki, "Sorption and transport of carbon dioxide in a polyimide from 3.3',4,4'-biphenyltetracarboxylic dianhydride and dimethyl - 3,7 -diaminodibenzothiophene -5,5'-dioxide", Polymer, 31 (1990) 673-678.

Polymer Science & Engineering Group   Telphone : (0212) 333941
Chemical Engineering Division   Telex   : 0145-266
National Chemical Laboratory   Fax   : (0212) 330233
Pune - 411 008, INDIA.

CURRICULUM VITAE

OF

AJAY Y. HOUDE

Personal Data :

Date and place of birth : February 24, 1964, Solapur (India)

Languages Known : English, Hindi, Kannada and Marathi

Academic Qualifications :

* Ph.D.[#](Chemistry)   University of Poona, Pune, India

* M.Sc.(Polymer Chemistry)   Shivaji University, Kolhapur, India
                                June 1986, Ist class (61.3%).

* B.Sc.(Chemistry)   Shivaji University, Kolhapur, India
                                June 1984, IInd class (58.7%).

[#] Thesis entitled " Sorption and Permeation of Gases in Polymers", submitted to University of Poona in September 1991.

Experience and Research Activities :

6/2/1987 till date :

Research Fellow (Ph.D. degree) National Chemical Laboratory, Pune, India. Broad area of research is "Membrane Separations".

* Selected and synthesized new polymers for gas separation which exhibited higher flux and selectivity for CO_2 / CH_4 and O_2 / N_2 separation.

* Designed and constructed high pressure sorption and permeation apparatus. Obtained experimental data at high pressures.

* Experience with DSC, DMA and WAXD. Studied effect of high pressure gas exposure and plasticizer addition on physical, mechanical and transport characteristics of glassy polymers.

7/30/1986 to 6/1/1987 :

Research chemist on the project 'Super Absorbing Polymers (JALSHAKTI)' sponsored by Indian Organic Chemicals Limited, Bombay at National Chemical Laboratory, Pune, India. Synthesised and characterized super absorbing polymers which absorbed 400 - 500 grams water / gram of polymer. The product is now commercialized for agriculture purpose.

Honors and Awards :

* 6/2/1987 till date : Research Fellowship awarded by Department of Science and Technology, Govt. of India, New Delhi, India.

* Awarded Certificate of Merit for paper entitled, "Permeation and Conditioning Effects in Phenolphthalein based Polysulfone", presented at 'POLYMERS 91', held at National Chemical Laboratory, Pune, India. January 1-4, 1991.

* Awarded Certificate of Merit for standing first in the B.Sc. examination, 1984.